

**MOBILITY MANAGEMENT PROTOCOLS FOR  
LOW POWER AND LOSSY NETWORKS**

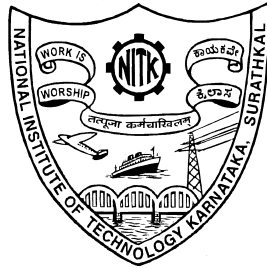
**Thesis**

Submitted in partial fulfilment of the requirements for the degree of

**DOCTOR OF PHILOSOPHY**

by

**SHRIDHAR SANSHI**



**DEPARTMENT OF INFORMATION TECHNOLOGY  
NATIONAL INSTITUTE OF TECHNOLOGY KARNATAKA  
SURATHKAL, MANGALORE - 575025**

**MAY, 2019**



## **Declaration**

I hereby *declare* that the Research Thesis entitled “Mobility Management Protocols for Low power and Lossy Networks” which is being submitted to the National Institute of Technology Karnataka, Surathkal in partial fulfilment of the requirements for the award of the Degree of Doctor of Philosophy in Information Technology is a *bonafide report of the research work carried out by me*. The material contained in this thesis has not been submitted to any University or Institution for the award of any degree.

Shridhar Sanshi  
Register No.: 155071IT15F03  
Department of Information Technology

Place: NITK Surathkal

Date:



## **Certificate**

This is to *certify* that the Research Thesis entitled “Mobility Management Protocols for Low power and Lossy Networks” submitted by Shridhar Sanshi (Register Number: 155071IT15F03) as the record of the research work carried out by him, is *accepted as the Research Thesis submission* in partial fulfilment of the requirements for the award of degree of Doctor of Philosophy.

Dr. Jaidhar CD  
Research Guide  
Assistant Professor  
Department of Information Technology  
NITK Surathkal - 575025

Chairman - DRPC  
(Signature with Date and Seal)



This thesis is  
dedicated to  
**My Parents**





## **Acknowledgements**

Foremost, I express my sincere and deepest gratitude to my supervisor, Head of the Department, Information Technology department, and Research Progress Assessment Committee members for their continuous support and encouragement.

I thank all the teaching and non-teaching staff of department of Information Technology and my fellow doctoral students for their cooperation.

Last, but not the least, I would like to thank my family: my parents, wife, brother, sister, in-laws, and siblings for their emotional support.

(Shridhar Sanshi)



## Abstract

The Internet of Things (IoT) is emerging as a new paradigm for information systems as things are seamlessly integrated with computation and communication capabilities. The Wireless Sensor Network (WSN) is a key component of the IoT environment which is typically composed of large-scale resource-constrained devices, that exploit the Multi-Hop data delivery over wireless links. Recently, the Internet Protocol (IP) based WSN has gained popularity due to the many opportunities it provides for direct communication with the WSN as well as remote access to the sensor data. On the other hand, assigning IP for sensor devices raises numerous challenges due to its resource constraints. Nevertheless, the Internet Engineering Task Force has developed the IPv6 over low power wireless personal area network (6LoWPAN) adaptation layer that enables IPv6 communication over the IEEE 802.15.4 layer, and also standardized the IPv6 Routing Protocol for Low power and Lossy Networks (RPL), to route packets over the 6LoWPAN adaptation layer.

The RPL is a gradient-based routing protocol with bidirectional links that aim to build a robust Multi-Hop mesh topology based on the routing metrics and constraints. However, several issues remain open for improvement and specification, in particular with respect to node mobility that arises in real-time scenarios. Several examinations have illustrated that the RPL is affected under mobility. There are various solutions proposed in the literature to support mobility in the RPL, with limitations. In order to address these issues, this thesis aims to support mobility in the RPL with enhanced performance. The effects of mobility in the RPL is evaluated with different Objective Functions (OFs) such as Objective Function Zero, Energy-based Objective Function, Delay-Efficient Objective Function, and Minimum Rank with Hysteresis Objective Function under different mobility models. Subsequently, it proposes a Multimetrics based OF (MMOF) based on the node type by considering node properties as well as the link properties. It proposes new mechanisms to update the Preferred Parent Node (PPN) based on the control messages to maintain connectivity to the DODAG root. Further, various timers modules are incorporated into the proposed techniques in order to maintain up to date neighbour nodes.

To evaluate the efficacy of the proposed protocols, simulations were carried out by using Contiki based Cooja simulator by varying system and traffic parameters. The simulations were repeated for 3 times and average of the results were considered for evaluating the performance. Different evaluation metrics, namely, the Packet Delivery Ratio (PDR), power consumption, end-to-end delay, and the number of control mes-

sages were considered to evaluate the performance of the proposed protocols. Based on the obtained experimental results, it was observed that under mobility, the OFs have a direct effect on the evaluation metrics. The proposed MMOF along with a mechanism to update the PPN showed improved performance in terms of PDR and power consumption compared to other protocols.

*Keywords:* Mobile Node; Mobility; Objective Function; Preferred Parent Node; Routing protocol.



# Contents

<b>1</b>	<b>Introduction</b>	<b>1</b>
1.1	DETAILS OF IEEE 802.15.4 STANDARD . . . . .	2
1.2	DETAILS OF IPv6 OVER LOW-POWER WIRELESS PERSONAL AREA NETWORKS . . . . .	2
1.3	LOW POWER ROUTING PROTOCOLS OVER 6LoWPAN . . . . .	4
1.4	BACKGROUND OF RPL . . . . .	6
1.4.1	Characteristics of Low power Lossy Networks . . . . .	6
1.4.2	Overview of IPv6 Routing Protocol for Low power and Lossy Networks . . . . .	7
1.5	MOBILITY IN INTERNET OF THINGS . . . . .	10
1.6	MOTIVATION . . . . .	10
1.7	MAJOR CONTRIBUTIONS OF THE THESIS . . . . .	11
1.8	ORGANIZATION OF THE THESIS . . . . .	13
1.9	SUMMARY . . . . .	14
<b>2</b>	<b>Literature Survey</b>	<b>15</b>
2.1	LITERATURE REVIEW ON MOBILITY IN 6LoWPAN . . . . .	15
2.1.1	Mobility Support for Single Hop Communication in 6LoWPAN	15
2.1.2	Mobility Support for Multi-Hop Communication in 6LoWPAN	18
2.2	LITERATURE REVIEW ON MOBILITY IN RPL . . . . .	21
2.2.1	Mobility Support by Modifying Trickle Timer Algorithm in RPL . . . . .	21
2.2.2	Mobility Support by Adding an Additional layer in RPL . . . . .	24
2.2.3	Mobility Support by Mobile Node Movement Prediction in RPL	25
2.2.4	Mobility Support by Other Mechanisms in RPL . . . . .	27
2.3	OUTCOME OF LITERATURE SURVEY . . . . .	30
2.3.1	Problem Statement . . . . .	32
2.3.2	Research Objectives . . . . .	32
2.4	SUMMARY . . . . .	33
<b>3</b>	<b>Analysis of the Objective Function for the RPL under Mobility</b>	<b>34</b>

3.1	PERFORMANCE ANALYSIS OF RPL UNDER MOBILITY . . . .	34
3.1.1	Objective Function Zero . . . . .	34
3.1.2	Minimum Rank with Hysteresis Objective Function . . . . .	35
3.1.3	Energy based Objective Function . . . . .	35
3.1.4	Delay Efficient Objective Function . . . . .	36
3.1.5	Modified RPL in Contiki Operating System . . . . .	37
3.1.6	Simulation Environment and Parameters . . . . .	37
3.1.7	Results and Discussion . . . . .	38
3.2	MULTI METRICS BASED OBJECTIVE FUNCTION FOR LOW POWER AND LOSSY NETWORKS UNDER MOBILITY . . . . .	39
3.2.1	Objective Function for Fixed Router Node . . . . .	41
3.2.2	Objective Function for Mobile Node . . . . .	44
3.2.3	Simulation Results and Discussions . . . . .	46
3.2.4	Analysis of Power Consumption . . . . .	47
3.2.5	Analysis of Packet Delivery Ratio . . . . .	48
3.2.6	Analysis of End-to-End Latency . . . . .	48
3.3	SUMMARY . . . . .	49
<b>4</b>	<b>Design and Analysis of Mobility Aware Routing Protocols</b>	<b>50</b>
4.1	MOBILITY AWARE ROUTING PROTOCOL BASED ON DIO MES- SAGE FOR LOW POWER AND LOSSY NETWORKS . . . . .	50
4.1.1	Selection of Preferred Parent . . . . .	50
4.1.2	Preferred Parent Update . . . . .	51
4.1.3	Main Advantages . . . . .	52
4.1.4	Simulation Results and Discussion . . . . .	53
4.1.5	Analysis of Packet Delivery Ratio . . . . .	53
4.1.6	Analysis of Power Consumption . . . . .	55
4.1.7	Analysis of End-to-End Latency . . . . .	56
4.2	ENHANCED MOBILITY AWARE ROUTING PROTOCOL FOR LOW POWER AND LOSSY NETWORKS . . . . .	57
4.2.1	Objective Function for Selecting Preferred Parent . . . . .	57

4.2.2	Updating Preferred Parent for Mobile Node . . . . .	58
4.2.3	Simulation Results and Discussion . . . . .	63
4.2.4	Analysis of Power Consumption . . . . .	64
4.2.5	Analysis of Packet Overhead . . . . .	65
4.2.6	Analysis of Packet Delivery Ratio . . . . .	67
4.2.7	Analysis of Latency . . . . .	69
4.2.8	Evaluating the Impact of Fixed Router Node Density . . . . .	72
4.2.9	Discussions . . . . .	73
4.3	SUMMARY . . . . .	74
<b>5</b>	<b>Mobility Support Routing Protocols using Timer Functions for Low power and Lossy Networks</b>	<b>76</b>
5.1	ENHANCED MOBILITY ROUTING PROTOCOL FOR WIRELESS SENSOR NETWORK . . . . .	76
5.1.1	Selecting Preferred Parent for Fixed Router Node . . . . .	76
5.1.2	Selecting Preferred Parent for Mobile Node . . . . .	76
5.1.3	Procedure of the Enhanced Mobility RPL . . . . .	80
5.1.4	Performance Evaluation of the proposed Enhanced Mobility RPL . . . . .	83
5.1.5	Discussions . . . . .	90
5.2	FUZZY OPTIMIZED ROUTING METRIC WITH MOBILITY SUPPORT FOR RPL . . . . .	91
5.2.1	Routing Metric Selection . . . . .	91
5.2.2	Fuzzy Inference System . . . . .	92
5.2.3	Results and Discussion . . . . .	98
5.3	SUMMARY . . . . .	102
<b>6</b>	<b>Conclusions and Future Work</b>	<b>103</b>
	<b>References</b>	<b>106</b>



## List of Tables

1.1	Comparison of routing protocols for 6LoWPAN . . . . .	6
2.1	Summary of Mobility Support Protocols for Single Hop communication in 6LoWPAN . . . . .	18
2.2	Summary of Mobility Support Protocols for Multi-Hop communication in 6LoWPAN . . . . .	20
2.3	Summary of Mobility Support Protocols by Modifying Trickle Algorithm in RPL . . . . .	24
2.4	Summary of Mobility Support Protocols by Adding an Additional Layer in RPL . . . . .	25
2.5	Summary of Mobility Support Protocols by MN Movement Prediction in RPL . . . . .	27
2.6	Summary of Mobility Support Protocols by Other Mechanisms in RPL . . . . .	31
3.1	Simulation parameters . . . . .	38
3.2	Bonnmotion software parameters . . . . .	38
3.3	Current consumption of Tmote Sky . . . . .	43
3.4	Simulation parameters . . . . .	47
3.5	Bonnmotion software parameters . . . . .	47
4.1	Simulation Settings . . . . .	53
4.2	Simulation parameters . . . . .	63
4.3	Bonnmotion software parameters . . . . .	63
5.1	Simulation parameters . . . . .	83
5.2	Simulation parameters . . . . .	98

## List of Figures

1.1	Protocol Stack for 6LoWPAN (Chen et al. (2014)) . . . . .	3
1.2	6LoWPAN Architecture (Shelby & Bormann (2011)) . . . . .	4
1.3	ROLL Architecture . . . . .	5
1.4	Example of DODAG tree . . . . .	8
1.5	Example of Mobile Node in multi-hop mesh network . . . . .	11
2.1	Classification of Mobility Management Protocols for LLN . . . . .	16
3.1	Modified RPL in Contiki Operating System . . . . .	36
3.2	(a) Power Consumption under RWK mobility model (b) Power Consumption under RWP mobility model (c) Power Consumption under GM. . . . .	39
3.3	(a) PDR under RWK mobility model (b) PDR under RWP mobility model (c) PDR under GM. . . . .	40
3.4	(a) Latency under RWK mobility model (b) Latency under RWP mobility model (c) Latency under GM. . . . .	40
3.5	Structure of Tmote Sky . . . . .	42
3.6	MMOF for RPL in Contiki Operating System . . . . .	45
3.7	Power consumption with respect to (a) Traffic (b) Trickle timer. . . . .	47
3.8	PDR with respect to (a) Traffic (b) Trickle timer. . . . .	48
3.9	Latency with respect to (a) Traffic (b) Trickle timer. . . . .	49
4.1	Preferred Parent Update . . . . .	51
4.2	PDR with respect to (a) RWP model (30 nodes) (b) GM model (30 nodes) (c) RWP model (50 nodes) (d) GM model (50 nodes) . . . . .	54
4.3	Power Consumption with respect to (a) RWP model (30 nodes) (b) GM model (30 nodes) (c) RWP model (50 nodes) (d) GM model (50 nodes) . . . . .	55
4.4	Latency with respect to (a) RWP model (30 nodes) (b) GM model (30 nodes) (c) RWP model (50 nodes) (d) GM model (50 nodes) . . . . .	56
4.5	Enhanced-RPL in Contiki Operating System . . . . .	58
4.6	Candidate_Parent_Table fields . . . . .	59
4.7	New_Parent_Table fields . . . . .	59
4.8	Scenarios due to Mobile Node Movement . . . . .	62

4.9	Power consumption in grid(G) [random(R)] topology with respect to Speed, Trickle timer, Traffic: (a), (c), (e) [(b), (d), (f)] . . . . .	66
4.10	Packet overhead in grid(G) [random(R)] topology with respect to Speed, Trickle timer, Traffic: (a), (c), (e) [(b), (d), (f)] . . . . .	68
4.11	PDR in grid(G) [random(R)] topology with respect to Speed, Trickle timer, Traffic: (a), (c), (e) [(b), (d), (f)] . . . . .	70
4.12	Latency in grid(G) [random(R)] topology with respect to Speed, Trickle timer, Traffic: (a), (c), (e) [(b), (d), (f)] . . . . .	71
4.13	Impact of Fixed Router Node density on (a) PDR, (b) power consumption, (c) end-to-end latency, and (d) packet overhead . . . . .	74
5.1	Modified DAO message . . . . .	78
5.2	Enhanced Mobility RPL in Contiki Operating System . . . . .	79
5.3	Example of different mobility scenario . . . . .	83
5.4	Impact of Data Traffic on (a) Packet Deliver Ratio, (b) Radio Messages, (c) Power Consumption, and (d) end-to-end delay . . . . .	84
5.5	Impact of Speed on (a) Packet Deliver Ratio, (b) Radio Messages, (c) Power Consumption, (d) and end-to-end delay . . . . .	86
5.6	Impact of Fixed Router Node on (a) Packet Deliver Ratio, (b) Radio Messages, (c) Power Consumption, and (d) end-to-end delay . . . . .	87
5.7	Hospital Environment Monitoring . . . . .	88
5.8	Hospital Monitoring Application (a) Packet Deliver Ratio, (b) Radio Messages, (c) Power Consumption, (d) and end-to-end delay . . . . .	90
5.9	Block diagram of Fuzzy Inference System . . . . .	93
5.10	Membership function for input routing metrics: (a) ETX (b) RE (c) RSSI (d) MT . . . . .	93
5.11	Membership Function of output variable:VL:Very Low, L:Low, ML:Moderate Low, M:Moderate, MH:Moderate High, H:High, VH:Very High . . . . .	94
5.12	Route Construction in FL-RPL . . . . .	95
5.13	Impact of Data Traffic on (a) Packet Deliver Ratio, (b) Radio Messages, (c) Power Consumption, and (d) end-to-end delay . . . . .	99
5.14	Impact of Speed on (a) Packet Deliver Ratio, (b) Radio Messages, (c) Power Consumption, (d) and end-to-end delay . . . . .	100
5.15	Impact of Fixed Nodes on (a) Packet Deliver Ratio, (b) Radio Messages, (c) Power Consumption, and (d) end-to-end delay . . . . .	101

## List of Abbreviations

<b>Abbreviation</b>	<b>Meaning</b>
6LoWPAN	IPv6 over Low-Power Wireless Personal Area Networks
AAA	Authentication, Authorization, and Accounting
AODV	Ad-hoc On-Demand Distance Vector
AP	Access Point
BMP-RPL	Bayesian model Mobility Prediction RPL
BRPL	Backpressure RPL
CoA	Care of Address
Co-RPL	Corona mechanism based RPL
CPN	Candidate Parent Node
CR	Communication Range
CSPMIPv6	Cluster Sensor PMIPv6
DAG	Directed Acyclic Graph
DAO	Destination Advertisement Object
DIO	Destination Oriented Directed Acyclic Graph Information Object
DIS	Destination Oriented Directed Acyclic Graph Information Solicitation
Dist	Distance
Dist_Var	Distance Variation
DLoWMob	Distributed Network-based Intra-PAN mobility scheme for 6LoWPAN
DODAG	Destination Oriented Directed Acyclic Graph
DYMO	Dynamic Mobile Ad-hoc Networks On-demand
DYMO-Low	Dynamic Mobile Ad-hoc Networks On-demand for 6LoWPAN
EC-MRPL	Energy Efficient and Mobility Aware Routing Protocol
EKF-MRPL	Mobility Support Protocol based on the Extended Kalman Filter
EM-RPL	Enhanced mobility routing protocol for wireless sensor network
ER	Edge Router
ERPL	Enhanced Routing Protocol for Low power and Lossy Networks
E-RPL	Energy efficient RPL
ETX	Expected Transmission Count
FA	Foreign Agent
FFD	Full Function Device
FL-RPL	Fuzzy Optimized Routing Metric with Mobility Support
FRN	Fixed Router Node
GI-RPL	Geographical Information RPL
GM	Gauss-Markov

GTM-RPL	Game-Theory based Mobile RPL
HiLow	Hierarchical routing
HMAG	Head MAG
HWSN6	Hospital Wireless Sensor Network
ICMPv6	Internet Control Message Protocol version 6
IETF	Internet Engineering Task Force
IoT	Internet of Things
IP	Internet Protocol
IPv6	Internet Protocol version 6
KP-RPL	Kalman positioning RPL
LLN	Low power and Lossy Networks
LMA	Local Mobility Anchor
LOAD	6LoWPAN Ad-hoc On-demand Distance Vector Routing
LoWMob	Network-based Intra-PAN mobility scheme for 6LoWPAN
M2P	Multipoint-to-Point
MAC	Medium Access Control
MAG	Mobile Access Gateway
MARPL	Mobility Aware Routing Protocol for Low power and Lossy Networks
ME-RPL	Mobility Enhanced RPL
MMOF	Multi Metrics based Objective Function
MN	Mobile Node
MNF	Mobile Node Flag
MIPv6	Mobile IPv6
Mod-RPL	Modified RPL
MoMoRo	Mobility support layer
MRHOF	Minimum Rank with Hysteresis Objective Function
MRPL	Modified Adaptive RPL
mRPL	mobility-enabled RPL
mRPL+	mobility-enabled RPL+
MSP	Mobility Support Points
MT	Mobility Timer
MT-RPL	Mobility Triggered-RPL
OF	Objective Function
OF0	Objective Function Zero
OFDE	Delay-Efficient Objective Function

OFE	Energy-based Objective Function
OS	Operating System
P2M	Point-to-Multipoint
P2P	Point-to-Point
PA	Proxy Agent
PAN	Personal Area Networks
PDR	Packet Delivery Ratio
PMIPv6	Proxy Mobile IPv6
PPN	Preferred Parent Node
RA	Router Advertisement
RWK	Random Walk
RWP	Random Waypoint
RD	Remaining Distance
RE	Residual Energy
Reverse-RPL	Reverse trickle algorithm based RPL
RFC	Request For Comments
RFD	Reduced Function Device
RL-RPL	Reinforcement Learning based RPL
ROLL	Routing Over Low power and Lossy Networks
RPL	Routing Protocol for Low power and Lossy Networks
RPL-VANET	RPL tuning in VANET
RSSI	Received Signal Strength Indicator
S-AODV	Sink Routing Table over AODV
SH-WSN6	Soft Handover for mobile WSNs
SLMA	Sensor Local Mobility Anchor
SMAG	Sensor Mobile Access Gateway
SMH	Seamless Mobility Handover
SPMIPv6	Sensor Proxy Mobile IPv6
SRPL	Standard RPL
TTL	Time to Live
UDGM	Unit Disk Graph Model
UDP	User Datagram Protocol
VANET	Vehicular Networks
WPAN	Wireless Personal Area Network
WSN	Wireless Sensor Networks



# Chapter 1

## Introduction

It is estimated that there will be 40 to 50 billion devices connecting to the Internet in the near future. Connecting such a massive number of devices to the Internet will be a difficult and challenging task (Atzori et al. (2010)). A new technology domain, namely, the Internet of Things (IoT), is emerging to provide the solution with the aim of connecting things around the world (Sundmaeker et al. (2010)). The focus in IoT is on two parts, Internet, which offers to the global network infrastructure with configurable and scalable capabilities with standard communication protocols, while things refer to physical devices or virtual objects, which have physical attributes, virtual personalities and identities, and use smart interfaces. IoT essentially connects things to provide useful information of the surrounding environment through the Internet (Atzori et al. (2010)).

Wireless Sensor Networks (WSN) is an important component of IoT where the sensor nodes collect information of the surrounding environment and contextual information, which it then sends over the Internet on behalf of the user. To attain a pervasive or ubiquitous computing environment, the sensor nodes must be enabled with Internet Protocol (IP) based networks (Rodrigues & Neves (2010)). The enablement of IP in sensor nodes would boost the management and sharing of distributed resources. However, sensor nodes are characterized by low computing, power constraints, low memory, and reduced radio coverage, hence adding an IP protocol to these constrained nodes is a challenging task (Dunkels et al. (2003)).

Initially, it was considered that the IP protocol was too heavy to implement in resource constrained devices. Nevertheless, advances in technology helped reconsider the misunderstanding about IP protocol usage over resource constrained devices (Hui & Culler (2008); Durvy et al. (2008)). The Internet Engineering Task Force (IETF) defined Internet Protocol version 6 (IPv6) over Low-Power Wireless Personal Area Networks (6LoWPAN) and IPv6 Routing Protocol for Low power and Lossy Networks (RPL) (Winter et al. (2012)) standards allowing the sensor node to have IPv6 addresses to connect to the Internet. The 6LoWPAN network comprises of sensor nodes, which are compliant to the IEEE 802.15.4 standard. The RPL is the default standard for routing packets over 6LoWPAN network.



## 1.1 DETAILS OF IEEE 802.15.4 STANDARD

The IEEE 802.15.4 is one of the popular standard for WSN ([Singh et al. \(2008\)](#)) that defines physical and Media Access Control (MAC) layer standards. The physical layer defines three modes of operations: (i) 868 MHz with data rate of 20 Kbps, (ii) 915 MHz with data rate of 40 Kbps, and (iii) 2.4 Gz (direct sequence spread spectrum) with data rate of 250 Kbps. To access the radio channel, it uses the Carrier Sense Multiple Access with Collision Avoidance protocol. Each device in the Wireless Personal Area Network (WPAN) can be identified by a unique 64-bit IEEE address similar to the ethernet network interface card address or the 16-bit short address allocated during the registration process. The length of the frame is restricted to 127 octets due to limited buffering capabilities and use of low power wireless links for communication. In WPAN, two types of nodes are defined, namely, the Full-Function Device (FFD) and the Reduced-Function Device (RFD). The FFD devices are capable of routing/forwarding data, can interact with other FFDs, and can assign a short address to the RFDs. The RFD has limited functionality compared with the FFD, which has minimal resources and low memory capabilities. The RFD can immediately and only connect and send its physical measurements to a single FFD.

A Personal Area Network (PAN) consists of a PAN coordinator, FFDs, and RFDs. The PAN coordinator is responsible for setting up and managing the PAN. It has overall information of the network and assigns a unique PAN ID for each PAN by listening to other networks. The PAN coordinator selects a radio frequency within which the network operates. The devices in the PAN scan for the channel in which the coordinator is operating and send a request to join the network. The PAN coordinator can assign 16 bit short address for the devices, if it accepts the request ([Adams \(2006\)](#)).

## 1.2 DETAILS OF IPv6 OVER LOW-POWER WIRELESS PERSONAL AREA NETWORKS

The IETF defined 6LoWPAN standard that allows a sensor node to have IPv6 addresses and connect to the Internet. It comprises of sensor nodes, which are compliant with the IEEE 802.15.4 standard. An adaptation layer is added between the data link-layer and the network layer to support the IPv6 protocol over the IEEE 802.15.4 standard as shown in [Figure 1.1](#). The 6LoWPAN adaptation layer has been defined in Request for

<b>Application Layer</b>	
<b>UDP</b>	<b>ICMP</b>
<b>IPv6 Network Layer</b>	
<b>6LoWPAN Adaptation Layer</b>	
<b>IEEE 802.15.4 MAC Layer</b>	
<b>IEEE 802.15.4 PHY Layer</b>	

Figure 1.1: Protocol Stack for 6LoWPAN ([Chen et al. \(2014\)](#))

Comments (RFC) 4919 ([Kushalnagar et al. \(2007\)](#)) and RFC 4944 ([Mulligan \(2007\)](#)). The 6LoWPAN goals, assumptions, and problem statement are described in RFC 4919 and RFC 4944 that defines the frame format of transmission of IPv6 packets, procedure for the IPv6 auto configuration, link local address, IPv6 header compression, fragmentation, reassembly, and delivery of a frame to the IEEE 802.15.4 link layer. The WSN is a subtype of 6LoWPAN, where the nodes are of low cost, low power, small size, etc., and which are developed to perform sensing and/or controlling physical parameters of the surrounding environment. Some of the salient features of the 6LoWPAN are as follows:

- At the physical layer, maximum allowable packet size is 127 octets supporting a 102 octets size in the MAC layer. The security at the link layer adds 21 octets of overhead resulting in 81 octets for data payload at the MAC layer.
- Support for both the IEEE 64-bit extended address and the 16-bit short address.
- Data rates of 20 Kbps (868 MHz), 40 Kbps (915 MHz), and 250 Kbps (2.4 GHz) for each of the presently defined physical layers.
- Normally all RFDs work on battery power.
- A large number of devices are expected to be deployed in during the network lifetime.
- The location of the devices are typically not fixed and may vary from time to time (mobile in nature).

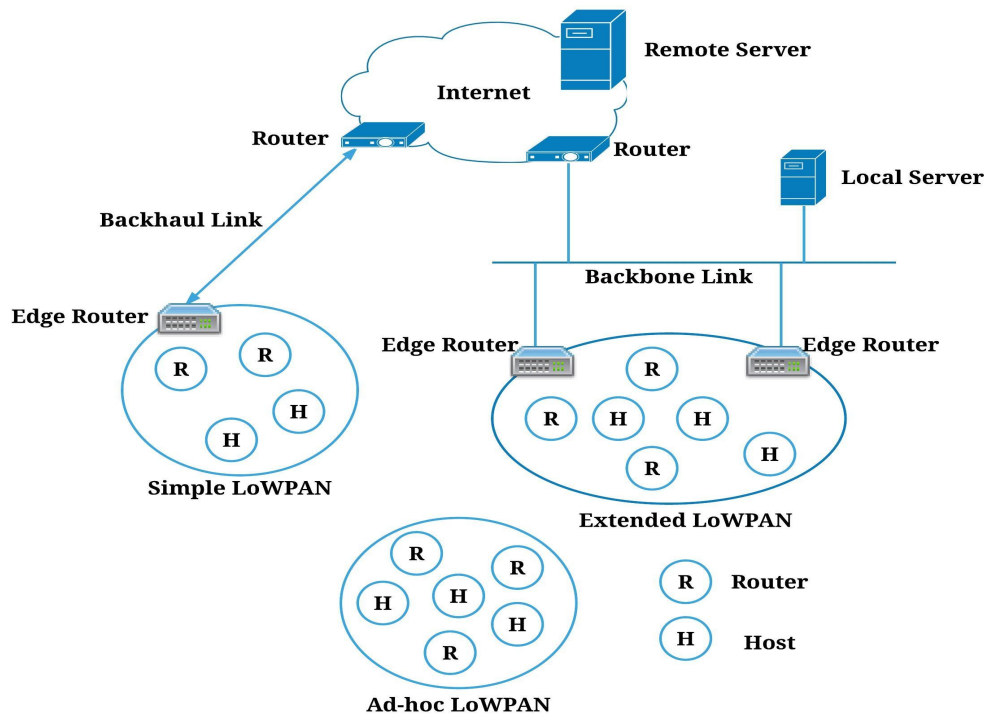


Figure 1.2: 6LoWPAN Architecture (Shelby & Bormann (2011))

Generally, the 6LoWPAN network is connected with the Internet through the Edge Router (ER), so all the packets are forwarded and received through the ER. The 6LoWPAN network is classified into three different types as Simple LoWPANs, Extended LoWPANs, and Ad hoc LoWPANs as shown in Figure 1.2. A Simple LoWPAN is connected to another IP network through an ER. An Extended LoWPAN consists of multiple ERs, which are connected to the backbone network. In the case of Ad-hoc LoWPAN network, the nodes operate themselves without any ER, but it is not connected to the Internet.

### 1.3 LOW POWER ROUTING PROTOCOLS OVER 6LoWPAN

To enable routing over the 6LoWPAN, few attempts were made to develop a lightweight protocol for resource constrained devices. These routing protocols were based on two routing schemes, viz., mesh-under and route-over schemes. In the mesh-under scheme, all the nodes in the network are considered to be reachable by sending a single IP datagram, since the forwarding of the datagram is performed at the data link layer or the 6LoWPAN adaptation layer, whereas in the route-over scheme, the decision of routing is taken at the network layer by considering each node as the IP router.

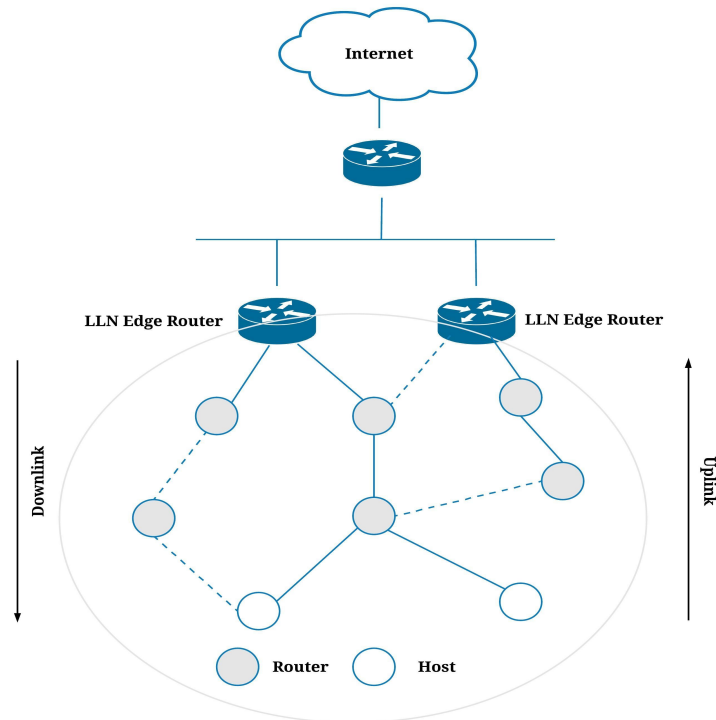


Figure 1.3: ROLL Architecture

In light of Ad-hoc On-Demand Distance Vector (AODV) protocol (Perkins et al. (2003)), the 6LoWPAN Ad-hoc On-demand Distance Vector Routing (LOAD) (Chang et al. (2010)), Sink Routing Table over AODV (S-AODV) (Cao & Lu (2010)), and Dynamic Mobile Ad-hoc Networks On-demand for 6LoWPAN (DYMO-Low) Routing (Kim et al. (2007)) are proposed. The LOAD is a variant of the AODV protocol in which the route is selected based on the link quality and the number of hops between the source and the destination node. Whereas, the S-AODV is optimized for the traffic that usually flows to the sink node, thereby reducing the traffic of route discovery by using the sink routing table. The Dynamic Mobile Ad-hoc Networks On-demand (DYMO) (Chakeres (2008)) protocol is a modified version of the AODV protocol operating on top of the IP layer. However, due to high resource utilization, the DYMO protocol has been revised and proposed as the DYMO-Low protocol. The DYMO-Low protocol that operates directly on the IEEE 802.15.4 link layer to reduce the power consumption of the node. To achieve scalability, a new Hierarchical routing (HiLow) (Kim (2005)) protocol was proposed. In HiLow, the node decides to become a coordinator, if it does not find any coordinator in its personal operating space and assigns a short address 0, otherwise it joins the coordinator, and a new short address is assigned by the coordinator.

Table 1.1: Comparison of routing protocols for 6LoWPAN

Protocol	Energy	Routing scheme	Routing approach	Local re-pair	Scalability	Memory usage	Mobility
AODV (Perkins et al. (2003))	High	Not applicable	Reactive	Yes	Low	High	Mobile
LOAD (Chang et al. (2010))	Low	Router-over	Reactive	Yes	Low	Medium	Mobile
S-AODV (Cao & Lu (2010))	Low	Mesh-under	Reactive	No	Low	Medium	Static
DYMO-low (Kim et al. (2007))	Low	Mesh-under	Reactive	No	Low	Medium	Mobile
HiLow (Kim (2005))	Low	Router-over	Hierarchical	No	High	Low	Static
RPL (Winter et al. (2012))	Low	Router-over	Proactive	Yes	High	Low	Static

Nevertheless, the protocols did not perform better in Low power and Lossy Networks (LLN), therefore, a new protocol that meets the requirements of LLN was required. In 2008, the IETF created a Routing over Low power and Lossy Networks (ROLL) working group to develop an efficient routing protocol that operates on 6LoWPAN adaptation layer. The ROLL working group standardized the RPL protocol and released the RFC 6550 for RPL in 2012. Figure 1.3 shows the ROLL architecture for the RPL. Table 1.1 shows the comparison of low power routing protocols designed for 6LoWPAN networks.

## 1.4 BACKGROUND OF RPL

### 1.4.1 Characteristics of Low power Lossy Networks

The ROLL working group mainly designed the RPL to operate in the LLN. The LLN exhibited certain unique features that the routing protocol had to consider for successful operation. The main features of the LLN depicted in RFC 6550 are as follows:

1. The LLN consists of thousands of nodes that are resource constrained in terms of memory, limited processing capability, and power as most of the nodes are battery operated.
2. The constrained nodes are operating in the lossy networks that normally consist

of lossy links that support low data rates.

3. The LLN supports different traffic flows, Multipoint-to-Point (M2P), Point-to-Multipoint (P2M), and Point-to-Point (P2P).

The ROLL workgroup also published several key requirements by taking several example applications. Some of the crucial industrial requirements [Pister et al. \(2009\)](#) for routing in LLN are presented as follows:

- **Traffic Support:** The routing protocol for LLN must have the potential to support periodic data, event data, and to transfer the bulk of data in multiple packets.
- **Reliability:** It must be able to deliver packets within a bounded latency, while ensuring correct data, and also guaranteeing maximum disruption time mandating upper bound for route maintenance.
- **Device-Aware:** Since most of the nodes are battery operated, they have to take into account long-term and short-term energy consideration, and hence, the protocol must ensure minimum energy consumption.
- **Protocol Performance:** It must be able to converge and establish connectivity to the newly added node within a time frame. It must also ensure route computation before selecting a path to the destination.
- **Mobility Support:** It must support the network dynamics that arise due to node changing its position and ensure mobile node connectivity to the network within a few seconds.
- **Security:** Routing protocol must be secured so that it is not manipulated by unauthenticated nodes and ensure that the attackers do not affect the routing performance.

#### 1.4.2 Overview of IPv6 Routing Protocol for Low power and Lossy Networks

To meet the requirements of the LLN, the IETF has standardized the RPL protocol. The RPL is designed specially to route packets over a network that has the characteristics of a lossy nature and consists of resource constraint devices. It is a distance-based gradient routing protocol, which constructs a Destination-Oriented Directed Acyclic

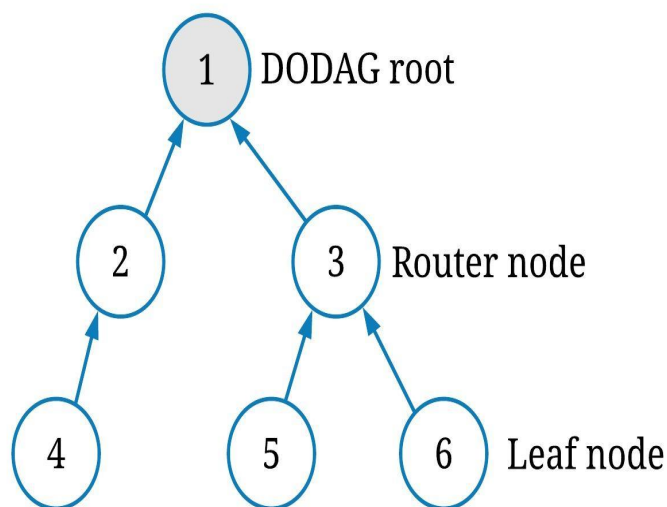


Figure 1.4: Example of DODAG tree

Graph (DODAG) tree on top of the physical network. The nodes in the DODAG tree are directed towards the DODAG root node that is connected to an external network. Figure 1.4 shows an example of the DODAG tree, which consists of three types of nodes that perform differently in the routing mechanism.

- **DODAG root:** It is responsible for creating a DODAG tree and collecting information from all the nodes in the tree topology. It is also responsible for connecting the LLN to the Internet.
- **Router node:** The router node associated with the DODAG tree in the RPL protocol is responsible for generating traffic and also for forwarding data packets to other nodes. It acts as an intermediate node between the DODAG root and the leaf node.
- **Leaf node:** The leaf node is the end node of the DODAG tree. It is only responsible for generating data traffic in the RPL protocol.

The RPL protocol uses different Internet Control Message Protocol version 6 (ICMPv6) messages to build and maintain the DODAG tree. The important control messages used in the RPL to build a DODAG tree are:

1. The DODAG Information Solicitation (DIS) message is a multicast message used to trigger a DODAG Information Object (DIO) message from its neighbouring nodes when the node is not a part of any DODAG.

2. The DIO message consists of crucial parameters to build a DODAG tree. Each node transmits a DIO message to inform its DODAG ID, rank, RPL Instance ID, and other parameters to join the DODAG tree and establishes a path towards the root node for its neighbours.
3. A Destination Advertisement Object (DAO) message is used to create a downward path from the DODAG root to the node. This message is transmitted when the nodes select their Preferred Parent Node (PPN). The PPN records the reverse route information, and in turn, send a DAO message to its PPN again, until it reaches the DODAG root.
4. A DAO-Acknowledgment is transmitted to acknowledge the receipt of a unicast DAO message.

The construction of the DODAG begins with the root sending necessary information like the RPL Instance ID and rank among others through the DIO message. The rank is a scalar value that specifies the relative distance to the root. Upon receiving the DIO message, the non-root node adds a sender of the DIO to its candidate parent list as the Candidate Parent Node (CPN). Then, the node selects its PPN among the CPNs based on the Objective Function (OF) to forward its traffic to the root node. Depending on the type of application, different routing metrics are used to define the OF. The RPL divides the network into multiple instances and forwards the traffic, based on the OF. The selection of the OF is critical for the success of the RPL protocol. The OF uses routing metrics and constraints for selection of an optimized path in the DODAG tree topology. The routing metrics can be based on link properties or node properties that are additive (but not necessarily) along the path to the root node. The RPL supports node metrics such as hop count, node state, node energy, etc., and link metrics such as throughput, latency, link reliability, etc. The RFC 6551 ([Vasseur et al. \(2012\)](#)) describes different routing metrics supported by the RPL. The standard OFs defined for the RPL are the Objective Function Zero (OF0) ([Thubert \(2012\)](#)), which is based on the hop count routing metric, and the Minimum Rank with Hysteresis Objective Function (MRHOF) ([Gnawali \(2012\)](#)), which is based on the Expected Transmission Count (ETX). The OF is advertised in the metric container of the DIO control message that is transmitted based on the trickle timer algorithm ([Levis et al. \(2004\)](#)).



The trickle timer algorithm is used in the RPL to achieve fast convergence and reduce the energy consumption of the nodes by reducing the transmission frequency of the DIO messages. It is based on “polite gossip” strategy to maintain and exchange the information with the neighbouring nodes. The main idea behind the algorithm is to transmit DIO messages more frequently, if the node information is not consistent with the neighbouring nodes, otherwise the DIO transmission frequency is reduced. The maximum interval time is given by  $I_{max} = I_{min} \times 2^{I_{double}}$ , where  $I_{min}$  is the minimum interval and  $I_{double}$  is the maximum time  $I_{min}$  value can be doubled.

## 1.5 MOBILITY IN INTERNET OF THINGS

Due to advancement in IoT technology, mobility support for the sensor nodes has become a fundamental requirement for many applications. In such applications, the sensor nodes are often carried by people or animals, mounted on moving vehicles, integrated with machines, etc. Numerous research works have been carried out considering the cooperation between fixed and mobile sensor nodes. In healthcare and medical applications, the patients are monitored continuously for their vital signs, diagnostics, and drug administration that are reported in real-time. In hazardous environments such as oil refineries, the vital signs of workers are collected continuously in order to monitor their health situation. There are also other reasons of mobility like physical movements due to network performance, changes in the radio channel, failure of the node, and sleep schedules (Oliveira et al. (2011)). Figure 1.5 shows an example of a Mobile Node (MN) within an RPL tree moving towards another Fixed Router Node (FRN).

## 1.6 MOTIVATION

As the number of applications of WSN is increasing day-by-day, there is an urgent need to connect the WSN to the Internet. In numerous applications, the data gathered by the sensor nodes are used for decision making, so there is a need for the data to be transferred over the Internet. Therefore, the 6LoWPAN was proposed for low power devices to use the IPv6 protocol to connect to the Internet. The RPL protocol, which is specifically designed for routing over 6LoWPAN, is capable of fulfilling the precise requirements of the WSN. One of the important features supported by the RPL is mobility management that allows the devices to connect to the Internet even when the devices are mobile. The mobility of the nodes can enlarge WSN applications, support communica-



Objective Function (OFDE), and MRHOF is carried out under different mobility models.

The OF supported by the standard RPL did not yield better performance since it used a single metric. Therefore, an OF based on Multimetrics (MMOF), which combines multiple routing metrics for FRNs and MNs, has been proposed. From the simulation results, it was observed that the proposed MMOF showed better performance compared to other chosen OFs of the RPL.

To improve the reliability, a Mobility Aware Routing Protocol for LLN (MARPL) that updates the PPN information soon after it receives the DIO message has been proposed. In MARPL, the MN is aware of its mobility and updates the PPN information without waiting for the route expiration time. To measure the effectiveness of the proposed MARPL, simulation works were carried out on a Contiki-based Cooja simulator for different mobility models. The obtained simulation results showed that the proposed MARPL performed better compared to the standard RPL for healthcare applications.

The Enhanced Routing Protocol for LLNs (ERPL) updates the PPN of the MN quickly whenever the MN moves away from the already selected PPN. Also, a new objective function that takes the mobility of the node into an account while selecting a PPN has been proposed. The performance of the ERPL was evaluated with varying system and traffic parameters under different topologies, similar to most real-life networks. The simulation results showed that the proposed ERPL reduced power consumption, packet overhead, and end-to-end latency and increased the Packet Delivery Ratio (PDR) compared with MRPL and SRPL protocols.

To prevent the MNs from selecting a PPN that is not in communication range, an Enhanced mobility routing protocol for wireless sensor network (EM-RPL) that incorporates modules to support the mobility of nodes has been proposed. The main goal of the EM-RPL is to increase network reliability and efficiency by selecting a route that is more stable and reduces the frequency of the route discovery process. The performance of the proposed EM-RPL was evaluated in the Contiki-based Cooja simulator and compared with the performance of other protocols that support mobility in the RPL. The simulation results demonstrated that the EM-RPL improved PDR and minimized power consumption by allowing the MNs to select a more stable path.

The fuzzy optimized routing metric with mobility support (FL-RPL) was proposed to enhance the performance of the RPL. The Fuzzy Inference System considers various routing metrics to pick a suitable candidate parent as the PPN to forward the data to the sink node. Further, timer functions were added to maintain consistent neighbours to support mobility and seamless connectivity. The FL-RPL was implemented and tested with different parameter settings for real-life scenario. The simulation results showed that the proposed solution increased PDR by approximately 12% while reducing power consumption by 20% compared with related works.

## **1.8 ORGANIZATION OF THE THESIS**

The remaining chapters of this dissertation are organized as follows:

Chapter 2 presents the existing works with respect to mobility support routing protocols for IoT. Basically, it highlights the literature review on 6LoWPAN and RPL that support node mobility in the network. Based on literature outcomes, it defines the problem statement and research objectives.

Chapter 3 scrutinizes the effect of OF under mobility by considering different mobility models. It compares the performance of the RPL that uses different OFs in terms of PDR, power consumption, and end-to-end latency by varying the number of MNs in the network. Further, a new OF was designed and implemented for FRNs and MNs by considering multiple routing metrics. It compares the performance of the proposed OF with the standard OFs and the OFs proposed in the literature.

Chapter 4 discusses the proposed mobility aware routing protocol that updates the PPN based on the DIO message from the neighbour nodes. The performance of the proposed technique is evaluated in terms of PDR, power consumption, and latency under different mobility models. Additionally, the simulations were carried by varying the density of the nodes in the network. Further, a new enhanced mobility aware routing protocol is discussed. The enhanced mobility protocol uses the OF for selecting the PPN based on node type along with a technique to update the PPN. Its performance is analyzed in random topology as well as grid topology with important evaluation metrics.

Chapter 5 discusses the proposed mobility support routing protocol using timer

functions for the LLN. At first, the proposed enhanced mobility protocol for WSN is discussed. Its performance is evaluated for elderly monitoring application and hospital environment monitoring application under different parameter settings. Then, the proposed protocol based on the fuzzy logic technique is discussed. Its performance is compared with related works in the literature in terms of PDR, power consumption, radio messages, and end-to-end delay.

Finally, Chapter 6 provides the conclusions on the entire thesis work and future directions.

## **1.9 SUMMARY**

This Chapter introduces routing protocols designed for lossy networks. It gives insight into the characteristics and challenges of the LLN. It gives an overview of the IEEE 802.15.4, 6LoWPAN, and RPL standards. This chapter also presents an outline of the contribution and structure of the thesis.

## Chapter 2

# Literature Survey

This Chapter highlights previous works regarding mobility support protocols related to 6LoWPAN and RPL. These protocols are classified on the basis of route-over and mesh-under mechanisms. The route-over protocols are classified on the basis of Additional Layer, modifying the trickle algorithm, predicting MN movement, and Other Mechanisms. The mesh-under protocols are classified based on the support for Single Hop and Multi-Hop communication. Figure 2.1 shows the organization of the mobility management protocols for the LLN. The performances of these protocols are evaluated with respect to packet overhead, handover delay, end-to-end delay, and PDR.

### 2.1 LITERATURE REVIEW ON MOBILITY IN 6LoWPAN

Routing protocols that are designed to support the mobility of the nodes over the mesh-under are classified into two categories as Single Hop communication and Multi-Hop communication.

#### 2.1.1 Mobility Support for Single Hop Communication in 6LoWPAN

Mobility support protocols that are proposed for the 6LoWPAN using Single Hop communication work with the router in one hop communication. Protocols such as Hospital Wireless Sensor Network (HWSN6), Sensor Proxy Mobile IPv6 (SPMIPv6), Cluster-based Proxy Mobile IPv6 (CSPMIPv6), Inter-Mario, and Soft Handover for mobile WSNs (SH-WSN6) are identified as Single Hop communication protocols.

Jara et al. (2009) proposed an HWSN6 protocol that was suitable for a hospital scenario. The idea was to use a fixed IPv6 address to avoid registering Care of Address (CoA) when the mobile node visited another network thus, reducing signalling cost that occurred during the registration of the CoA to its home agent. It utilized nodes with high resources such as sink nodes and gateways to exchange control messages on behalf of the MN. Further, it provided security to protect the patient's private information. However, the protocol depended on the beacon messages that were sent periodically by the Foreign Agent (FA) for movement detection, and thereby, increased the delay. Additionally, the route optimization between the MN and the home network was not

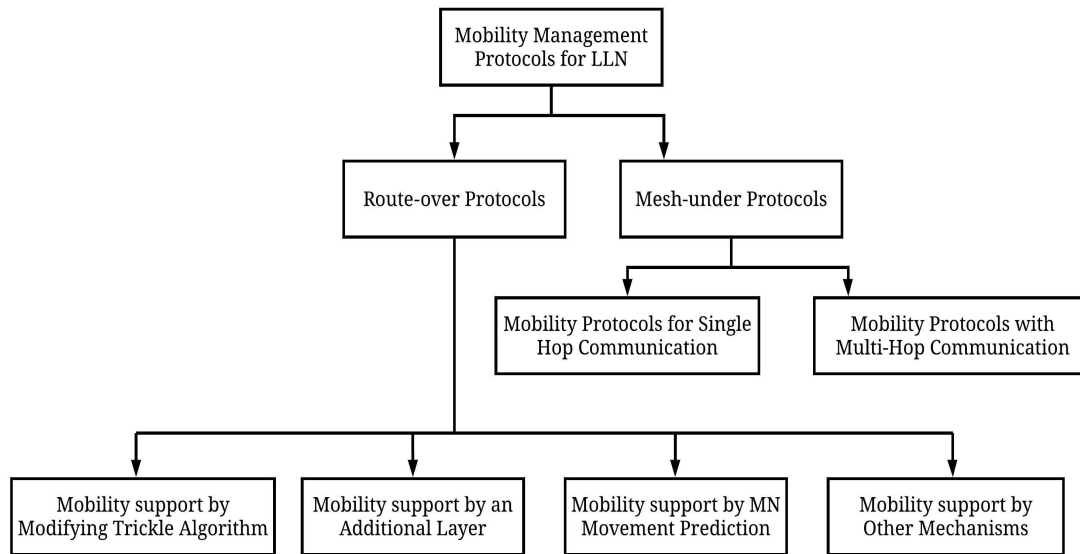


Figure 2.1: Classification of Mobility Management Protocols for LLN

considered, which increased the end-to-end delay.

Similarly, [Islam et al. \(2010\)](#) proposed a protocol to monitor a patient's status in a hospital and named it SPMIPv6. It was an enhanced version of the Proxy Mobile IPv6 (PMIPv6) designed to support localized mobility, especially focusing on energy efficiency. The entity Sensor Local Mobility Anchor (SLMA) was responsible for maintaining accessibility to the sensor node even when the node was mobile. It maintained the Sensor Mobile Access Gateway (SMAG) information table, binding cache entry, and performed encapsulation and decapsulation. It reduced the message required for MN registration by incorporating the Authorization, Authentication and Accounting (AAA) service. Another important entity in the network was SMAG, which detected the movement of the MN and initiated exchange of signalling messages with the SLMA, instead of the MN. The SPMIPv6 performed better compared with the Mobile IPv6 (MIPv6) and PMIPv6 in terms of signalling cost and transmission cost. The SPMIPv6 still suffered from handoff latency, single point failure, and Local Mobility Anchor (LMA) overhead.

To overcome the limitations of the SPMIPv6, [Jabir et al. \(2012\)](#) proposed a new protocol named the Cluster Sensor PMIPv6 (CSPMIPv6). This protocol enhanced the architecture of the SPMIPv6 by grouping the Mobile Access Gateways (MAGs). Each group was maintained and controlled by a cluster head (HMAG), which was selected

during installation and configuration. The primary purpose of the MAG and LMA was like the SPMIPv6, that is, to provide accessibility to the MNs, to detect node movement, and initiate mobility signalling. The advantage of adding HMAG was to reduce the overhead of LMA by maintaining local mobility management, providing route optimization for intra-cluster and inter-cluster interaction, and to reduce handoff latency. It also integrated the functions of the AAA services and thus, reduced the cost of the MN registration. However, adding an entity to the network increased the end-to-end delay, handoff latency, and also the protocol was not applicable for a large number of sensor nodes because of its static tree structure (Silva et al. (2014)).

Ha et al. (2010) proposed inter-MARIO to decrease the handover delay during the inter-PAN mobility. It followed the make-before-break approach, by making the partner node to act as an Access Point (AP). This node preconfigured future handover by predicting next location based on the movement detection algorithm using signal strength indicator of the MN, sent MN information to the neighbour PAN, and neighbour PAN information to the MN. As the configuration information was already known to the FA, it can send a surrogate binding update message to the home agent for MNs' handover, thus, reducing handover latency and data loss.

When an MN is in the range of multiple Access Points (APs), it is difficult for the MN to choose between multiple APs. Petajajarvi & Karvonen (2011) proposed soft handover technique (SH-WSN6) to address this challenge. The decision of joining the APs was achieved based on the connection quality comparison algorithm. The remote resource directory was proposed in the architecture, which maintained the information of the resources and interfaced to reach the MN. When an MN receives a Router Advertisement (RA) message, which is sent periodically by the AP, it checks whether the node is already registered with the AP or not, and if not, it sends a registration message to the AP. In this protocol, the MN was allowed to join multiple APs at the same time. Although it reduced unnecessary handover process and removed unreliable links, the protocol suffered from frequent transmission of RA, which increased the traffic load and energy consumption.

Table 2.1 summarizes the protocols that are discussed to support mobility for Single Hop communication in the 6LoWPAN.



Table 2.1: Summary of Mobility Support Protocols for Single Hop communication in 6LoWPAN

Authors	Protocol	Mobility Support	Remarks
Jara et al. (2009)	HWSN6	Mobility supports for hospital scenario	Fixed Global IPv6 address
Islam et al. (2010)	SPMIPv6	SLMA was responsible for maintaining accessibility	Single point of failure
Jabir et al. (2012)	CSPMIPv6	Grouping of LMA into clusters	Reduced registration cost
Ha et al. (2010)	Inter-MARIO	Prediction based on movement detection	Signaling overhead by the partner node
Petajajarvi & Karvonen (2011)	SH-WSN6	The choice for selecting AP if multiple APs are present is done based on connection quality comparison algorithm	Frequent transmission of RA messages

### 2.1.2 Mobility Support for Multi-Hop Communication in 6LoWPAN

In the 6LoWPAN, the nodes have limited communication range and consume significant amount of energy to interact with the ER. Researchers have proposed Multi-Hop communication protocols for the 6LoWPAN networks to minimize power consumption in transmitting the packets to the ER, especially, when a node moves away from the ER.

Network-based Intra-PAN mobility scheme for 6LoWPAN named, LoWMob was proposed (Bag et al. (2009)) to support Multi-Hop communication. In LoWMob, the static nodes of the inter-PAN area are responsible to forward the packets from the MN to/from the ER. LoWMob adds mobility support at the adaptation layer so as to reduce the signalling cost of the static nodes. This new adaptation layer supports mobility packet formats such as `join_request`, `association_request`, `new_node`, and location update packets. Also, the protocol proposed a Distributed version LoWMob named DLoWMob, which included Mobility Support Points (MSP) to disperse the traffic concentrated at the gateways and to provide an efficient path between the source and the destination in the 6LoWPAN. Moreover, the protocol discussed security considerations. However, the LoWMob was suitable only for Intra-PAN mobility scenario.

Multi-hop based inter-PAN mobility was proposed with the objective to move all mobility related tasks to PAN devices (Bag et al. (2008)). It provided mobility support at the adaptation layer in order to reduce the number of bits transmitted across the

wireless link by the PAN devices. It also provided additional information regarding the surrounding PANs to the border nodes to reduce the handover time. The performance depended on the signalling cost subjected to provide mobility in the network. The results were compared with the Hierarchical Mobile IPv6, and it was observed that the proposed method required less number of bits when the speed and packet entry rate of the MN was increased. Based on a similar concept, a network assisted mobility for 6LoWPAN was proposed [Bag et al. \(2009\)](#). The idea was to reduce the signalling cost during registration of a new address by using a fixed address for the MN. It predicted future MN location and buffered the packets in order to reduce packet loss. Although the node did not change its position, it periodically sent location update message, which resulted in energy consumption.

FFDs are considered as more powerful devices with high resources compared with the MN. [Zinonos & Vassiliou \(2010\)](#) proposed an inter-mobility support protocol for the 6LoWPAN Networks in which the FFDs were responsible for providing mobility support for the MN by acting as Proxy Agents (PAs). These PAs suggested that the MN should join new proxy devices for better performance as and when required. The PA reduced handoff delay and packet loss either by predicting or by speedily responding to the handover event using the link layer information. Another mobility paradigm that uses PA was proposed, namely, the Mobile IP-Based Protocol for Wireless Personal Area Networks in Critical Environments ([Jara et al. \(2011\)](#)). The PA was mainly responsible for movement direction detection and guaranteed low latency during hand-off. Additionally, it could perform authentication related operations. In case of correct prediction, the handover delay was reduced significantly, whereas in the case of wrong prediction, the handover delay was more.

[Kim et al. \(2012\)](#) proposed a 6LoWPAN sensor node mobility scheme based on the PMIPv6 in which the PMIPv6 could detect the PAN attachment of the MN so as to support Multi-Hop communication. In this scheme, the MN actively scanned the available channels and determined whether it had moved out of its current PAN. The RA notified the current point of the attachment of MN to the gateway. The performance of the node mobility scheme was affected due to the maximum load on the gateway. A protocol proposed by authors [Teo et al. \(2015\)](#) also supported Multi-Hop communication based on the PMIPv6. The main idea was to maintain the route trace table at each FFD, which

Table 2.2: Summary of Mobility Support Protocols for Multi-Hop communication in 6LoWPAN

Authors	Protocol Name	Mobility Support	Remarks
<a href="#">Bag et al. (2009)</a>	LowMob	Support for mobility packet formats.	Support only for Intra-PAN mobility.
<a href="#">Ha et al. (2010)</a>	Inter-PAN	PAN devices support for inter-mobility.	Overhead to inform all other PAN devices.
<a href="#">Bag et al. (2009)</a>	Inter-PAN Network Assisted Mobility Protocol	Predicts future MN location.	Location update message has to be sent even the node does not change location.
<a href="#">Zinonos &amp; Vassiliou (2010)</a>	Inter-Mobility	Proxy agents are responsible for supporting mobility.	Communication between the old proxy and new proxy node consume energy.
<a href="#">Jara et al. (2011)</a>	Mobile IP based Protocol	Intra mobility is supported by GinMAC.	High handoff latency in case of wrong prediction.
<a href="#">Kim et al. (2012)</a>	Node Mobility based on PMIPv6	Gateway handles mobility related signaling.	The MN sends a frequent beacon message which consumes significant energy of the MN.
<a href="#">Chen et al. (2014)</a>	Enhanced Group Mobility	Modified RS and RA to carry necessary of all the nodes in the group.	Selection of coordinator sensor node was not discussed.
<a href="#">Ha et al. (2017)</a>	Intra-MARIO	Predicts link disconnection based on the RSSI value.	Polling consume significant energy.

had information about the previous source address, so that it was easy to route a reply from the other side. However, the protocol suffered from round trip delay. In ([Chen et al. \(2014\)](#)), the PMIPv6 supports for group mobility for 6LoWPAN that reduces the number of control messages. The RA and router solicitation were modified to carry the required information of all the nodes in the group in one message to further reduce the handoff delay. The protocol did not discuss the selection of the coordinator for the group of nodes. Further, scanning for an available channel consumed the energy of the sensor node.

To support the 6LoWPAN characteristics and adapt to 6LoWPAN architecture, ([Wang et al. \(2012\)](#)) proposed mobility support protocol for 6LoWPAN. In this protocol, the cluster tree structure compatible with the IPv6 network was introduced. Due to the cluster tree, the IPv6 address could be compressed by reducing the size of the header

and reduced flooding by communicating only to the cluster head . Similarly, [Xiaonan & Hongbin \(2016\)](#) proposed a Seamless Mobility Handover (SMH) based on the hierarchical IPv6 address structure to reduce the handover cost and delay during mobility handover. The advantage of the address structure was that it was conducive to address the compression so that the header size could be reduced and the CoA did not need to be registered to the Home Address, thereby reducing control messages. However, the static nodes became a bottleneck for the operation of the network. Furthermore, the structure of the tree was not balanced, which increased the latency to reach from the leaf node to the root node. To support Intra-PAN, recently a fast mobility management protocol was proposed [Ha et al. \(2017\)](#). The MN movement was detected as per the adaptive polling based strategy on the basis of link quality estimation and predicted link status. After detecting the movement of the MN, a FastRejoin mechanism was used to reduce the handoff delay. However, the protocol required the MN to send frequent beacon messages.

Table 2.2 summarizes the discussion of mobility support protocols for Multi-Hop communication in the 6LoWPAN.

## **2.2 LITERATURE REVIEW ON MOBILITY IN RPL**

In literature, several works have been carried out on RPL to provide mobility support, which signified the importance of mobility support for the RPL. The proposed solutions were classified into four categories based on 1) Modifying the Trickle Algorithm, 2) Adding an Additional Layer, 3) MN Movement Prediction, and 4) Solutions based on Other Mechanisms.

### **2.2.1 Mobility Support by Modifying Trickle Timer Algorithm in RPL**

[Hong & Choi \(2011\)](#) proposed a protocol named DAG based Multi-path Routing (DMR) to provide robustness towards mobility, and also, to enhance the routing performance of the MNs. The main idea was to construct a DODAG by using link quality and maintain connectivity upon route failure, by using sibling nodes to forward the traffic. The sink node was responsible for constructing and maintaining the DODAG topology by broadcasting the necessary information through a DIO message. In DMR, a DODAG node recorded the sibling node information in the routing table so that the packets were

forwarded to the sink node in case of link failure. The performance of the DMR was analyzed by using the NS-2.34 simulator. In the simulation, the FRNs were deployed randomly, while the MN followed the random waypoint (RWP) mobility model to move across the simulation area.

Lee et al. (2012) proposed a fixed DIO timer with values ranging from  $I_{min}$  to  $I_{max}$  for Vehicular Networks (VANET) (RPL-VANET). The trickle timer was disabled to avoid transmissions of outdated DIO messages that did not match the current DODAG topology. The ETX probe messages were transmitted without any delay to support the MN to select an appropriate PPN. To prevent a loop in the network topology, parent ID was added to the DIO message. The MN discards any DIO message that matches its ID in the DIO message. With a large DIO timer, the packet overhead was reduced, but frequent disconnections were inevitable. The RPL-VANET protocol was analyzed using the Qualnet 4.5 simulator in which 10 nodes were separated by 250m and moving in a straight line of length 5000m. The speed of the MN was varied for 25mph, 45mph, and 65mph to analyze the behaviour of the RPL-VANET at higher speeds.

Tian et al. (2013) introduced a new metric based on geographical information along with a strategy for tuning the RPL (GI-RPL). The GI-RPL built a tiny DODAG based on the node distance in the forward direction and it selected the PPN based on the greedy algorithm. The DIO message was set to adapt to changing topology based on the velocity and radio range of the node. The radio range was divided into a neighbour region and process region, where the neighbour region was used for communicating with the neighbour nodes, and the process region was used for sensing the distance and direction of the MN. A node in the process region with forwarding direction remained active, while in the backward direction remained in sleep mode to save energy. The performance of the GI-RPL was analyzed using the Cooja simulator by considering evaluation metrics such as PDR, delay, and packet overhead. The MN was made to move in a straight road for 4200m in which 14 FRNs were separated by 300m. However, this strategy was suitable only for VANETs.

Cobârzan et al. (2014) proposed a reverse trickle algorithm to provide mobility support to the RPL (Reverse-RPL). It was based on the assumption that the MN stayed longer with a new PPN, and the more time it spent with the same PPN the more likely

it was to go away from that PPN. Therefore, the trickle algorithm started with the maximum time period to send DIO message and reduced the time period by half after sending a DIO message. The standard trickle algorithm was switched to reverse trickle algorithm when an MN joined the PPN. By contrast, the standard trickle algorithm was restored when the last MN left the PPN. The performance of the Reverse-RPL was analyzed using the WSNNet simulator, wherein the FRNs were deployed in a  $425m \times 425m$  simulation area in a grid fashion. The MNs were deployed in a random fashion and followed the Billiard linear trajectory and the random trajectory.

The authors [Gara et al. \(2016\)](#) modified the trickle timer to handle changes in the network topologies (MRPL). The main idea was to adjust the DIO message interval based on the distance and velocity of the node. To compute the distance, the node sent position information through control messages, and the distance was computed using the Euclidean distance formula. Further, a new OF by the combination of ETX and Received Signal Strength Indicator (RSSI) was used to select the PPN. The performance of the MRPL was analyzed using the Cooja simulator and considered evaluation metrics were overhead, average delay, average power consumption, and average PDR. The Tmote Sky node was used for simulation provided by the Contiki platform. The MN followed the RWP mobility model with speeds varying from 0 to 10 m/s. The simulation results showed that the proposed technique increased the PDR. However, the protocol required more control messages whenever the MN moved out of the PPN's communication range. Therefore, it suffered from delay in updating the PPN.

The authors [Park et al. \(2017\)](#) proposed a modified energy efficient RPL (E-RPL), where the velocity and the angle between the neighbour nodes and the MN were calculated for selecting the PPN. The distance was measured based on the RSSI value, while the speed and direction of the MN was determined based on the Doppler frequency of the received signal. The time interval between the solicitation messages was dynamically set based on distance and speed. However, the protocol experienced some delay in updating the PPN, whenever the MN moved out of the PPN's communication range. The performance of the E-RPL was analyzed using MATLAB. The simulations were performed by deploying the FRNs in the grid topology, random topology, and linear arrangements. Several experiments were carried out to analyze the performance by varying the speed of the MN with respect to packet loss rate, cumulative transfer count,

Table 2.3: Summary of Mobility Support Protocols by Modifying Trickle Algorithm in RPL

Authors	Protocol Name	Objective Function	Mobility Support	Remarks
<a href="#">Hong &amp; Choi (2011)</a>	DMR	LQI	Path redundancy	Support routing through sibling nodes
<a href="#">Lee et al. (2012)</a>	RPL-VANET	ETX	Fixed DIO timer	Frequent path failures
<a href="#">Tian et al. (2013)</a>	GI-RPL	Geographical information	Adaptive DIO period	Applicable for only VANET
<a href="#">Cobârzan et al. (2014)</a>	Reverse-RPL	ETX	Reverse Trickle algorithm	Performance reduces due to sudden movement
<a href="#">Gara et al. (2016)</a>	MRPL	ETX , RSSI	Adaptive DIO period	Delay in updating PPN
<a href="#">Park et al. (2017)</a>	E-RPL	ETX	Adaptive DIO period	Delay in updating PPN

and energy consumption.

Table 2.3 shows the summary of the mobility support protocols by the modifying trickle timer algorithm in the RPL.

### 2.2.2 Mobility Support by Adding an Additional layer in RPL

The authors [Cobârzan et al. \(2015\)](#) introduced a Mobility-Triggered RPL (MT-RPL) cross-layer between layers 2 and 3 to support mobility. It took advantage by linking the L2 triggers and the X-Machiavel ([Kuntz et al. \(2013\)](#)) preamble sampling MAC protocol. The X-Machiavel is a slightly modified version of the X-MAC preamble sampling MAC protocol. The X-Machiavel protocol alters the behaviour of the X-MAC to support MN transmissions in both idle and busy channels. In the idle channel, the static nodes forward the MN packets opportunistically, while in the busy channel, the MN takes possession of a reserved medium for transmission of its packets. The RPL registers an L2 trigger and use channel stealing or opportunistic forwarder by the X-Machiavel protocol. The rank of the node is included in the layer 2 header so that the node can decide to act as an opportunistic forwarder or take possession of a reserved medium for an ongoing communication. The MT-RPL was evaluated in the WSNNet simulator, where the FRNs were deployed in the grid topology and the random topology. The MNs followed the Billiard random trajectory across the  $100m \times 100m$  simulation area. The performance of the MT-RPL was evaluated in terms of the number

Table 2.4: Summary of Mobility Support Protocols by Adding an Additional Layer in RPL

Authors	Protocol Name	Objective Function	Mobility Support	Remarks
<a href="#">Cobârzan et al. (2015)</a>	MT-RPL	ETX	Cross-layer implementation	High packet overhead
<a href="#">Ko &amp; Chang (2015)</a>	MoMoRo	ETX, LQI, RSSI	Link estimation using fuzzy logic	High packet overhead

of control messages and energy consumption.

The authors [Ko & Chang \(2015\)](#) introduced a mobility support layer (MoMoRo) to the existing RPL. The main goal of the MoMoRo layer was to re-establish bidirectional routes between the nodes when the routes were affected by mobility. In order to do that, the MoMoRo sent probe messages once it identified disconnectivity in the network. The MoMoRo used link quality estimators such as ETX, RSSI, and symbol error rate variance to identify change in the channel environment. Link quality estimation was given to the fuzzy logic estimator to ascertain good quality links. Additionally, an adaptive scheme was proposed to determine the threshold values for the fuzzy sets. The MoMoRo was evaluated in the test bed by deploying the Tmote Sky nodes in an office building. The simulation results were analyzed with respect to end-to-end packet reception ratio, packets overhead, and end-to-end number of transmission for static network, a combination of static nodes and mobile nodes, and fully mobile network. Adding an additional layer increased packet overhead, which in turn, increased the power consumption of the sensor nodes.

Table 2.4 shows the summary of the mobility support protocols by adding an Additional Layer in the RPL.

### 2.2.3 Mobility Support by Mobile Node Movement Prediction in RPL

The authors [Soma et al. \(2016\)](#) proposed a new strategy using the Bayesian mobility prediction technique to provide mobility support for the WSN (BMP-RPL). A new stability metric was proposed using the prediction model to build links according to topology changes. In the BMP-RPL, a node learns about its neighbours after collecting hello beacons from them, and then it calculates neighbour distribution using the Gaussian law based on mean and standard deviation velocity that is advertised by the neighbour nodes. Based on the velocity and neighbor, the stability of the path is de-



terminated. The performance of the proposed technique was evaluated using the Cooja simulator. In the simulation, a fixed Cooja mote was deployed in the grid topology and the MNs followed RWP mobility model with a speed of 2m/s. The simulations were performed in two scenarios where the total number of nodes in the simulation varied such as 10, 15, 20, 25, 30, and 35. In the first scenario, 6 nodes were configured as MNs, while in the second scenario, 9 nodes were configured as MNs. The packet loss ratio and route stability were considered for evaluating the proposed techniques by comparing with other techniques.

The authors [Barcelo et al. \(2016\)](#) proposed a new strategy using the Kalman positioning to support mobility in the RPL (KP-RPL). In the KP-RPL, the MN discarded parents that could not be reached due to position errors and selected a PPN based on end-to-end ETX estimations obtained from the Kalman filter. The Kalman filter was used to predict and improve the accuracy of the MNs position by considering velocity estimates. Each node redefined the confidence region based on the Kalman filter and created a blacklist of nodes that were not reachable. The authors used the MATLAB for evaluation in which 100 anchor nodes were deployed in a square grid and an MN was made to move around the simulation area at a speed of 2m/s. The simulation results were evaluated with respect to PDR and average power consumption under different scenarios.

The authors [Bouaziz et al. \(2017b\)](#) used the extended Kalman filter to predict the non-linear movement of the MN (EKF-MRPL). The new PPN selection was based on the movement direction of the MN with the extended Kalman filter. The MN position was assessed accurately by using an extended Kalman filter on the RSSI values obtained from the trilateration method by considering the direction of the MN. The PPN was selected based on the nearest node in the direction of the movement. The performance of the EK-MRPL was evaluated using the Cooja simulator. Some fixed nodes were deployed in the grid fashion, where an MN moved around the simulation area at a speed of 2m/s in a non-linear movement trajectory based on the random walk (RWK) mobility model. The results were evaluated in terms of PDR, handover delay, energy consumption, and signalling cost. However, these models consumed significant power that reduced the network lifetime as the nodes had low processing capacity and low power.

Table 2.5: Summary of Mobility Support Protocols by MN Movement Prediction in RPL

Authors	Protocol Name	Objective Function	Mobility Support	Remarks
<a href="#">Soma et al. (2016)</a>	BMP-RPL	Stability metric	Mobility prediction using Bayesian model	Low responsiveness
<a href="#">Barcelo et al. (2016)</a>	KP-RPL	ETX, RSSI	Kalman positioning and blacklisting	High processing cost
<a href="#">Bouaziz et al. (2017b)</a>	EKF-MRPL	RSSI	Extended Kalman filter	High processing cost
<a href="#">Bouaziz et al. (2017a)</a>	EC-MRPL	RSSI	Mobility prediction using Burst of control messages	High packet overhead

The authors [Bouaziz et al. \(2017a\)](#) proposed an energy efficient and mobility aware routing protocol (EC-MRPL). The main idea was to predict a new attachment before the disconnection and to reduce the MN involvement for signalling the control messages to save energy. The PPN was responsible for the MN movement detection, transmission of data packets to/from the MN, and in finding a new PPN, if the connectivity to the MN degraded. The PPN was changed only after receiving confirmation of connection to a new PPN to increase the reliability of the data packets. The EC-MRPL was evaluated by using the Cooja simulator. The simulations results were evaluated in terms of PDR, power consumption, handover delay, and signalling cost.

Table 2.5 shows the summary of the protocols proposed to support mobility by Movement Prediction in the RPL.

#### 2.2.4 Mobility Support by Other Mechanisms in RPL

To increase route stability, [Korbi et al. \(2012\)](#) proposed a procedure that dynamically managed the DIS interval based on the number of PPN changes (ME-RPL). This approach allowed non-MNs to predict MN behaviour by assuming that an MN continues to remain inconsistent in the near future, if the MN was inconsistent for several past intervals. An MN continues to remain stable if it is showed few inconsistencies for several past intervals. Based on this assumption, the DIS interval was reduced to half if the node changed the PPN beyond the threshold UpDIS value. If the node changed the PPN below the threshold DownDIS value, then the DIS interval was increased by multiplying with 2. The performance of the ME-RPL was evaluated in the Cooja simulator

under linear and grid topology. The results were evaluated in terms of packet loss rate and route stability by considering different scenarios. It was found that the transmission of the DIS interval increased the packet overhead.

The authors [Gaddour et al. \(2014\)](#) proposed an extension to the standard RPL, which used the corona mechanism to support mobility (Co-RPL). The basic idea was to create coronas around the Directed Acyclic Graph (DAG) root, which allowed localization of the RPL routers in motion. The MN selected the PPN based on the corona ID and ranks of the parent nodes to prevent any loop in the network. The DIO Control messages were transmitted periodically by the DAG roots in order for the neighbours to update the routing path. On path failures, the MNs packets were forwarded to the neighbors until they found an alternate path through another parent node. The Co-RPL was evaluated using the Cooja simulator where the fixed nodes are randomly deployed in the simulation area. The simulation results were evaluated in terms of packet loss ratio, energy consumption, and average delay by varying the DODAG roots, packet transmission rate, and speed of the MN. However, even though the protocol increased the PDR, it consumed more power and increased control packet overhead in the network.

The authors [Gara et al. \(2015\)](#) proposed a methodology that focused on health and medicare applications (Mod-RPL). The body central units collected vital information from the patients and forward it to the sink node so that appropriate decisions could be taken at the appropriate time. The Mod-RPL allowed the continuous monitoring of patients, even when they were mobile. The main idea was to configure the MN as a leaf node, whereby it could operate differently compared with a fixed node. The fixed node operated as defined by the standard RPL. The performance of Mod-RPL was evaluated using the Cooja simulator. The simulation consisted of 39 Tmote sky nodes that were uniformly distributed in a bi-dimensional grid and about 20 nodes were configured as MNs with speeds varying from 0 to 2m/s. The PDR, power consumption, packet overhead, and delay were considered as evaluation metrics.

The authors [Fotouhi et al. \(2015\)](#) proposed a smart-hop mechanism (mRPL) to support mobility for the nodes. The main idea was to detect a good quality link by sending a burst of control messages and analyzing the quality of the link from the average of the received signal strength. Upon detecting a good quality link, the MN continued the data

transmission. If the quality of the link was below the threshold value, it entered into discovery phase while continuing data transmission to the PPN. In the discovery phase, the MN sends a burst of DIS control messages to its neighbours for selecting a better PPN. It compares the average RSSI value of the potential parents obtained from the DIO control message and compared with the threshold value and selects the PPN, if the value is higher than the threshold value. [Fotouhi et al. \(2017\)](#) proposed a new mechanism that guaranteed interoperability between a fixed node and the MN (mRPL+). In mRPL+, the MN selected a new PPN before disconnecting from the serving PPN. The mRPL+ proposed soft hand-off and hard hand-off for maintaining seamless connectivity in the network. The soft hand-off was initiated when a neighbour node observed good quality link by overhearing the packets of the MN in their vicinity. The proposed mRPL and mRPL+ were evaluated using the Cooja simulator. The MN followed a specific path in the simulation area with speeds ranging from 0.5 to 2m/s. However, the protocols were not efficient when the node changed its position suddenly.

The authors [Ancillotti et al. \(2017\)](#) proposed a link quality estimation strategy using the machine learning technique (RL-RPL). The quality of the link was monitored asynchronously and synchronously to increase responsiveness to changing network conditions. In asynchronous monitoring, reactive and proactive mechanisms were used to monitor the quality of the link based on the RSSI value and the ETX of the received packets from the neighbour nodes. The proactive mechanism was designed to anticipate topology changes, which were activated after successful transmission of the packet to the PPN, whereas the reactive mechanism was designed to handle unexpected network disruptions, which were activated after a transmission failure on a stable link. The simple moving average filter was used to estimate the quality of the link efficiently. In synchronous monitoring, the reinforcement learning technique was used to control active probe messages. The network was divided into multiple clusters and forwarded control probe messages based on cluster ID. The performance of the RL-RPL was evaluated in the Cooja simulator with evaluation metrics such as packet loss rate, energy consumption, and packet overhead.

The authors [Tahir et al. \(2018\)](#) proposed a Backpressure RPL (BRPL) to improve the throughput of the network by varying data traffic and node mobility. The BRPL used the QuickTheta algorithm to support data traffic dynamics, and the QuickBeta

algorithm to adjust network dynamics. The QuickTheta algorithm adjusted the traffic data dynamically based on network traffic congestion levels. An exponential weighted moving average was used to maintain the queue length. The QuickBeta algorithm was used to identify the mobility condition of the nodes by monitoring one-hop neighbours for a time. The QuickBeta algorithm can be tuned based on the mobility awareness of the nodes in the network. The performance of the BRPL was evaluated using the Cooja simulator for a mobile network, whereas for the static networks, real life IoT test bed experiments were conducted. Evaluation metrics such as packet loss rate, energy consumption, and communication overhead were used.

The authors [Kharrufa et al. \(2018\)](#) proposed a game-theory based mobile RPL (GTM-RPL) to improve the throughput of the MNs. The main idea of the proposed GTM-RPL was to control the transmission rate, timers, and operation mode using the Nash equilibrium to optimize its performance. A game model was designed by assuming that the MNs competed for the transmission of data to the sink node. Each action of the MN such as data rate, change in PPN, and trickle parameters that affected the performance of other nodes was considered. The GTM-RPL used the RSSI value and the link quality indicator to monitor the link quality cost in the game model. The GTM-RPL was evaluated in the Cooja simulator for hospital environmental monitoring and elderly monitoring applications. The Tmote sky nodes were deployed over the application area and the MNs were made to move around the simulation area based on the RWP mobility model with a speeds ranging from 0 to 2m/s.

Table 2.6 shows the summary of the protocols proposed to support mobility by Other Mechanisms in the RPL.

### **2.3 OUTCOME OF LITERATURE SURVEY**

It was observed from the literature that many mobility management protocols had proposed to support mobility in the 6LoWPAN (Section 2.1) as well as the RPL (Section 2.2) for IoT. As discussed in Section 2.1.1 supports of mobility in Single Hop communication in 6LoWPAN, most of the protocols were affected by single point failure, where the decision of the forwarding data takes place. Some protocols did not consider route optimization between the node and the home network because of which the performance of the protocols was affected drastically. Some protocols used a high number of con-

Table 2.6: Summary of Mobility Support Protocols by Other Mechanisms in RPL

Authors	Protocol Name	Objective Function	Mobility Support	Remarks
Korbi et al. (2012)	ME-RPL	ETX	Dynamic DIS interval	High packet overhead
Gaddour et al. (2014)	Co-RPL	ETX	Corona Mechanism	Drastically increases the control message overhead
Gara et al. (2015)	Mod-RPL	ETX	Modified RPL for healthcare	Delay in updating PPN
Fotouhi et al. (2015)	mRPL	RSSI	Immediate beaconing with hard hand-off	High energy consumption
Fotouhi et al. (2017)	mRPL+	RSSI	Immediate beaconing with hard and soft hand-off	High energy consumption
Ancillotti et al. (2017)	RL-RPL	LQE	Machine learning technique	High packet overhead
Tahir et al. (2018)	BRPL	ETX	Back pressure routing	Delay in updating PPN
Kharrufa et al. (2018)	GTM-RPL	LQI, RSSI	Game Theory	Low responsiveness

control messages that impacted on overhead, and also resulted in high energy consumption while increasing end-to-end delay. Additionally, such protocols did not perform accurately for a large number of nodes in the network. Section 2.1.2 discussed the various mobility support protocols that supported Multi-Hop communication in the 6LoWPAN. Some of the protocols provided mobility support for Intra-PAN, while some protocols supported Inter-PAN mobility in the network. Further, some protocols employed prediction technique to support mobility that predicted the MN location. However, their performance was affected due to frequent transmission of the control messages.

It was noted that the previous mobility solutions were based on the mesh-under, in Section 2.2, protocols provided mobility solution using the route-over approach. The protocols discussed in Section 2.2.1 modified the trickle timer algorithm to provide mobility support. The performance of these protocols did not improve much as they sent DIO messages based on the assumption that did not hold true for all situations. Further, the protocols did not discuss updating the PPN, when the MN changed its location. From the discussion carried out in Section 2.2.2, it was found that adding an additional layer increased packet overhead, which in turn increased power consump-

tion. Section 2.2.3 discussed related work that supported the mobility of the nodes by predicting the MN movement. However, the performance drastically reduced, if the MN suddenly changed its position. Finally, Section 2.2.4 discussed protocols that used different mechanisms such as machine learning technique, game theory based solution, and backpressure based techniques. However, these protocols did not consider all aspects of node characteristics and failed to achieve the requirements of low power networks.

From the literature survey, it was evident that most of the proposed solutions were evaluated using the Contiki-based Cooja simulator. The fixed nodes in the networks were deployed based on random or grid fashion, where the MNs moved around the simulation area based on the RWP or RWK mobility models with speeds ranging from 0 to 2m/s. It was observed that the Tmote Sky platform is popular among researchers. Further, to evaluate the performance of the protocols, evaluation metrics such as PDR, power consumption, signal overhead, and end-to-end delay were used.

### **2.3.1 Problem Statement**

In order to address these issues and challenges, the research problem is defined as, “To design and develop mobility management protocols for Low power and Lossy Networks and to measure the performance of the proposed protocols via simulation with important evaluation parameters”.

### **2.3.2 Research Objectives**

The research objectives are defined as:

- 1). To design and develop a Movement Detection or Movement Direction Detection Algorithm/Technique.
- 2). To design and develop a Preferred Parent Node update mechanism.
- 3). To simulate and verify the correctness of the proposed Mobility Management Protocols for Low power and Lossy Networks using a simulator with evaluation parameters namely end-to-end delay, PDR, and power consumption.

## **2.4 SUMMARY**

In this chapter, the existing state-of-the-art mobility support protocols based on Single Hop communication protocols and Multi-Hop communication protocols for 6LowPAN were discussed. Discussion about existing literature pertaining mobility support by Modifying the Trickle Algorithm, MN Movement Prediction, and by adding an Additional Layer were also carried out in this chapter. It also discussed the existing works with respect to Other Mechanisms to support mobility in the RPL. Finally, the problem definition and research objectives for designing a mobility support routing protocol for lossy networks was highlighted.



## Chapter 3

# Analysis of the Objective Function for the RPL under Mobility

The RPL is a fairly simple distance vector routing protocol. It constructs the DAG rooted towards one node usually, the DAG root using the OF. The RPL is designed to choose an optimized path to its destination based on the defined OF, while the OF uses a routing metric to construct the DAG. The OF can use any of the routing metrics like the ETX, hop count, remaining energy, end-to-end delay, RSSI, local traffic, etc. or a combination of any of these routing metrics. The choice of the OF plays a crucial role in obtaining better performance for the network scenario.

### 3.1 PERFORMANCE ANALYSIS OF RPL UNDER MOBILITY

In the present work, four different OFs were considered and implemented in the Contiki RPL to study the behaviour of the RPL in different mobility models. The primary goal of the simulation work is to ascertain which OF performs better in a mobile environment. As far as it was possible to ascertain, the absence of work focusing on different OFs with respect to mobile environment provided the motivation for the present work. The OFs considered were MRHOF ([Gnawali, 2012](#)), OF0 ([Thubert, 2012](#)), OFE ([Kamgueu et al., 2013](#)), and OFDE ([Gonizzi et al., 2013](#)). For the mobility models, Gauss-Markov (GM), RWK, and RWP mobility models were considered.

#### 3.1.1 Objective Function Zero

OF0 is the default OF for interoperability in the RPL. It does not use any routing metric to select the route towards the sink node, but uses the rank of the node to select the optimized route to the sink node. The hop count is used to measure rank of a node. The hop count is defined as the distance from the sensor node (sender) to the sink node in terms of intermediate sensor nodes (hops). The rank of the sink node is zero, which then increases with the scalar value (`step_of_rank`) down the link towards the leaf nodes.

### 3.1.2 Minimum Rank with Hysteresis Objective Function

The MRHOF was proposed by the ROLL working group and is the default OF used for the formation of the DAG in the RPL. It is based on incremental metric with the target to limit the routing metric, and by default, it uses the ETX as the link metric, which is the expected transmissions required by the node to accomplish the task of delivering the packet to its destination. It distinguishes the more reliable path that requires less number of packet transmissions. The value of ETX varies from one to infinity with one as 100 percent throughput and the throughput decreases as the ETX value increases. As per (Gnawali, 2012), the value of the ETX was calculated by measuring the probability that a packet reaches its neighbour ( $D_f$ ) successfully and the probability that an acknowledgment packet is successfully received ( $D_r$ ).

$$ETX = \frac{1}{D_f \times D_r} \quad (3.1)$$

The node calculates the path metric to reach the destination through each of its neighbour as per (Gnawali, 2012):

$$Pathcost = ETX(m) + MinPathcost(m) \quad (3.2)$$

Where,  $ETX(m)$  is the  $ETX$  value for the neighbour  $m$  and  $MinPathcost(m)$  is the advertised  $ETX$  value of neighbour  $m$ . The node selects the neighbour node with minimum  $Pathcost$  as its PPN. The MRHOF also uses the minimum hysteresis to decrease churn in response to small variations in the routing metric.

### 3.1.3 Energy based Objective Function

Since energy is considered as an important parameter in WSN, the authors Kamgueu et al. (2013) proposed an OF by considering the nodes' remaining energy as the routing metric in the RPL. In Equation (3.3),  $PW_i$  represents the path cost of the  $i^{th}$  node to the sink node. The path cost of the  $i^{th}$  node is the minimum path cost between the PPN and its own energy. The sink node sets the value as  $MAX_{energy}$ . The node selects a neighbour that advertises the highest path cost value as a parent. As per (Kamgueu

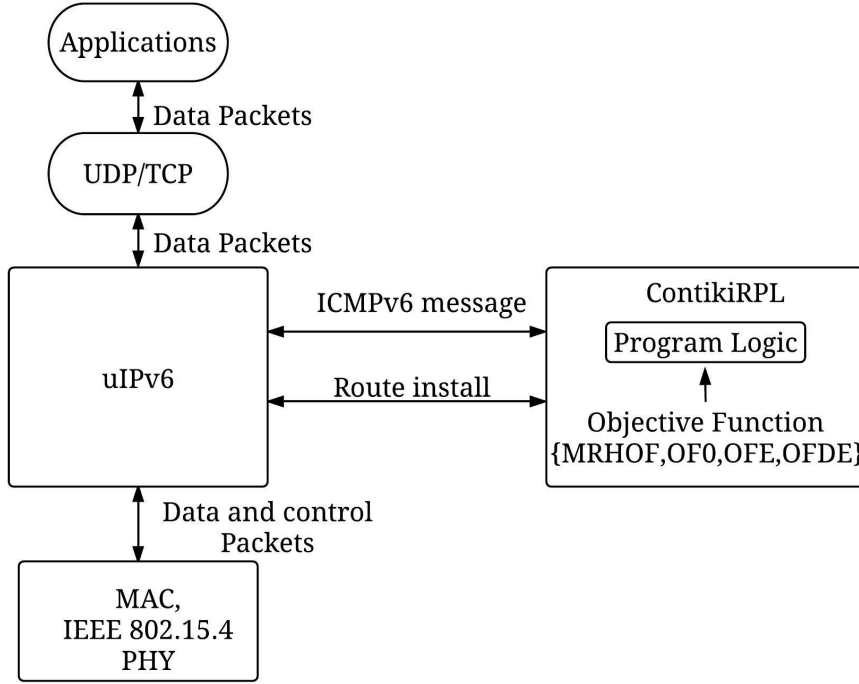


Figure 3.1: Modified RPL in Contiki Operating System

et al., 2013), the path cost is calculated as:

$$PW_i = \min[\max_{j \in N_i}(PW_j), E_i] \quad (3.3)$$

Where,  $N_i$  is the set of neighbours towards the sink node, and  $E_i$  represents the energy of the  $i^{th}$  node.

### 3.1.4 Delay Efficient Objective Function

The authors [Gonizzi et al. \(2013\)](#) proposed a routing metric to minimize average delay to reach the sink node. The routing metric is defined as the cumulative sum of delay at every hop along the route towards the sink node. The node chooses its PPN from its neighbours with minimum sum of average delay advertised by a neighbour node along with delay to reach that neighbour node. As per ([Gonizzi et al., 2013](#)), it can be expressed as:

$$Average\_Delay = Average\_Delay_i + D_f \quad (3.4)$$

Where,  $Average\_Delay_i$  is the delay announced by the  $i^{th}$  neighbour node,  $D_f$  indicates the forwarding latency between the node and its  $i^{th}$  neighbour node.

### 3.1.5 Modified RPL in Contiki Operating System

Figure 3.1 shows the modified RPL in the Contiki operating system; the program logic uses an OF defined by the application to choose a PPN among its neighbour nodes. The Algorithm 1 shows the generalized pseudocode to select the PPN among the neighbour nodes.

---

**Algorithm 1:** Preferred Parent ()

---

**Input** : NeighborTable of C  
**Output**: PreferredParent of C

- 1 Initialize: *MAX\_METRIC*
- 2 *PreferredParent* = *NULL*
- 3 **for** *c* in *NeighborTable* **do**
- 4     **if** *c.metric* < *MAX\_METRIC* **then**
- 5         *MAX\_METRIC* = *c.metric*
- 6         *PreferredParent* = *c*
- 7 **if** *PreferredParent* = *NULL* **then**
- 8     send(DODAG Information Solicitation message)
- 9 **else**
- 10    send(*PreferredParent*)

---

### 3.1.6 Simulation Environment and Parameters

The Cooja simulator provided by the Instant Contiki 2.6 (Jevtić et al., 2009; Dunkels, 2012), a well-known simulator for IoT and is also called as the cross-level emulator. It operates on the Contiki Operating System (OS), which is a lightweight open source OS running on the sensor nodes. It supports standards like IPv6, 6LoWPAN, RPL, etc. to provide low power communications. To simulate the lossy behaviour of the network, in the present work, the Unit Disk Graph Model (UDGM) (Kuhn et al., 2003) available in the simulator was used. The node transmission range was set to 50 metres. The RWK, RWP, and the GM mobility models were considered to analyze the performance of the RPL with different OFs. For the simulation, 30 nodes were randomly deployed in the simulation area. Number of MNs were varied to 3, 6, 9, 12, and 15 nodes out of the 30 nodes in the simulations to investigate the behaviour of the RPL in terms of power consumption, end-to-end latency, and PDR. The well-know Bonnmotion software (Aschenbruck et al., 2010) was used in the present work to generate mobility patterns. Table 3.1 shows the parameters used in the simulation work and Table 3.2 presents the

parameters set in the Bonnmotion software to generate the mobility patterns.

Table 3.1: Simulation parameters

<b>Simulation Parameters</b>	<b>Value</b>
Radio Model	UDGM
Node density	30
Simulation area	100m × 100m
Transmission range	50m
Mote Type	Tmote Sky
Mobility Model	RWK, RWP and GM
Simulation time	600s

### 3.1.7 Results and Discussion

The simulation experiments were conducted by varying the percentage of the MNs in the network under different mobility models. The obtained results were compared and analyzed.

**Power consumption:** Figure 3.2 shows the average power consumption of the nodes during simulation under RWK, RWP, and the GM mobility models by varying the MNs count in the network. Initially, all the sensor nodes were static, and the average energy consumption of the nodes with the OFE performed better compared with the other OFs. However, an increment of MNs in the network increased the power consumption. The reason for power consumption was that the nodes required several retransmissions to successfully deliver the packets to the sink node. For all the mobility models, the MRHOF performed better in the case of MNs as it required less number of retransmission of packets compared with the other three OFs.

**PDR:** Figure 3.3 shows the PDR during the simulation under RWK, RWP, and the GM mobility models by varying the MNs count in the network. Initially, all the sensor nodes were static, and therefore, all the OFs showed similar behaviour. However, an increment of MNs decreased the PDR of all the OFs in all the mobility models consid-

Table 3.2: Bonnmotion software parameters

<b>Settings</b>	Simulation area	Min speed	Max speed	Mobile nodes
<b>Value</b>	100m × 100m	4Km/hour	6Km/hour	3, 6, 9, 12, 15

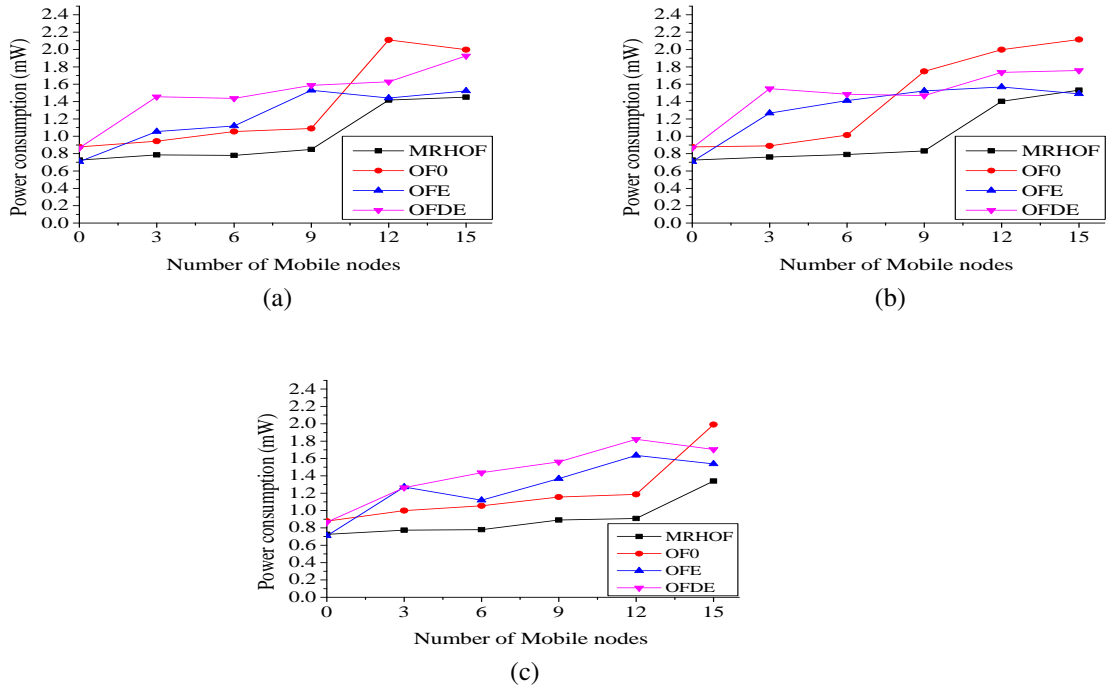


Figure 3.2: (a) Power Consumption under RWK mobility model (b) Power Consumption under RWP mobility model (c) Power Consumption under GM.

ered. Again, the MRHOF performed better in all the mobility models compared with the other three OFs. The reason was that the other OFs did not consider the quality of the links while choosing the PPN, which led to the dropping off some packets.

**End-to-End Latency:** Figure 3.4 shows the behaviour of latency during simulation under RWK, RWP, and the GM mobility models by varying the MNs' count in the network. Initially, the OF0 performed better compared with the other three OFs as it was based on the shortest path. However, as the mobile node count increased, the end-to-end latency also increased. This demonstrated that having the shortest path does not guarantee lower end-to-end latency because the intermediate node could be congested due to the mobility of the nodes. The OFDE performed better in all the mobility models as the next hop was selected based on lower latency to reach the sink node.

### 3.2 MULTI METRICS BASED OBJECTIVE FUNCTION FOR LOW POWER AND LOSSY NETWORKS UNDER MOBILITY

Since the OF, supported by the standard RPL, did not consider the mobility of the node while selecting a PPN, it used only a single metric. In the present work, an OF based on Multi Metrics (MMOF) for FRN and MN was proposed. For the FRNs, ETX, RE,

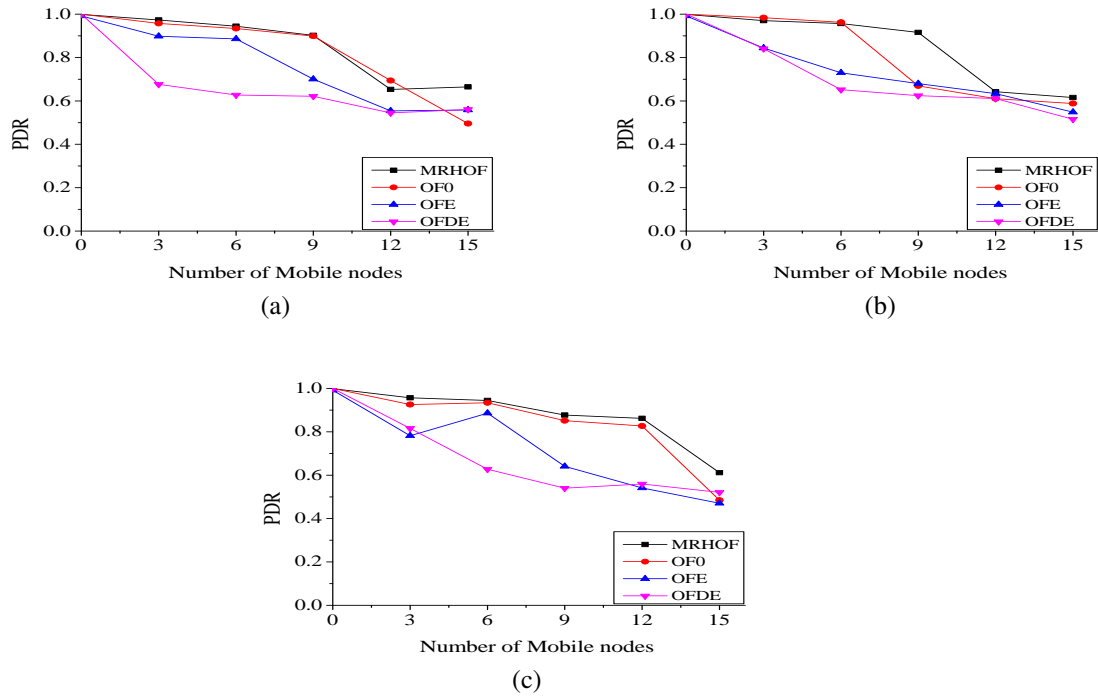


Figure 3.3: (a) PDR under RWK mobility model (b) PDR under RWP mobility model (c) PDR under GM.

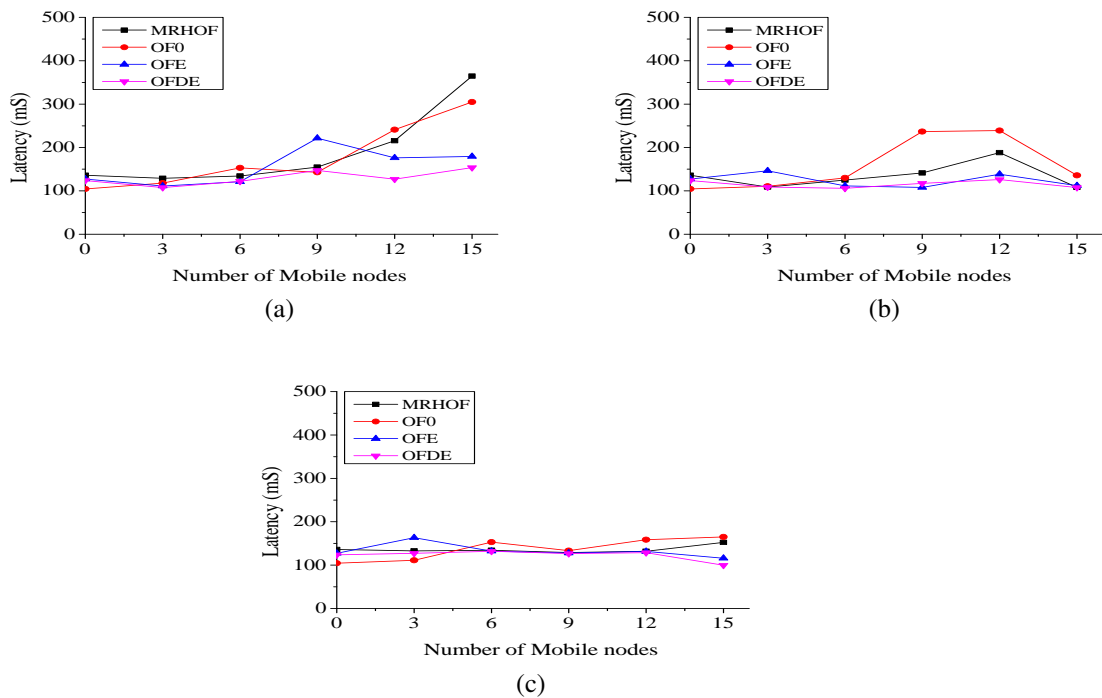


Figure 3.4: (a) Latency under RWK mobility model (b) Latency under RWP mobility model (c) Latency under GM.

and Distance (Dist) metrics were considered for selecting a PPN that had high energy, minimum distance, and high-quality link. For the MNs, ETX, Dist, and direction of the MN were considered, as the position of the MN plays an important role in selecting the PPN. Each OF is discussed in detail in the following sub-sections.

### 3.2.1 Objective Function for Fixed Router Node

The choice of PPN among its candidate parents was done based on the proposed MMOF and it was calculated by considering three different routing metrics such as  $ETX$ ,  $RE$ , and  $Dist$ . The MMOF was calculated as given in Equation (3.5).

$$MMOF = \alpha \frac{ETX_{curr}}{ETX_{max}} 100 + \beta (100 - \frac{RE_{curr}}{E_{total}} 100) + \gamma \frac{Dist_{curr}}{Dist_{max}} 100 \quad (3.5)$$

Where,  $\alpha$ ,  $\beta$ , and  $\gamma$  are weights assigned to routing metrics ETX, RE, and Dist, respectively, such that  $\alpha + \beta + \gamma = 1$ . The weights can be altered according to the priority of the metrics.  $ETX_{curr}$  was the current link quality,  $ETX_{max}$  was the maximum value that an ETX can take,  $RE_{curr}$  was the remaining energy of the node,  $E_{total}$  was the energy of the node during deployment,  $Dist_{curr}$  was the current distance from the node, and  $Dist_{max}$  was the maximum distance that a node can communicate with another node. The calculation of each routing metric is explained in the following sub-sections.

#### Expected Transmission Count based Routing Metric

ETX is the number of expected transmissions required by a node to accomplish the task of delivering the packet successfully to its destination. The value of ETX is calculated by measuring the probability that a packet reaches the neighbour ( $D_f$ ) successfully and the probability that an acknowledgment packet is successfully received ( $D_r$ ) as given in Equation (3.6).

$$ETX_{curr} = \frac{1}{D_f \times D_r} \quad (3.6)$$

#### Residual Energy based Routing Metric

It is the amount of energy remaining before the node runs out of its energy. It is calculated by subtracting the amount of energy depleted from the total energy of the node, as



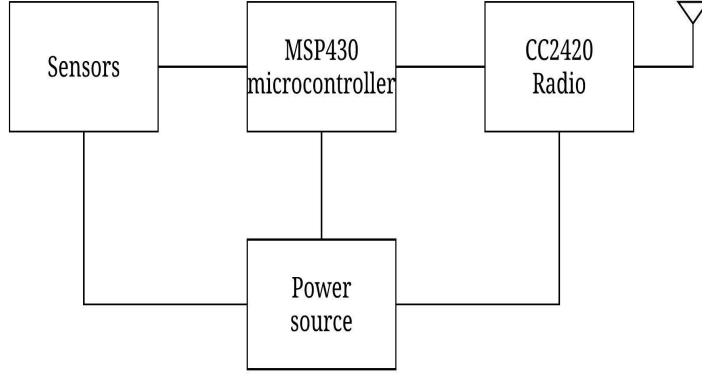


Figure 3.5: Structure of Tmote Sky

given in Equation (3.7).

$$RE_{curr} = E_{total} - E_{depletion} \quad (3.7)$$

Where,  $E_{total}$  is the initial energy of the node and  $E_{depletion}$  is the energy consumed by the node. The energy depletion  $E_{depletion}$  of the node is defined as the sum of energy consumed during processing, communicating, and sensing. As per [Dunkels et al. \(2007\)](#), it is calculated as in Equation (3.8).

$$E_{depletion} = V \times (I_{ap}T_{ap} + I_{lp}T_{lp} + I_{tx}T_{tx} + I_{rx}T_{rx} + \sum_i I_{ni}T_{ni}) \quad (3.8)$$

Where,  $V$  is the supply voltage,  $I_{ap}$ ,  $I_{lp}$ ,  $I_{tx}$ ,  $I_{rx}$ , and  $I_{ni}$  is the current required by the microcontroller in active mode, in low power mode, transmission mode of the communicating device, receiving mode of the communication device, and sensors, respectively, and  $T_{ap}$ ,  $T_{lp}$ ,  $T_{tx}$ ,  $T_{rx}$ , and  $T_{ni}$  is the activity duration of the microcontroller in active mode, in low power mode, transmission mode of the communicating device, receiving mode of the communication device, and sensors, respectively.

In this work, the Tmote Sky provided by the Cooja simulator was used ([Jevtić et al. \(2009\)](#)). The Tmote Sky is an ultra-low power wireless module specifically designed for sensor networks. Figure 3.5 shows the structure of a Tmote Sky. It has a built-in IEEE 802.15.4 compliant CC2420 radio implementing physical layer functions and also few medium access control layer functions. Taking the IEEE 802.15.4 characteristics and low power operations into account, the CC2420 provides a reliable wireless

Table 3.3: Current consumption of Tmote Sky

Module	State	Current
CPU	Active	600 $\mu$ A
	Idle	3 $\mu$ A
Radio	Transmit	17.4 mA
	Receive	19.2 mA
SHT11	Active	0.55mA

communication.

Table 3.3 shows the current consumption of the Tmote Sky taken from the data sheet provided by the manufacturer (Sky (2006); Amiri (2010)). In the present work, only sources which consumed more energy were used and the rest were ignored.

#### Distance based Routing Metric

The distance routing metric selected a node with the minimum distance as the PPN to avoid long-distance communication, and thereby addressed its concerns regarding reduction of transmission range of the node. The received signal strength diminished with the distance raised to the  $n^{th}$  power, where  $n$  is the path loss exponent, which depends on the environment. Therefore, the route with minimum distance is generally more energy efficient than one with a longer distance.

The distance is determined using the RSSI value based on the empirical model. The advantage of using an RSSI value is that it uses less costly hardware and can be implemented in low power devices.

The CC2420 has an on-chip RSSI register, which provides an 8-bit digital value (RSSI\_VAL) averaged over 8 symbol periods (Texas-Instruments (Texas-Instruments)). The status bit (RSSI\_VALID) signifies when the value is adequate. The RSSI register value is determined and continuously updated for each symbol when the RSSI\_VALID bit is set.

To adjust the error in RSSI\_VAL due to variation in antenna radiation pattern, a known RSSI offset is added to the RSSI\_VAL, which is a function of the environment or position of the node and its value is discovered empirically during system development from the front end gain. The  $RSSI$  value was computed as per Equation (3.9) (Kumar

et al. (2009)).

$$RSSI = RSSI\_VAL + RSSI\_OFFSET \text{ [dBm]} \quad (3.9)$$

Where,  $RSSI\_VAL$  is the 8-bit register value and  $RSSI\_OFFSET$  set to approximately -45 dBm (Texas-Instruments (Texas-Instruments)).  $RSSI\_OFFSET$  was added to compensate an error in  $RSSI\_VAL$ . For example, if the  $RSSI\_VAL$  is -40 dBm, then -45 dBm ( $RSSI\_OFFSET$ ) is added to obtain -85 dBm  $RSSI$  value. The distance was calculated using the relationship between the  $RSSI$  value and the power of the received signal as per (Kumar et al. (2009)).

$$RSSI \propto 10 \log\left(\frac{1}{D^n}\right)$$

$$RSSI = -10n \log(D) + C \quad (3.10)$$

Where,  $D$  is the distance between the MN and the parent node, ' $n$ ' is the path loss exponent factor, and  $C$  is some fixed constant. Equation (3.10) can be rewritten as:

$$RSSI = -m \log(D) + C \quad (3.11)$$

Where, ' $m$ ' is the slope of linear equation between  $\log(D)$  and  $RSSI$ . From Equations (3.10), (3.11), the path loss exponent factor was calculated as:

$$n = \frac{m}{10} \quad (3.12)$$

### 3.2.2 Objective Function for Mobile Node

The MN has the ability to change its location in the network. Due to mobility, if the MN is effectively distant from its parent node then the route towards the parent node becomes inconsistent. Therefore, mobility has to be given more priority over other routing metrics. A new routing metric  $Dist\_Var$  was defined to identify the change in position of the MN over a period of time. The MMOF for the MN was calculated using multiple routing metrics, i.e.,  $ETX$ ,  $Dist$  and  $Dist\_Var$  as given in Equation (3.13).

$$MMOF = \alpha \frac{ETX_{curr}}{ETX_{max}} 100 + \beta \frac{Dist_{curr}}{Dist_{max}} 100 + \gamma \frac{Dist\_Var}{Dist_{max}} 100 \quad (3.13)$$

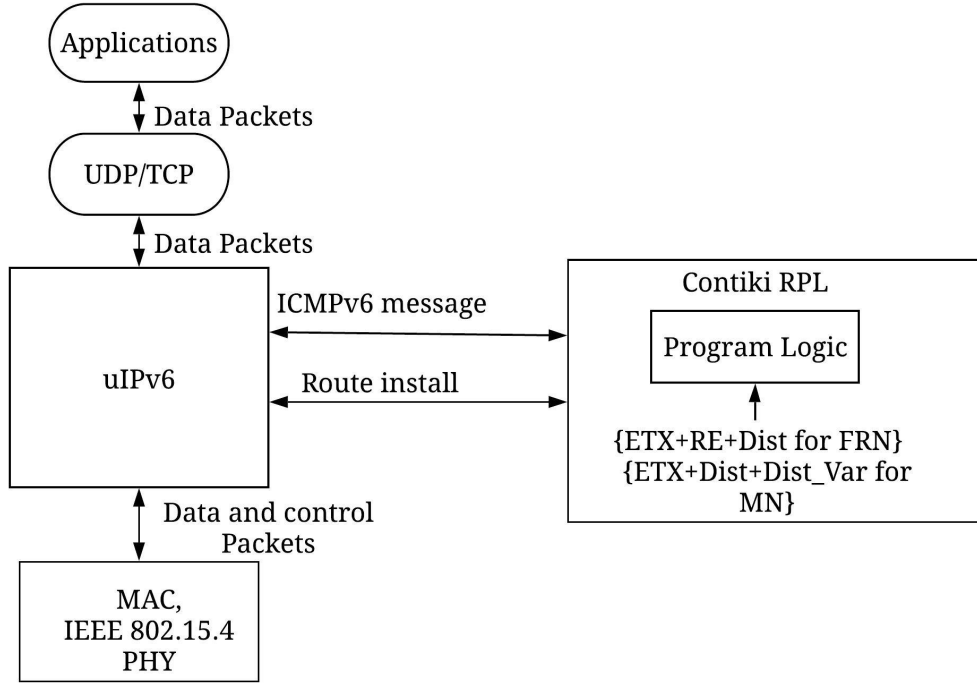


Figure 3.6: MMOF for RPL in Contiki Operating System

Where,  $\alpha$ ,  $\beta$ , and  $\gamma$  are weights assigned to ETX, Dist, and Distance Variation (Dist\_Var), respectively, such that  $\alpha + \beta + \gamma = 1$ . The weights can be altered according to the priority of the metrics. The  $ETX_{curr}$  is the link quality,  $ETX_{max}$  is the maximum value that an ETX can take,  $Dist_{curr}$  is the distance from the node,  $Dist_{max}$  is the maximum distance that a node can communicate and this routing metric is given highest priority among other routing metrics, and  $Dist\_Var$  is the distance variation of the node over a period of time.  $ETX_{curr}$  and  $Dist_{curr}$  were calculated according to Equations (3.6) and (3.11), respectively, whereas  $Dist\_Var$  was calculated using the formula given in Equation (3.14).

$$Dist\_Var = Dist_{t_2} - Dist_{t_1} \quad (3.14)$$

Where,  $Dist_{t_1}$  and  $Dist_{t_2}$  are the distances from the node calculated at the time of receiving successive DIO messages. The  $Dist_{t_1}$  and  $Dist_{t_2}$  were determined using RSSI as per Equation (3.11).

Figure 3.6 shows the MMOF for the RPL in the Contiki operating system in which the program logic uses the proposed MMOF defined for FRNs and MNs in order to

select the PPN. Algorithm 2 shows the procedure involved to select the PPN. For selecting the PPN, the node determines the path cost for each candidate parents using the MMOF and selects a candidate parent which has the least path cost as the PPN.

---

**Algorithm 2:** Preferred Parent Node Selection()

---

```

1 PreferredParent = NULL
2 MAX_OF = Maximum_Value
3 if Candidate_Parent_Table == TRUE then
4   foreach CPN ∈ Candidate_Parent_Table do
5     if CPN.OF < MAX_OF then
6       MAX_OF = CPN.MMOF
7       PreferredParent = CPN
8 if PreferredParent then
9   Send(DAO message to PreferredParent)
10 else
11   Broadcast DIS control message

```

---

### 3.2.3 Simulation Results and Discussions

The sub-section discusses the performance of the proposed MMOF evaluated using Cooja simulator (Jevtić et al. (2009); Dunkels (2012)). The performance of the proposed MMOF was compared with the MRHOF (Gnawali (2012)), OF0 (Thubert (2012)), OFE (Kamgueu et al. (2013)), and OFDE (Gonizzi et al. (2013)). In this simulation, 1 sink node, 30 FRNs, and 9 MNs were used in random topology. The routing metric *Dist* was given higher priority compared with the other two metrics, and therefore,  $\beta$  was set to 0.4, whereas  $\alpha$  and  $\gamma$  were set to 0.3. In random topology, the FRNs were placed randomly such that at least one FRN was in the communication range of other FRNs, similar to an actual environment. The detailed simulation parameters used in the present work are shown in Table 3.4. To generate the mobility traces, the Bonnmotion software (Aschenbruck et al. (2010)) was used, and the parameters that were set in the Bonnmotion software are shown in Table 3.5. The simulation results were obtained by varying the number of packet transmissions and the trickle timer in random topology.

*Reason for Varying Traffic:* Packets get lost when the MN moves away from communication range of the PPN and requires retransmission of such packets to be delivered successfully to the destination. To analyze the performance of the MMOF, the packet

Table 3.4: Simulation parameters

Simulation parameter	Values
Radio model	UDGM
Transmission range	30m
Mote Type	Tmote Sky
Simulation area	100m × 100m
Node density	FRN: 30, MN:9
Mobility model	RWP
Simulation time	600 seconds

Table 3.5: Bonnmotion software parameters

Settings	Simulation area	Maximum speed	Nodes	Interval time
Value	100m × 100m	1.5 m/s	9	10s

transmission rate was set to 1 packet per 2 minutes, 1 packet per minute, 2 packets per minute, and 3 packets per minute.

*Reason for Varying Trickle Timer:* Since the PPN was updated based on the OF obtained from the DIO message, which in turn broadcasted based on the trickle timer. Hence, the trickle timer was varied to analyze the performance of the MMOF. At first,  $[I_{min}, I_{doubling}]$  was fixed to [12, 1], then  $[I_{min}, I_{doubling}]$  was set to [10, 8],[12, 8], and [14, 8]. To measure the performance of the MMOF, power consumption, PDR, and end-to-end latency evaluation metrics were considered.

### 3.2.4 Analysis of Power Consumption

Figure 3.7 shows the power consumption in random topology with varying number of packet transmissions (3.7a) and trickle timer (3.7b). In general, the power consumption is directly dependent on the number of packets transmitted over the network. As shown

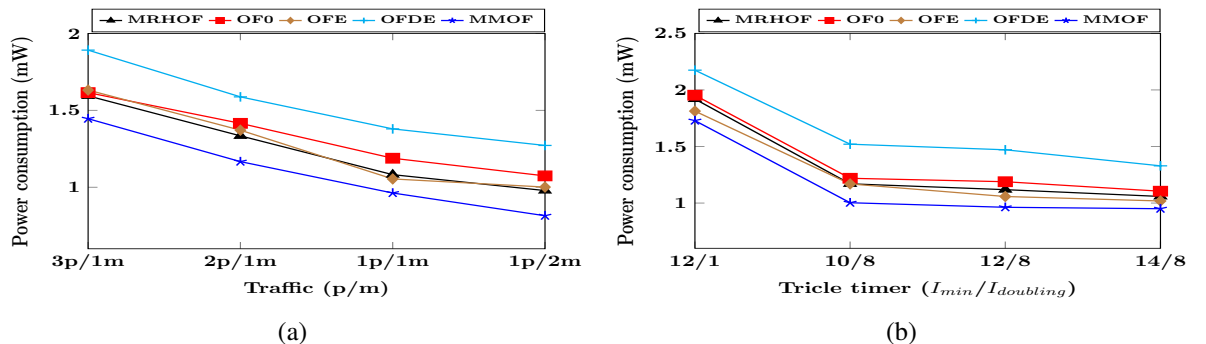


Figure 3.7: Power consumption with respect to (a) Traffic (b) Trickle timer.

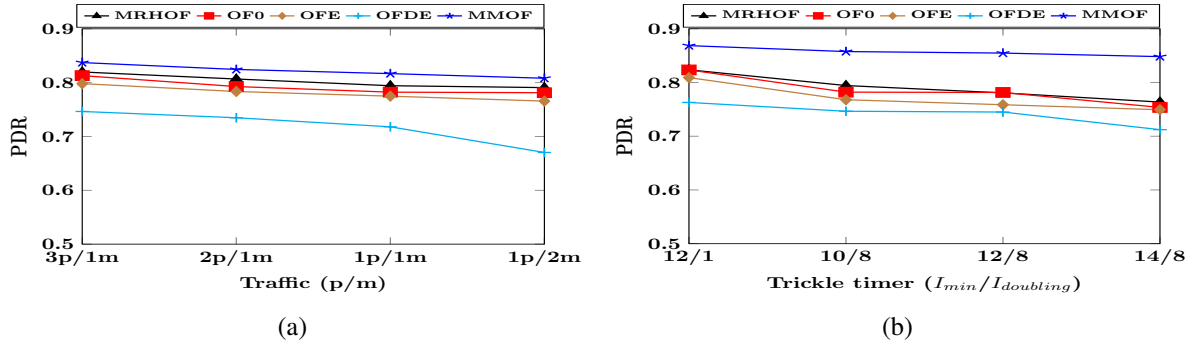


Figure 3.8: PDR with respect to (a) Traffic (b) Trickle timer.

in Figure 3.7, the power consumption decreased as the number of data packets and control packets reduced.

The OFDE and OFE consumed more power as they required retransmission of the packets. In case of OF0 and MRHOF, the PPN was selected irrespective of its distance to the PPN, consuming more power. In contrast, the MMOF consumed less power compared with the other OFs as it selected a node with minimum distance from the PPN and also high ETX value that reduced the number of retransmissions.

### 3.2.5 Analysis of Packet Delivery Ratio

Figure 3.8 shows slight decrease in PDR with the varying number of packet transmissions (3.8a) and trickle timer (3.8b). In general, the PPN is updated based on the OF, which is determined from the DIO message. Therefore, the decrease in DIO messages reduced the PDR as the packets were transmitted to an inconsistent PPN.

The OFDE, OFE, and OF0 ignored the link quality and showed less PDR. The MRHOF showed better PDR. However, if the node is distant and moving away from the PPN, then the packets get lost. In contrast, the PPN was selected based on the position and link quality in the MMOF and thus outperformed the other OFs.

### 3.2.6 Analysis of End-to-End Latency

Figure 3.9 shows end-to-end latency with varying number of packet transmissions (3.9a) and trickle timer (3.9b). In general, the latency increases if more number of packets is injected over the network, since each node requires some amount of time to process the received packet. As seen in Figure 3.9, latency is high initially and gradually decreases as the number of packets transmitted into the network.

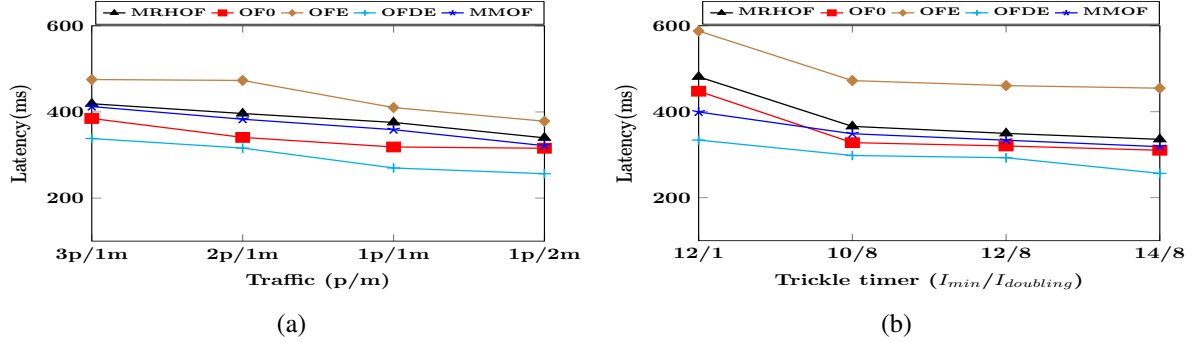


Figure 3.9: Latency with respect to (a) Traffic (b) Trickle timer.

The OFE and MRHOF have higher latency compared with the proposed MMOF. However, the MMOF has higher latency compared with the OF0 and OFDE. While selecting a PPN, the MMOF does not consider end-to-end delay to the root node.

### 3.3 SUMMARY

In Section 3.1, the performance of the RPL was investigated by considering different OFs, namely, MRHOF, OF0, OFE, and OFDE under three different mobility models such as RWK, RWP, and the GM. The obtained simulation results demonstrated that under mobility, the OFs have a direct effect on PDR, power consumption, and end-to-end latency. Furthermore, the MRHOF performed better in terms of PDR and power consumption. However, the OFDE achieved better results in terms of end-to-end latency compared with the other OFs in all the mobility models used in the simulation work.

In Section 3.2, an MMOF was proposed that minimized the energy consumption of the nodes while selecting a PPN based on the combination of minimum distance, maximum energy, high-quality link, and direction of the node. The performance of the MMOF was evaluated and compared with the MRHOF, OF0, OFE, and the OFDE. The simulation results showed that the MMOF exhibits reduced power consumption, increased PDR compared to the other chosen OFs such as OF0, OFE, and OFDE, and lower latency compared to MRHOF and OFE.



## **Chapter 4**

# **Design and Analysis of Mobility Aware Routing Protocols**

Due to the mobility of the nodes, the RPL experiences packet loss, this requires retransmission and significantly consumes node energy. In order to address this issue, in the present work new mobility aware routing protocols are proposed.

### **4.1 MOBILITY AWARE ROUTING PROTOCOL BASED ON DIO MESSAGE FOR LOW POWER AND LOSSY NETWORKS**

Due to the mobility of the nodes, the RPL suffers from frequent disconnection of communication links with neighbouring nodes that induces data loss, high energy consumption, and transmission delays. In order to address these issues, there is a need for an efficient mobility aware RPL. In the present work, a Mobility Aware Routing Protocol for LLN (MARPL) has been proposed, which is an improved RPL. The primary objective of the MARPL is to increase reliability and to reduce power consumption so that it is suitable for networks, where some nodes are mobile by nature.

The proposed MARPL for MNs with its selection of PPN, updating PPN, and its main benefits are discussed in the following sub-sections.

#### **4.1.1 Selection of Preferred Parent**

Initially, the DODAG root node sends a DIO message with its parameters to the nodes in its proximity. The nodes that receive the DIO message compute the OF and select the DODAG root node as their PPN and then transmit their information. The process is repeated until all the nodes are a part of the DODAG tree. The nodes in the network are frequently in an inconsistent state due to mobility, and therefore, the trickle timer algorithm increases the transmission of the DIO messages. Further, the packets from the node that had selected the MN as their PPN are lost, when the MN changes its position. To overcome this issue, the MNs in the MARPL are not permitted to send DIO messages to its neighbour nodes and are therefore, not selected as PPN. Thus, in the MARPL, only the FRNs are allowed to become PPN.

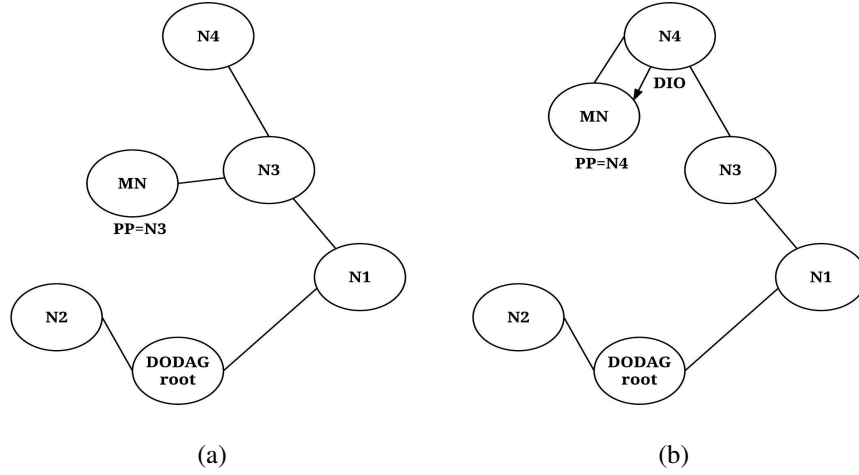


Figure 4.1: Preferred Parent Update

To avoid a loop in the DODAG tree, the static nodes are allowed to select their PPN only if the candidate parent rank is higher than its rank value. The rank value of the nodes increases from the leaves to the root node. When a node selects its PPN, it calculates the new rank ( $Rank_N$ ) based on the information obtained from the DIO message by adding the base rank ( $Rank_B$ ) with the minimum rank increase value as given in Equation (4.1).

$$Rank_N = Rank_B + Min\_Rank\_Increase \quad (4.1)$$

#### 4.1.2 Preferred Parent Update

In the MARPL, the static nodes send DIO messages based on the trickle timer algorithm. Whenever the nodes receive a DIO message, they add the sender node information into the candidate parent list, if the sender information is not already present in the list. A new node implies a new parent node along the direction of the MN path.

The MN computes the OF for the new parent node and compares it with the threshold value. If the OF of the new parent node is less than that of the threshold, then it is selected as a PPN for the MN and added to its neighbour's list, otherwise, the OF is compared with the parent nodes in the candidate parent list and is replaced with a parent node with a higher OF than the new parent node. When a PPN route expires, the MN selects a PPN that has the least OF in the candidate parent list. The number of parents for the MN is fixed, and when it reaches maximum value, then the oldest parent node is

removed from the candidate parent list.

In Figure 4.1a, the node N3 was selected as the PPN for the MN node which had the least OF in its candidate parent list. If the MN node moves away from node N3 and reaches the vicinity of node N4, then the MN node selects N4 as its PPN as shown in Figure 4.1b.

Algorithm 3 shows the procedure to update the PPN for the MN. However, for the static nodes, the PPN is updated based on the standard RPL protocol.

---

**Algorithm 3:** Update Preferred Parent for Mobile node

---

**Input** : Neighbors of node N  
**Output:** Preferred Parent of node N

- 1 *PreferredParent* = *NULL*
- 2 *NewParent* = *NULL*
- 3 **do**
- 4 | send(DODAG Information Solicitation message)
- 5 **while** *fixed router node* == *TRUE*;
- 6 **if** *DODAG Information Object* == *TRUE* **then**
- 7 | *NewParent* = *DIO\_Instance\_ID*
- 8 | *P* = *rpl\_find\_parent(NewParent)*
- 9 | **if** *P* == *NULL* **then**
- 10 | | *NewParent.OF* < *Threshold*
- 11 | | *PreferredParent* = *NewParent*
- 12 | | *rpl\_add\_parent(Newparent)*
- 13 | | *NumParents*++
- 14 | **if** *NumParents* == *MaxParents* **then**
- 15 | | *rpl\_remove\_parent(oldest parent)*
- 16 **do not broadcast** DODAG Information Object message

---

#### 4.1.3 Main Advantages

Firstly, the MNs are not permitted to be selected as PPN by not allowing them to send DIO messages, and thus, the unnecessary retransmission of packets is eliminated. Secondly, the MN selects a new PPN before it is out of communication range of the current PPN so that the MN is always within the vicinity of the FRN at any time, due to which packets are not lost.

Table 4.1: Simulation Settings

Simulation parameter	Values
Radio model	UDGM
Transmission range	30 meters
Mote Type	Tmote Sky
Simulation area	100m × 100m
Node density	30, 50
Mobile Nodes	3, 6, 9, 12, 15 for 30 node density 5, 10, 15, 20, 25 for 50 node density
Simulation time	600 seconds

#### 4.1.4 Simulation Results and Discussion

The MARPL was simulated and analyzed using the Contiki Operating System-based Cooja simulator ([Jevtić et al. \(2009\)](#)). Extensive simulations were performed with varying density of the nodes (30 and 50) and varying the number of MNs (3, 6, 9, 12, 15 for 30 node density and 5, 10, 15, 20, 25 for 50 node density) in the network under RWP mobility model and the GM mobility model. To create mobility traces for the said mobility models, the Bonnmotion software ([Aschenbruck et al. \(2010\)](#)) was used. Table 4.1 indicates the parameters used in the simulation work. The performance of the proposed MARPL was compared with the Standard RPL (SRPL) ([Winter et al. \(2012\)](#)) and the Modified RPL (Mod-RPL) ([Gara et al. \(2015\)](#)) to measure the efficiency of the MARPL for healthcare applications.

To determine the efficiency of the proposed MARPL, important evaluation metrics such as average PDR, average power consumption, and average end-to-end latency were considered. The obtained simulation results are shown in Figures 4.2, 4.3, and 4.4.

#### 4.1.5 Analysis of Packet Delivery Ratio

In healthcare applications, the nodes send crucial data to the sink node, since rapid delivery of data packets is critical for the applications' success. Generally, these applications demand high PDR to achieve their intended goal. The average PDR is determined by the ratio of the sum of all the packets successfully delivered to the sink node to the sum of all the packets sent by the nodes in the network.

Figures 4.2a and 4.2b show PDR by varying the MNs from 3, 6, 9, 12, and 15

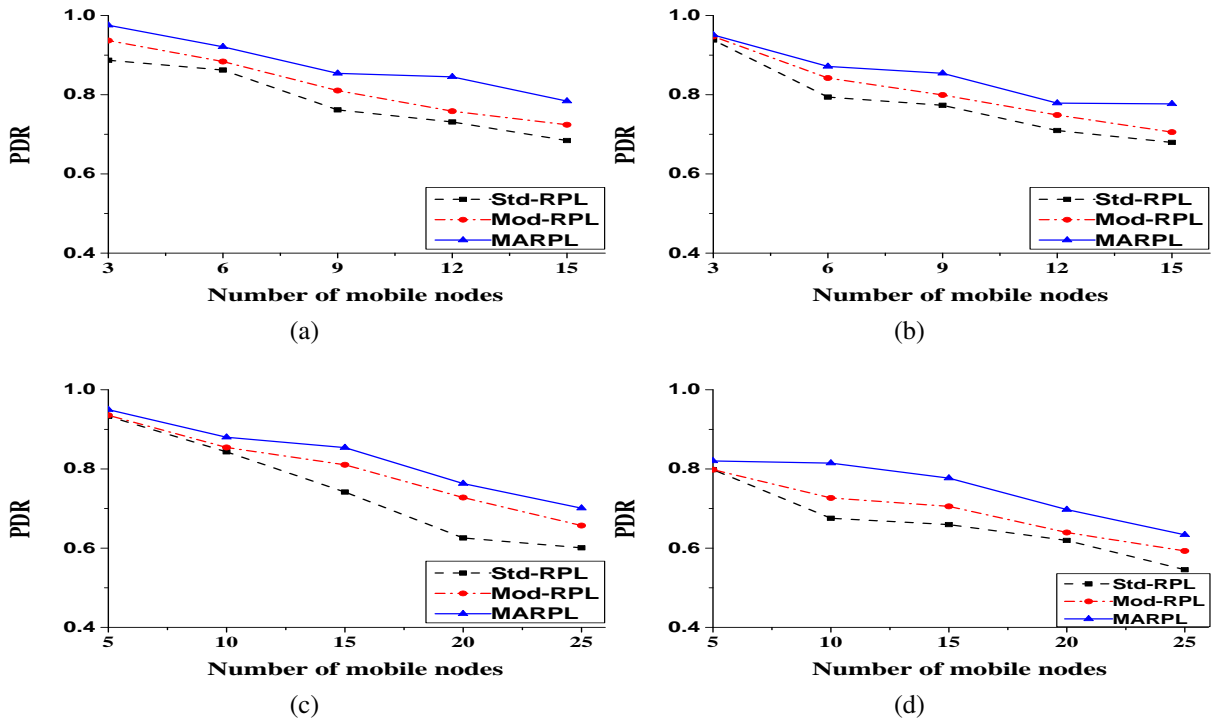


Figure 4.2: PDR with respect to (a) RWP model (30 nodes) (b) GM model (30 nodes) (c) RWP model (50 nodes) (d) GM model (50 nodes)

from a total number of 30 nodes with respect to RWP and GM, respectively. Similarly, Figures 4.2c and 4.2d illustrate the simulation experiments for 50 nodes by varying the MNs from 5, 10, 15, 20, and 25. The x-axis and y-axis represent the percentage of the MNs and the PDR of the network, respectively. The proposed MARPL showed better performance in terms of PDR compared with the SRPL and the Mod-RPL.

In the case of the SRPL, if the MN is elected as the PPN, the packets sent by the node will not be delivered if the PPN moves away from it, and this is also the reason for the decreasing PDR with the increase in percentage of the MNs. In the case of Mod-RPL, if the node moves away from the vicinity of the PPN, it takes a while to realize that it is no longer in the range of the PPN, and meanwhile, all the packets sent by the node are lost. Hence, the PDR also decreases with the increase in percentage of the MNs. Whereas in the case of MARPL, if the node moves away from the already selected PPN, it changes the PPN when it receives a DIO message from its new neighbour node. However, the DIO messages are transmitted according to the trickle timer, and therefore, it takes a while for the node to change its PPN, and this is the reason that the PDR decreases with the increase in the number of MNs.

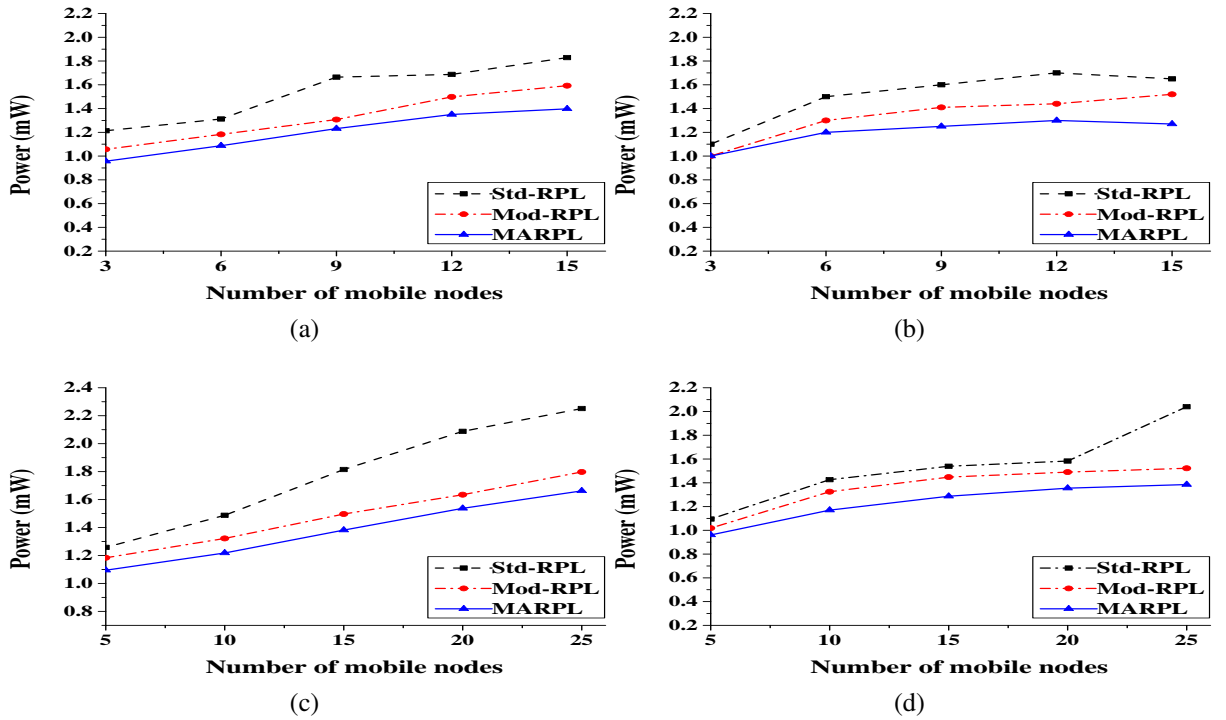


Figure 4.3: Power Consumption with respect to (a) RWP model (30 nodes) (b) GM model (30 nodes) (c) RWP model (50 nodes) (d) GM model (50 nodes)

#### 4.1.6 Analysis of Power Consumption

The WSN applications are optimized for power consumption to increase the lifetime of the sensor nodes. The power consumption is calculated based on the power state monitoring application that is inbuilt in the Cooja simulator.

Figures 4.3a and 4.3b show power consumption by varying the MNs from 3, 6, 9, 12, and 15 from a total number of 30 nodes with respect to RWP and GM, respectively. Similarly, Figures 4.3c and 4.3d demonstrate the simulations for 50 nodes by varying the MNs from 5, 10, 15, 20, and 25. The x-axis and y-axis represent the percentage of MNs and the average power consumption of the network in mill watts, respectively. From the results, it was observed that the MARPL consumed less power compared with the SRPL and Mod-RPL.

The SRPL consumed more power because of some nodes selected the MN as their PPN that would not be available after a certain period and caused frequent packet loss and also required more control messages. This was the reason for more power consumption when the number of MNs increased in the network. In the case of Mod-RPL, the PPN would not be available if the MN moved away from it. Therefore, the MN

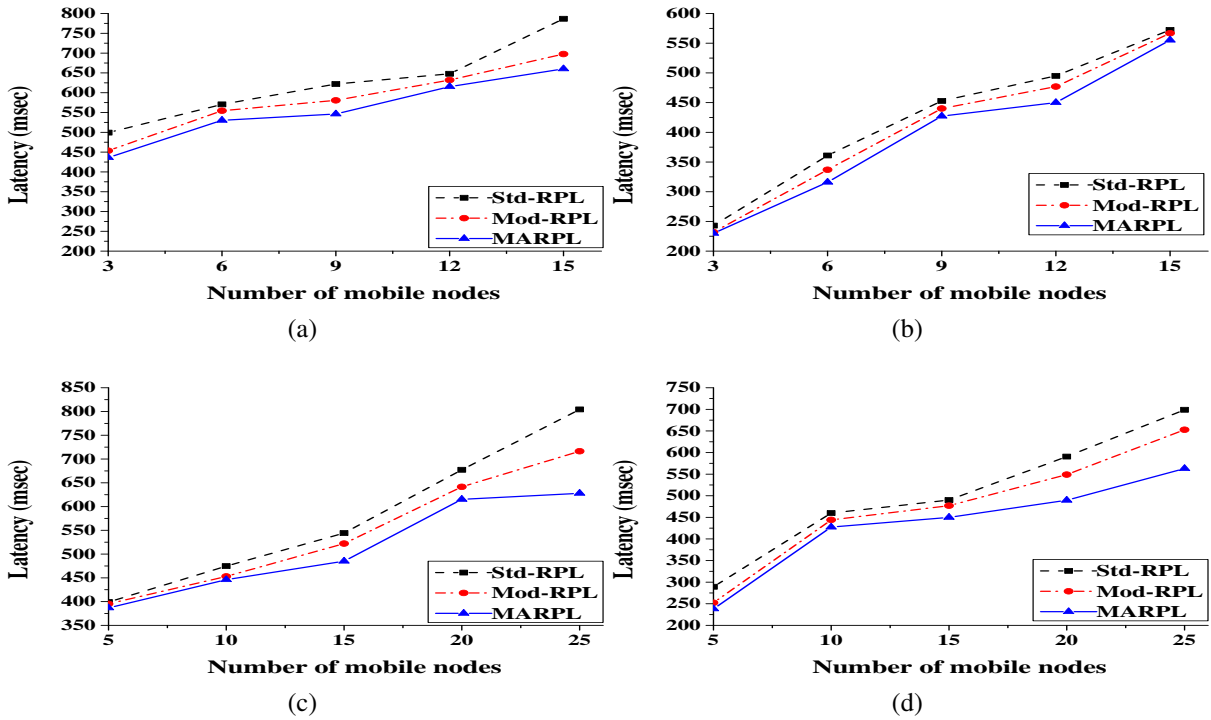


Figure 4.4: Latency with respect to (a) RWP model (30 nodes) (b) GM model (30 nodes) (c) RWP model (50 nodes) (d) GM model (50 nodes)

required several retransmissions, which consumed more power. Thus, when a number of MNs were more, the average power consumption increased.

#### 4.1.7 Analysis of End-to-End Latency

Some applications require packets to be delivered within a timeframe, and therefore it is considered as an important parameter for WSN. The average end-to-end latency is calculated as the ratio of time taken by the packets to reach the destination from the source to the total number of packets transmitted.

Figures 4.4a and 4.4b show end-to-end latency by varying the MNs from 3, 6, 9, 12, and 15 from a total number of 30 nodes with respect to RWP and GM, respectively. Similarly, Figures 4.4c and 4.4d present the simulation for 50 nodes by varying the MNs from 5, 10, 15, 20, and 25. The x-axis and y-axis represent the percentage of MNs and the end-to-end latency of the network in milliseconds, respectively. From the results, it was observed that the end-to-end latency of the MARPL was less compared with the SRPL and Mod-RPL.

In the SRPL, the packets took a longer route and also, if the nodes selected the MN

as their PPN along the path, then the packets reached the destination with higher end-to-end latency. In the case of Mod-RPL, the MN continued to send packets to the PPN that was at a longer distance, and therefore, increased the end-to-end latency. However in the case of MARPL, if the MN moved away from the PPN, it selected a new PPN, and hence, the end-to-end latency was less compared with the other protocols.

## **4.2 ENHANCED MOBILITY AWARE ROUTING PROTOCOL FOR LOW POWER AND LOSSY NETWORKS**

The Enhanced mobility aware routing protocol for Low Power and Lossy Networks (ERPL) was proposed to provide mobility support to the standard RPL, which included the following modifications:

- The MNs were not allowed to transmit DIO messages, and hence were not allowed to become the PPN, which reduced some amount of retransmissions and controlled packet overhead.
- The OF of the FRN used multiple routing metrics, i.e., ETX, RE, and Dist, which ensured that the link was of high quality, high availability, and consumed less power.
- The OF of the MN used multiple routing metrics, i.e., ETX, Dist, and Distance Variation (Dist\_Var). The Dist was given more priority which ensured that the MN selected the nearest PPN in the direction of the movement.
- Frequently updating neighbour nodes to avoid using an inconsistent link and to avoid selecting a PPN, which was away from the MN, minimized the energy consumption.

### **4.2.1 Objective Function for Selecting Preferred Parent**

The RPL classified the nodes into three classes, namely, DAG root, FRN, and leaf node. In the proposed work, another class of node, i.e., the MN, equipped with mobility engine was added. The MNs are capable of changing their location and moving around the network. Therefore, a different mechanism for the MN during the selection of the PPN was proposed. The OF for selecting the PPN for FRN is discussed in Section 3.2.1 and the OF for selecting a PPN for the MN is discussed in the Section 3.2.2. Figure 4.5 shows the ERPL in the Contiki operating system, in which the program logic uses the proposed new OF defined for mobility support in order to select a PPN.



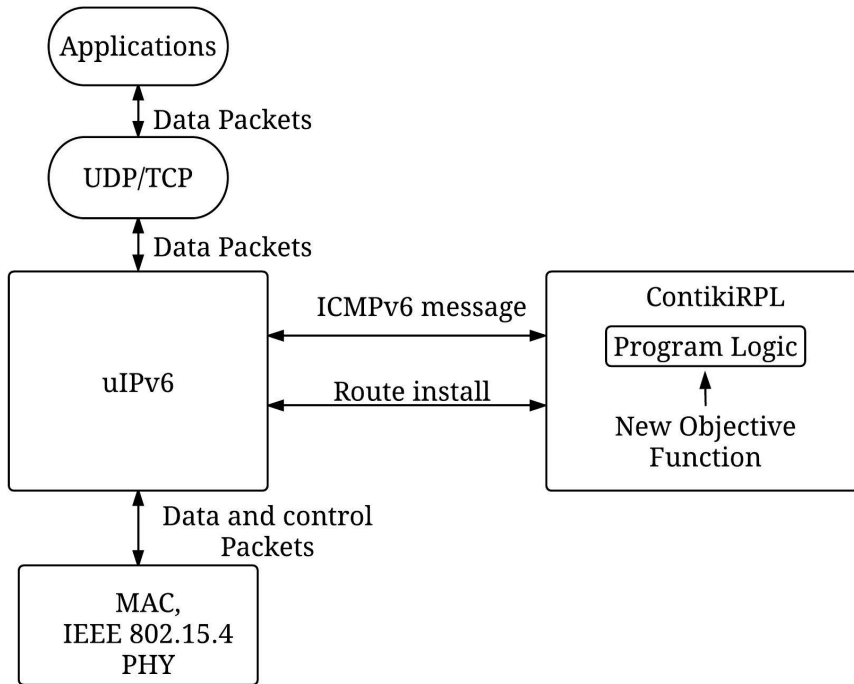


Figure 4.5: Enhanced-RPL in Contiki Operating System

#### 4.2.2 Updating Preferred Parent for Mobile Node

In case of the standard RPL, the PPN was updated periodically or when a link to the PPN expired. However, if the MN was effectively distant from the PPN, i.e., the MN was already out of the PPN communication range then, all the packets transmitted by the MN were lost and required retransmission for successful delivery. To overcome this problem, the proposed approach updates the PPN of the MN after receiving a DIO message from the CPN or at least two DIO messages from a new parent node. In order to update the PPN, the MN maintains two tables, namely, *Candidate Parent Table* and *New Parent Table* and the fields of these tables are given in Figure 4.6 and Figure 4.7. Where, ID uniquely identifies the node in the network, *Dist* indicates the distance between the parent node and MN, *Dist\_Var* designates whether the MN is moving towards or away from the parent node, *Lifetime* indicates duration until the entry remains in the *Candidate Parent Table* and *New Parent Table*.

Algorithm 4 shows the step-by-step procedure involved in updating the MN's PPN. However, updating the PPN for the FRN is the same as specified in the standard RPL protocol. Different scenarios that arise during the selection of the PPN due to MN mobility are described in the Section below. Figure 4.8 shows an example of the different

ID	Dist	Dist_Var	Lifetime
----	------	----------	----------

Figure 4.6: Candidate\_Parent\_Table fields

ID	Dist	Lifetime
----	------	----------

Figure 4.7: New\_Parent\_Table fields

scenarios.

1. T1:T2 MN joining the network
2. T2:T3 MN moving close to a new parent node
3. T3:T4 MN moving close to a CPN
4. T4:T5 MN moving away from the parent node

#### Mobile Node joining the Network

The steps involved in the MN joining the network are discussed in this section. Initially, the MN's *Candidate\_Parent\_Table* and *New\_Parent\_Table* are empty. Since, no parent nodes are available in the *Candidate\_Parent\_Table*, the MN keeps broadcasting DIS messages into the network until a parent node is available in the *Candidate\_Parent\_Table*. If it receives a DIO message from the parent node, it calculates the distance based on the *RSSI* value. If the measured distance is above the *threshold* then the parent node is added to the *New\_Parent\_Table* with all the information. If a node receives another DIO message from the same parent node within the *Lifetime*, then the *Dist\_Var* is computed. Then, the information of the parent node is added to the *Candidate\_Parent\_Table* by removing its entry in the *New\_Parent\_Table*. If this is the first CPN, then it is selected as the PPN, otherwise a CPN with the least OF is selected as the PPN.

In Figure 4.8 at T1, the MN keeps broadcasting DIS messages since there are no candidate parents, and at T2, the FRN6 is the only CPN, and therefore, it is selected as the PPN node.

#### Mobile Node Moving Close to a New Parent Node

The steps involved when a MN moves close to a new parent node are discussed in this scenario. When an MN receives a DIO message from a parent node, it checks if the parent node is already present in the *Candidate\_Parent\_Table*. If the parent node

---

**Algorithm 4:** Updating Preferred Parent

---

```
Input : Mobile Node MN
Output : PreferredParent of MN
1 Candidate_Parent_Table = NULL
2 New_Parent_Table = NULL
3 do
4   send(Broadcast DIS message)
5   if DIO == TRUE then
6     Instance = DIO.Instance
7     NP = New_Parent_Table.Find(Instance.ID)
8     if NP == NULL then
9       Dist = Calculate_Distance(RSSI)
10      if Dist > Threshold then
11        | New_Parent_Table.Add(Instance)
12      else
13        | Ignore DIO
14    else
15      Compute Dist_Var
16      Candidate_Parent_Table.Add(Instance)
17      New_Parent_Table.Remove(Instance)
18 while Candidate_Parent_Table == TRUE;
19 Call Procedure 1
20 if DIO == TRUE then
21   Instance = DIO.Instance
22   CPN = Candidate_Parent_Table.Find(Instance.ID)
23   if CPN == NULL then
24     NP = New_Parent_Table.Find(Instance.ID)
25     if NP == NULL then
26       Dist = Calculate_Distance(RSSI)
27       if Dist > Threshold then
28         | New_Parent_Table.Add(Instance)
29       else
30         | Ignore DIO
31     else
32       Dist = Calculate_Distance(RSSI)
33       Compute Dist_Var
34       Candidate_Parent_Table.Add(Instance)
35       New_Parent_Table.Remove(Instance)
36       Call Procedure 1
37   else
38     if CPN.ID == PreferredParent.ID then
39       Dist = Calculate_Distance(RSSI)
40       Compute Dist_Var
41       Candidate_Parent_Table.Update(CPN)
42     else
43       Dist = Calculate_Distance(RSSI)
44       Compute Dist_Var
45       Candidate_Parent_Table.Update(CPN)
46       Call Procedure 1
```

---

---

```

47 if PreferredParent.Lifetime == 0 then
48   | Candidate_Parent_Table_Remove(PreferredParent)
49   | PreferredParent = NULL
50   | Call Procedure 1
51 if CPN.Lifetime == 0 then
52   | Candidate_Parent_Table_Remove(CPN)
53 if CPN == FALSE then
54   | repeat Algorithm 4

```

---

is not present, then it searches in the *New\_Parent\_Table*. If the parent node is already present, then it determines the *Dist* from the *RSSI* of the DIO message, computes the *Dist\_Var*, adds the parent node to the *Candidate\_Parent\_Table*, removes its entry from the *New\_Parent\_Table* and checks if the parent node has potential to become a PPN. Otherwise, it determines the *Dist* from the *RSSI* of the DIO message and compares it with the *threshold*. If the *Dist* is greater than the *threshold*, then it is added to the *New\_Parent\_Table*, otherwise the DIO message is ignored.

In Figure 4.8 at T3 since the MN has moved closer to FRN4, and therefore has the least OF compared with FRN6 and FRN1, the FRN4 is selected as the PPN.

---

#### **Procedure 1 Preferred Parent Selection**

---

```

1 PreferredParent = NULL
2 MAX_OF = Maximum_Value
3 if Candidate_Parent_Table == TRUE then
4   | foreach CPN ∈ Candidate_Parent_Table do
5     | if CPN.OF < MAX_OF then
6       |   | MAX_OF = CPN.OF
7       |   | PreferredParent = CPN
8 if PreferredParent then
9   | Send(DAO message to PreferredParent)
10 else
11   | repeat Algorithm 4

```

---

#### **Mobile Node Moving Close to a Candidate Parent Node**

The MN moving close to a CPN is discussed here. When the MN receives a DIO message from the CPN, it checks if the CPN is already a PPN or not. If the CPN is

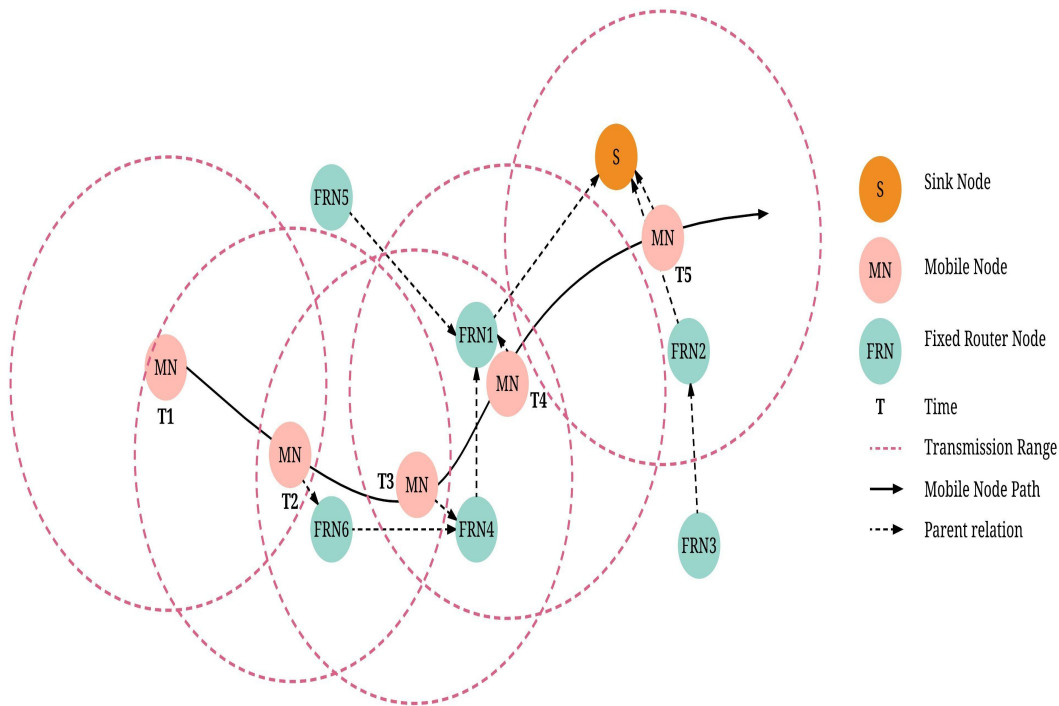


Figure 4.8: Scenarios due to Mobile Node Movement

already a PPN, then  $Dist$  is determined using the  $RSSI$  of the DIO message and the  $Dist\_Var$  is updated in the  $Candidate\_Parent\_Table$ , otherwise the corresponding parent node is updated and the CPN with the least OF is selected as the PPN.

In Figure 4.8 at T3, FRN4 is selected as the PPN and FRN1 is already a CPN of the MN. When an MN moves closer to FRN1 at T4, FRN1 has the least OF, and hence is selected as the PPN.

#### Mobile Node Moving Away from the Parent Node

In this scenario, the MN moving away from a parent node is discussed, i.e., either the CPN or a new parent. When the MN receives a DIO message from the parent node, it adds a timer or resets the timer in the corresponding  $Candidate\_Parent\_Table$  or  $New\_Parent\_Table$ . If the MN does not receive a DIO message before the  $Lifetime$  of the entry in the  $Candidate\_Parent\_Table$  or  $New\_Parent\_Table$  expires, it is then assumed that the MN has moved away from that parent node and is no longer reachable, and the entry of the parent node in the corresponding table is removed. If the removed parent node is PPN, then a new CPN is selected as the PPN with the least OF.

In Figure 4.8 at T4, FRN1 is selected as PPN. At T5, the MN moves away from the

Table 4.2: Simulation parameters

Simulation parameter	Values
Radio model	Unit Disk Graph Model
Transmission range	30m
Mote Type	Sky Mote
Simulation area	$100m \times 100m$
Node density	FRN: 30, MN:9
Mobility model	RWP
Simulation time	600sec

Table 4.3: Bonnmotion software parameters

Settings	Simulation area	Speed	Nodes
Value	$100m \times 100m$	(0.5, 1, 1.5, 2) m/s	9

FRN1, if it no longer hears any DIO messages from it. Therefore, the *Lifetime* expires and is removed from the *Candidate\_Parent\_Table* and sink node is selected as the PPN.

### 4.2.3 Simulation Results and Discussion

In order to evaluate the performance of the proposed ERPL, the Cooja simulator provided by the Instant Contiki 2.6 (Jevtić et al., 2009; Dunkels, 2012) was used, and the parameters used in the present work are shown in Table 4.2. To generate mobility traces, the Bonnmotion software (Aschenbruck et al., 2010) was used, and the parameters are shown in Table 4.3. The performance of the ERPL was compared with the SRPL (Winter et al., 2012) and the MRPL (Gara et al., 2016), which calculated the DIS interval using the distance and speed of the MN.

The simulation results were obtained by varying the speed of the MN, the number of packet transmissions, and the trickle timer under the grid and random topologies. In the grid topology, the FRNs were placed at a certain distance from each other, whereas in the case of random topology, the FRNs were placed randomly such that at least one FRN was in communication range of the other FRNs, similar to an actual environment.

**Reason for varying Speed:** The main goal of this work was to update the neighbours whenever the MN changed its position. Therefore, to analyze the performance of the ERPL, the MN speed was set to 0.5m/s, 1m/s, 1.5m/s, and 2m/s, which is in the range of human walking and running speed.

**Reason for varying Traffic:** Packets get lost when the MN moves away from the

communication range of the PPN and requires retransmission of the packets to be delivered successfully to the destination. To analyze the performance of the ERPL, the packet transmission rate was set to 1 packet per 2 minutes, 1 packet per minute, 2 packets per minute, and 3 packets per minute.

***Reason for varying Trickle timer:*** Since the PPN was updated based on the OF, which was obtained from the DIO message, which in turn was broadcast based on the trickle timer. Hence, the trickle timer was varied to analyze the performance of the proposed ERPL. At first, the timer was fixed to  $I_{min}$  value 12, then  $[I_{min}, I_{max}]$  was set to  $[10, 8]$ ,  $[12, 8]$ , and  $[14, 8]$ .

To measure the performance of the proposed ERPL, power consumption, packet overhead, PDR, and end-to-end latency were considered as evaluation metrics. The importance of these metrics and the results obtained from the simulations are explained below.

#### **4.2.4 Analysis of Power Consumption**

Energy consumption is an important factor for a successful sensor network operation since the sensor nodes are battery powered. To calculate power consumption, the power trace tool (Dunkels et al., 2011) available in the Cooja simulator was used. It uses power state monitoring to calculate the system power consumption.

Figure 4.9 shows the power consumption in the grid and random topologies, which were sub-categorized with respect to varying speed, trickle timer, and traffic.

From Figure 4.9a, it was found that proposed ERPL consumed an average 17% less power as compared with the SRPL, and on average 10% less power compared with the MRPL in the grid topology. In random topology, as shown in Figure 4.9b, it was observed that the ERPL consumed an average 12% less power compared with the SRPL, and on average 4% less compared with the MRPL by varying the speed of the MNs.

From Figure 4.9c, it was found that the ERPL outperformed with respect to the SRPL by 17% on average and the MRPL by 3% on average in the grid topology. In random topology, the ERPL outperformed on average by 15% compared with the SRPL and by 3% compared with the MRPL by varying the trickle timer, as shown in Figure 4.9d.

As shown in Figure 4.9e, the average power consumption of the proposed ERPL was 17% less compared with the SRPL and 10% less compared with the MRPL in the grid topology. In random topology, as shown in Figure 4.9f, the proposed ERPL consumed on average 21% less power compared with the SRPL and 9% less power compared with the MRPL by varying the traffic.

The main reason for the SRPL to consume more power was that there was a chance of the MN becoming a PPN, which would not be available after a certain period due to its movement. Therefore, the SRPL required more control messages and retransmission of packets, which resulted in consuming more power. In case of the MRPL, even though the MN was moving away and distant from the PPN, still the packets were being forwarded to it, which may have resulted in packet loss. Hence, the MRPL consumed more power. Another reason was that MRPL required control messages to find a new PPN when the MN moved away from the PPN. In contrast, the ERPL selected based on the direction of the MN movement. Therefore, the FRN which was very close to the MN was selected as the PPN. Hence, the ERPL showed improvement in all situations.

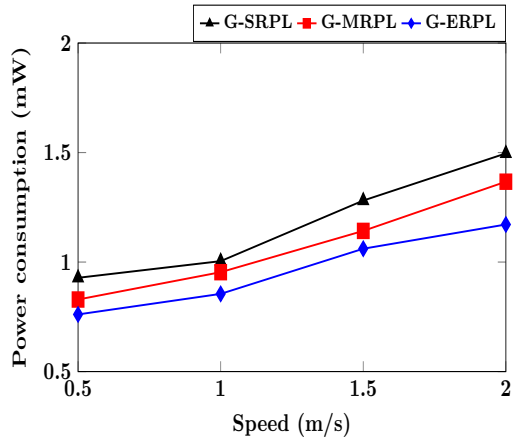
#### 4.2.5 Analysis of Packet Overhead

Control packets are essential for constructing, sustaining, and repairing routes in the network. Hence, they are considered as important components of the network. However, redundant transmission of control packets consumes more energy, overloads the network, and influences the transmission of other packets. Therefore, the RPL should contain the transmission of the control messages. The packet overhead was calculated as the total number of control messages, i.e., DIS, DIO, DAO, and DAO-ACK transmitted until completion of the simulation.

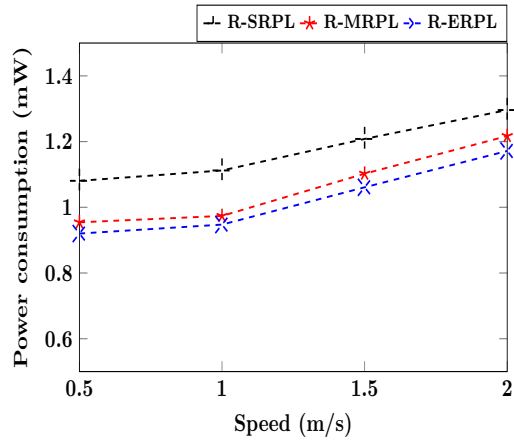
Figure 4.10 shows the packet overhead in the grid and random topologies, which were sub-categorized with respect to varying speed, trickle timer, and traffic.

Figure 4.10a and Figure 4.10b show the impact of the varying speed of the MNs on a number of control messages transmitted over the network in the grid and random topologies, respectively. The ERPL required on average 11% fewer control messages compared with the SRPL and 2% fewer control messages than the MRPL in the grid topology. In random topology, the ERPL requires on average 12% fewer control messages compared with the SRPL and 3% fewer control messages than the MRPL.

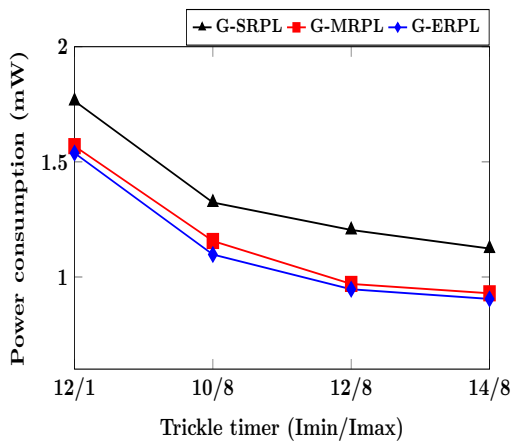




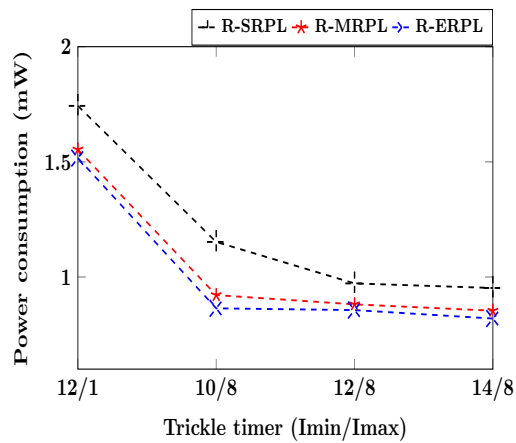
(a)



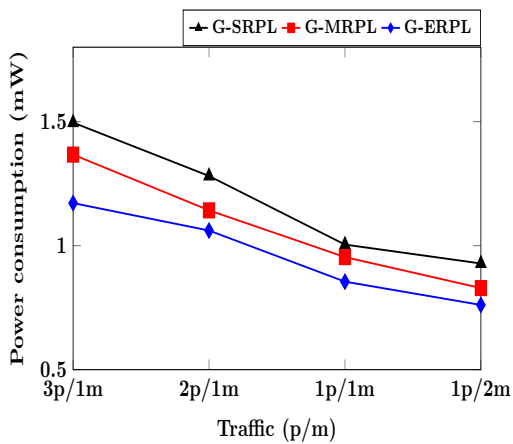
(b)



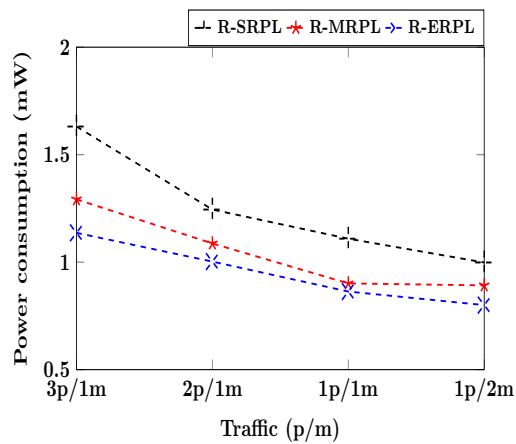
(c)



(d)



(e)



(f)

Figure 4.9: Power consumption in grid(G) [random(R)] topology with respect to Speed, Trickle timer, Traffic: (a), (c), (e) [(b), (d), (f)]

Figure 4.10c and Figure 4.10d show the impact of varying the trickle timer on a number of control messages transmitted over the network in the grid and random topologies, respectively. The ERPL requires on average 15% fewer control messages compared with the SRPL and 8% fewer control messages than the MRPL in the grid topology. In random topology, the ERPL requires on average 14% fewer control messages compared with the SRPL and 5% fewer control messages than the MRPL.

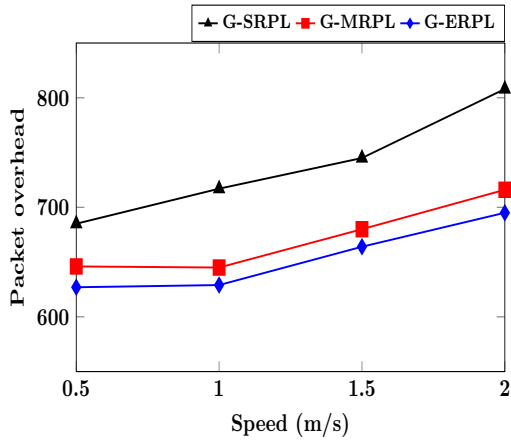
Figure 4.10e and Figure 4.10f show the impact of varying the traffic on a number of control messages transmitted over the network in the grid and random topologies, respectively. The ERPL requires on average 11% fewer control messages compared with the SRPL and 3% fewer control messages than the MRPL in the grid topology. In random topology, the ERPL requires on average 10% fewer control messages compared with the SRPL and 2% fewer control messages than the MRPL.

The reason for overhead in the SRPL is that the MNs were allowed to broadcast DIO messages, which significantly increased the number of control messages in the network. If the MN becomes a PPN for some node, then due to the mobility it is not available for the node after a certain period of time. To repair the path, the node sends control messages, which further increases the number of control messages in the network. In the MRPL, when the MN moves away from the PPN, the node solicits a DIS message in the network to which the neighbouring nodes reply with DIO messages. This procedure is repeated to update the PPN, which increases the control messages in the network. In contrast, in the ERPL, the MNs are not allowed to send DIO messages, and therefore, they are not selected as PPN at any movement. For updating the PPN, the FRN which is close to the MN is selected as the PPN. Therefore, it requires fewer control messages in all situations.

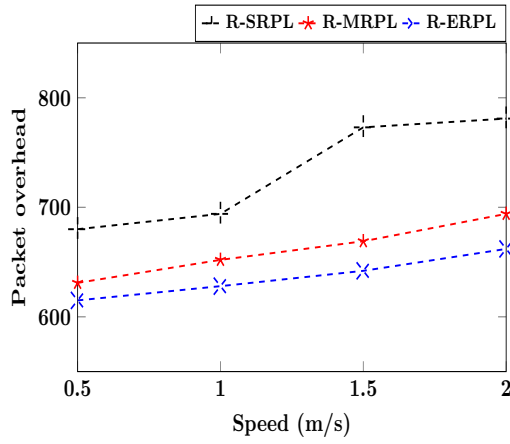
#### **4.2.6 Analysis of Packet Delivery Ratio**

Figure 4.11 shows the PDR under the grid and random topologies, which were sub-categorized with respect to varying speed, trickle timer, and traffic.

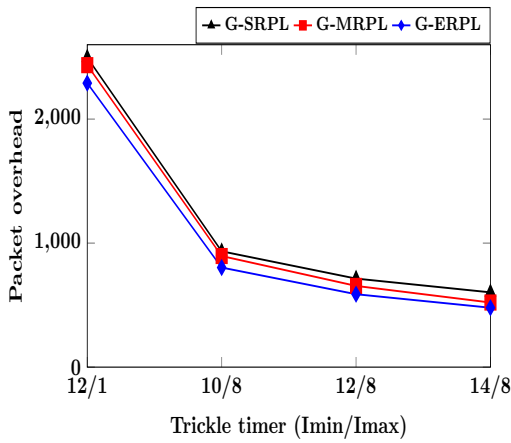
Figure 4.11a and Figure 4.11b show the influence of varying the speed on PDR over the network in the grid and random topologies, respectively. The average PDR in the grid topology showed 8% improvement for the ERPL compared with the SRPL and 3% improvement for the ERPL against the MRPL. In random topology, it was found that



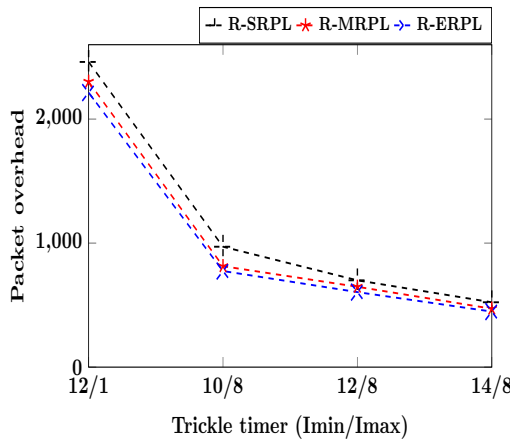
(a)



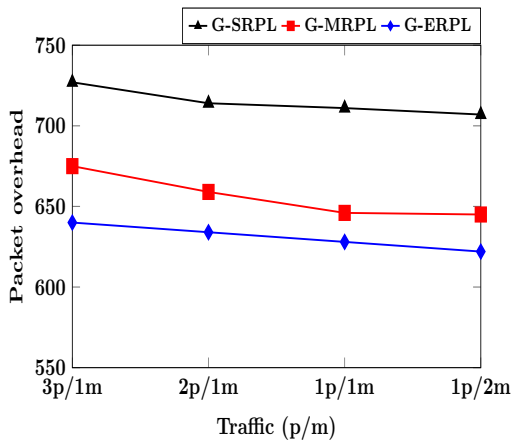
(b)



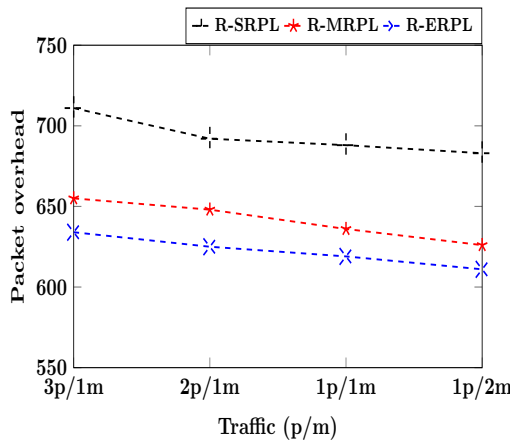
(c)



(d)



(e)



(f)

Figure 4.10: Packet overhead in grid(G) [random(R)] topology with respect to Speed, Trickle timer, Traffic: (a), (c), (e) [(b), (d), (f)]

the ERPL showed 10% better PDR against the SRPL and 6% better against the MRPL.

Figure 4.11c and Figure 4.11d show the impact of varying the trickle timer on PDR over the network in the grid and random topologies, respectively. The average PDR in the grid topology showed 16% improvement for the ERPL compared with the SRPL and 6% improvement in the ERPL against the MRPL. In random topology, it was found that the ERPL showed 11% better PDR against the SRPL and 5% better against the MRPL.

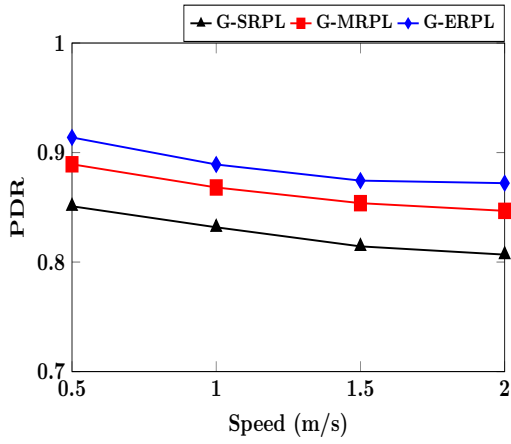
Figure 4.11e and Figure 4.11f show the impact of varying the traffic on PDR over the network in the grid and random topologies, respectively. The average PDR in the grid topology showed 9% improvement for the ERPL compared with the SRPL and 6% improvement in the ERPL against the MRPL. In random topology, it was found that the ERPL showed 7% better PDR against the SRPL and 3% better against the MRPL.

The reason for low PDR in the SRPL was that all the nodes were treated equally, irrespective of their mobility status. The PDR decreased drastically when an MN was selected as the PPN since the MN had changed its location, and the new PPN was not updated quickly. In the MRPL, the MN solicited DIS messages when the leaving time of the MN expired. To select a new PPN, the MRPL took some time, which resulted in packet loss. Another reason for the low PDR was that even though the MN was moving away and distant from the PPN, the data packets were still being forwarded to it, which resulted in packet loss. In contrast in the ERPL, a new PPN was selected when the MN moved close to another FRN without waiting for route expiration time. Hence, it showed better results in all situations.

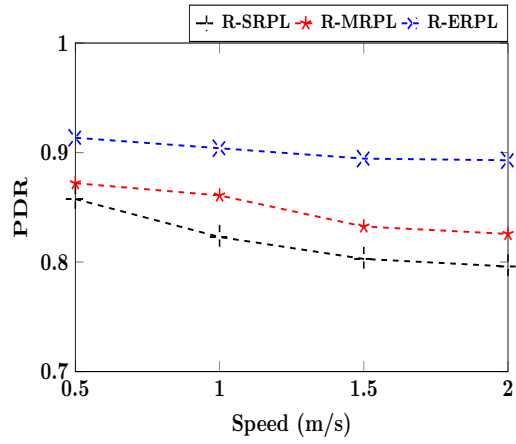
#### **4.2.7 Analysis of Latency**

This metric ought to be limited for applications that require real-time guarantees. It was calculated as the time taken by the data packets from the point of transmission to its reception at the sink node. Figure 4.12 shows the end-to-end latency under the grid and random topologies, which was sub-categorized with respect to varying speed, trickle timer, and traffic.

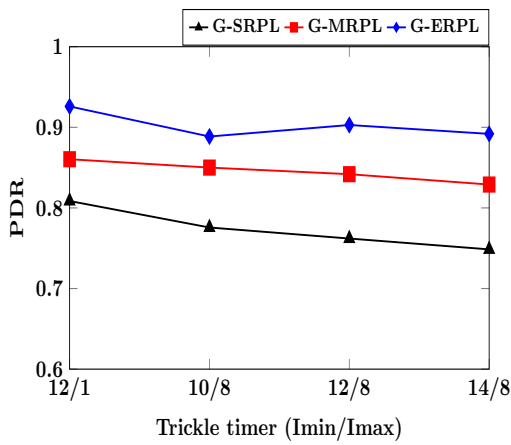
From Figure 4.12a, it was found that the ERPL data packets reached its destination faster than the SRPL by an average 8% and an average 5% compared with the MRPL in



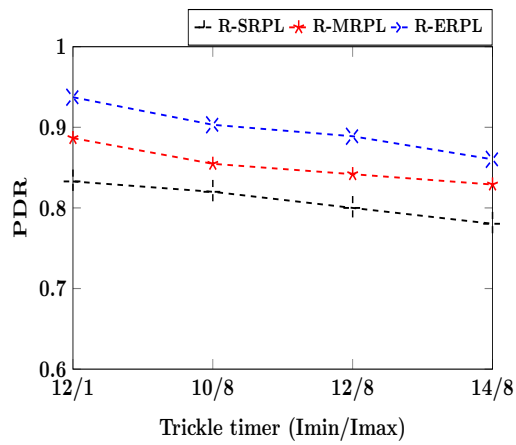
(a)



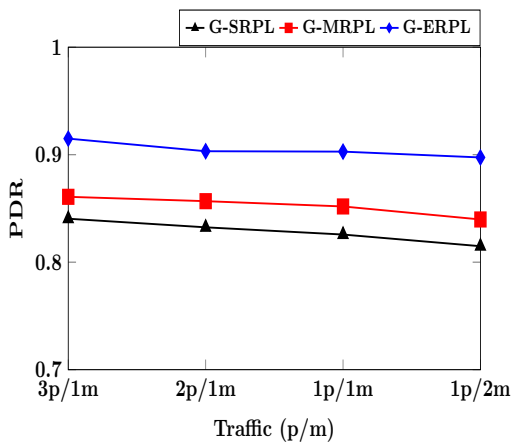
(b)



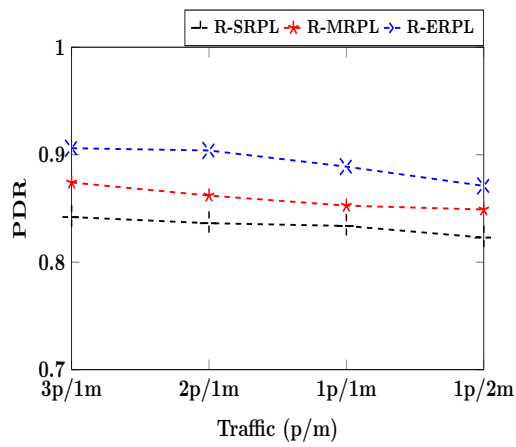
(c)



(d)

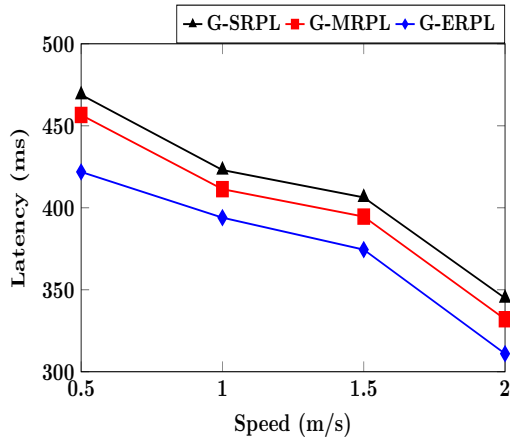


(e)

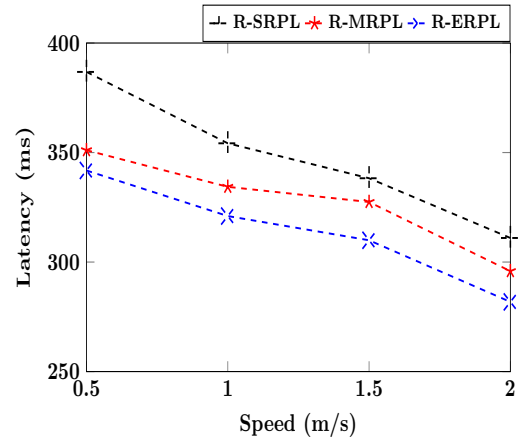


(f)

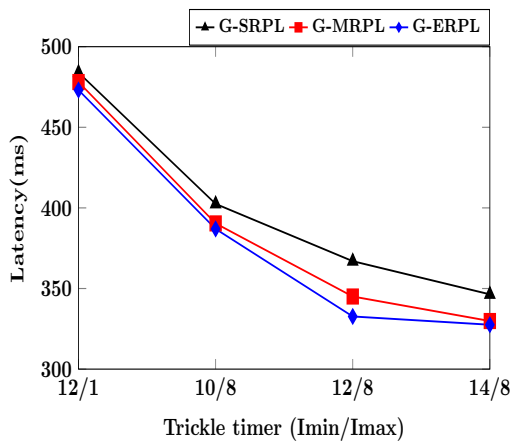
Figure 4.11: PDR in grid(G) [random(R)] topology with respect to Speed, Trickle timer, Traffic: (a), (c), (e) [(b), (d), (f)]



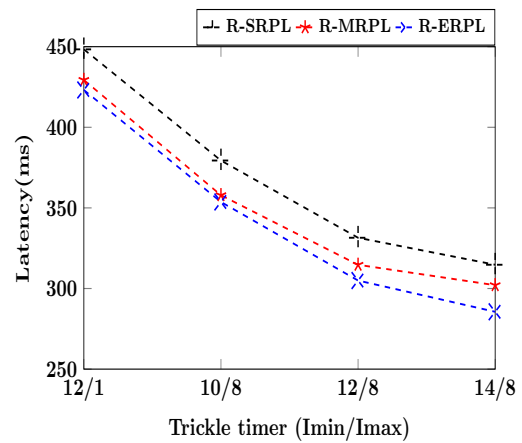
(a)



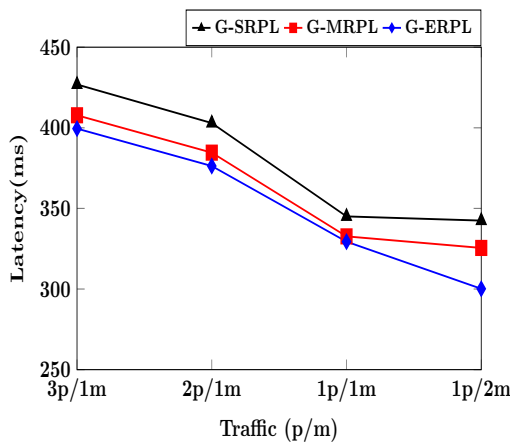
(b)



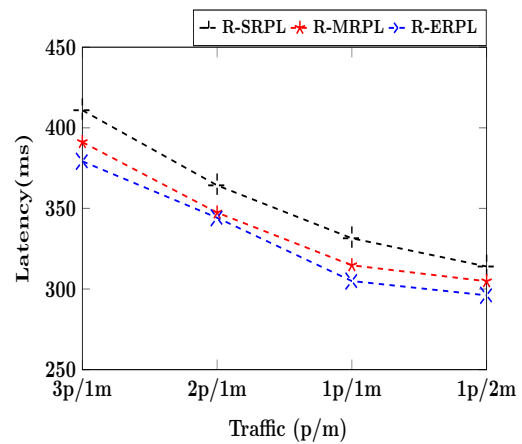
(c)



(d)



(e)



(f)

Figure 4.12: Latency in grid(G) [random(R)] topology with respect to Speed, Trickle timer, Traffic: (a), (c), (e) [(b), (d), (f)]

the grid topology. In random topology, as shown in Figure 4.12b, it was found that the ERPL data packets reached its destination faster by an average 9% compared with the SRPL and an average 5% compared with the MRPL by varying the speed of the MNs.

From Figure 4.12c, it was found that the ERPL data packets reached its destination faster than the SRPL by an average 5% and an average 2% compared with the MRPL in the grid topology. In random topology, as shown in Figure 4.12d, it was found that the ERPL data packets reached its destination faster by an average 7% compared with the SRPL and an average 2% compared with the MRPL by varying the trickle timer.

As shown in Figure 4.12e, it was found that the ERPL data packets reached its destination faster than the SRPL by an average 7% and on average 3% compared with the MRPL in the grid topology. In random topology, as shown in Figure 4.12f, it was found that the ERPL data packets reached its destination faster by an average 6% compared with the SRPL and on an average 2% compared with the MRPL by varying the traffic.

In case of SRPL, if the intermediate nodes along the path from source node to destination node are mobile nodes, then the data packets take a longer time to reach the destination. In case of MRPL, as the distance between the node and its PPN increased, the end-to-end latency also increased. In contrast, the ERPL made use of the distance as a routing metric while calculating the OF. Hence, it showed a slight improvement in all the situations.

#### **4.2.8 Evaluating the Impact of Fixed Router Node Density**

In this study, the performance of the ERPL was analyzed by varying the density of FRNs by 15, 20, 25 and 30 nodes in the random topology. In general, the proposed ERPL performance increases with the increase in density of the FRNs, as shown in Figure 4.13.

Initially, with 15 FRNs the proposed ERPL achieved approximately 81% of PDR. As the number of FRNs was increased to 30 nodes, the ERPL achieved approximately 89% of PDR. In general, as the density of FRNs increases, the MNs have more candidate parents that increase the probability of selecting the best parent with high-quality link, and thereby increase the PDR. However, with the low density of FRNs, the ERPL performed better compared with the SRPL and the MRPL, as shown in Figure 4.13a.

Figure 4.13b shows the average power consumption of the nodes in the network. The average power consumption of the ERPL decreases with the increase in FRNs. The power consumption of node includes the power spent over the transmission of control messages, i.e., DIS, DIO, DAO, and DAO-ACK messages. With less number of FRNs, the node requires more control messages for selecting a PPN, and therefore consumes more power. However, the ERPL consumed less power compared with the SRPL and the MRPL.

Figure 4.13c shows that the average delay of the ERPL reduces slightly with the increase in the number of FRNs. With less number of FRNs, there is a chance of selecting a PPN, which is far from the node. In the case of ERPL with increasing number of FRNs, there is a chance of selecting a PPN, which is near to the node. However, in the SRPL, the node selection was based only on the ETX value, which increased the delay.

Figure 4.13d shows the impact of varying the density of the FRNs on a number of control messages transmitted over the network. The total number of control messages increase with increase in FRNs as each node sends control messages to construct and maintain a DODAG tree. However, the number of control messages required for selecting a PPN decreases with the increase in FRNs since the MN rarely broadcasts DIS messages as there is more chance of finding a candidate parent with high density of FRNs.

#### 4.2.9 Discussions

The simulation results showed that the ERPL performed better by updating the PPN quickly whenever an MN moved away from the already selected PPN under different traffic and system parameters. Nevertheless, there were several considerations regarding the viability of the ERPL.

- A node must be able to recognize whether it is static or mobile in nature, as the MN is not allowed to transmit DIO messages.
- The PPN was selected based on the OF that included distance as a routing metric. The distance was calculated using the *RSSI* value, which is sensitive to interferences in real world scenarios.



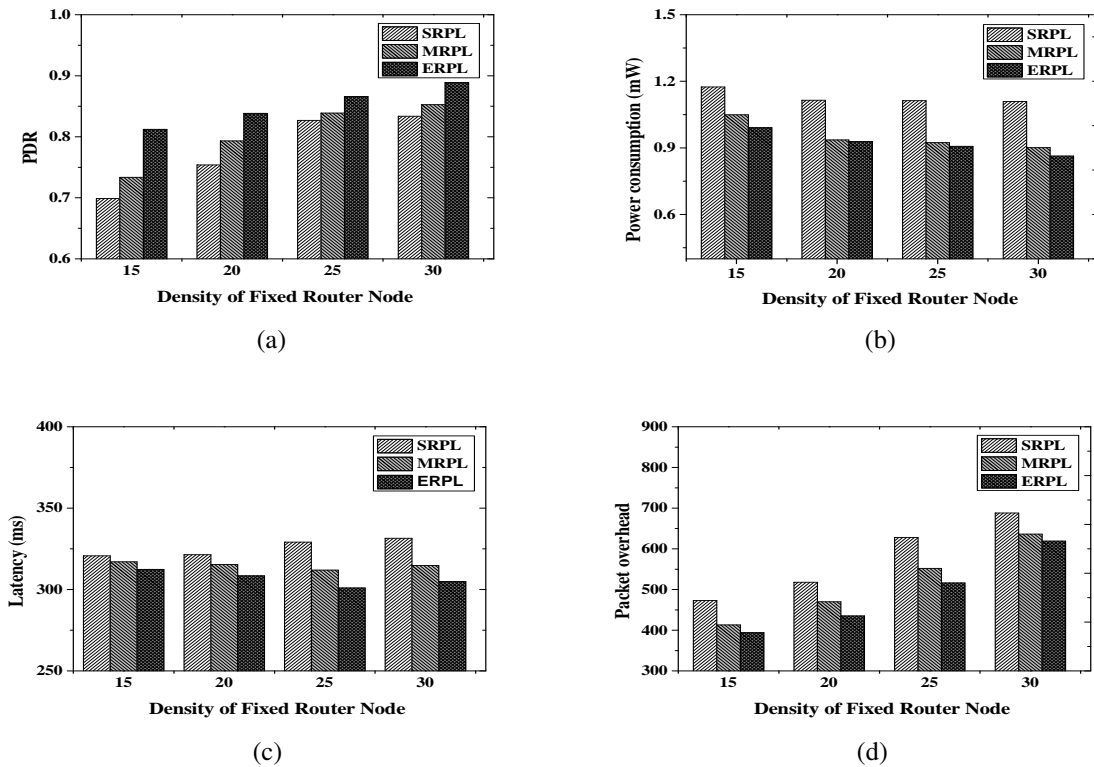


Figure 4.13: Impact of Fixed Router Node density on (a) PDR, (b) power consumption, (c) end-to-end latency, and (d) packet overhead

- The ERPL required the MNs to be in the range of at least one FRN since the MNs were not allowed to become PPNs.
- To achieve high performance, the ERPL required more number of FRNs in the network.
- Finally, the power consumption and packet overhead can be reduced further, if the ERPL predicts the path of the MN and selects an ideal FRN as a PPN.

### 4.3 SUMMARY

Section 4.1 proposed an MARPL in which the MN was aware of its mobility and updated the PPN information without waiting for route expiration time. To evaluate the robustness of the proposed MARPL, simulations were carried out on the Contiki based Cooja simulator for different mobility models. The results showed that proposed MARPL performed better with respect to healthcare applications compared with the standard RPL.

In Section 4.2, an ERPL was proposed to provide mobility support for the LLNs. In addition, a new OF was introduced that selected a PPN based on high quality, high availability, and low power consumption. On this basis, a mechanism to update the PPN for the MN was also proposed. The proposed ERPL was simulated using the Cooja simulator in order to verify its effectiveness. The obtained simulation results showed that the proposed ERPL outperformed the MRPL and the SRPL by achieving maximum 21% less power consumption, 15% less packet overhead, 9% low end-to-end latency, and the PDR had increased to 16%.

## Chapter 5

# Mobility Support Routing Protocols using Timer Functions for Low power and Lossy Networks

Due to disconnections of the communication links and slow reaction of the RPL under mobility, packets routed to the destination require retransmission, which significantly consumed node energy. To overcome these drawbacks, i.e., to repair the routes and reestablish a path to the destination node without significant delay, new mechanisms were proposed using timer modules.

### 5.1 ENHANCED MOBILITY ROUTING PROTOCOL FOR WIRELESS SENSOR NETWORK

In the present work, an EM-RPL was designed, simulated, and evaluated. The aim of the EM-RPL was to repair the routes and to re-establish a path to the destination node without significant delay by using multiple routing metrics and timer modules. The multiple routing metrics ensured an optimal path to the destination, while the timer modules maintained seamless connectivity to the destination node by updating the PPN whenever the MN moved out of communication range. The candidate parent list was updated to maintain consistent neighbours based on the neighbour's activity.

#### 5.1.1 Selecting Preferred Parent for Fixed Router Node

In the previous chapter 3, an MMOF was designed for selecting a PPN for the FRN. This OF used routing metrics ETX, RE, and Dist as given in Equation (3.5). The MMOF value was called for the CPNs, and the FRN selected the PPN among the CPNs that had the least MMOF value.

#### 5.1.2 Selecting Preferred Parent for Mobile Node

In the case of the RPL, the packets were lost due to the mobility of the nodes. When the MNs changed their position and moved out of communication range from the selected PPN, still they continued to forward the traffic. Also, the MNs selected a PPN periodically among the candidate parents based on the OF. However, the CPNs were not updated when they were not in communication range. Further, the MN was also

allowed to become a PPN resulting in increased packet loss. Therefore, the mobility in the RPL required careful consideration.

In order to overcome the aforementioned problems, modules were added to the RPL to remove inconsistent neighbours and to select a PPN, which was likely to remain for a longer duration. The modules and their importance of adding to support mobility in the RPL are briefly discussed in following sub-sections.

#### **Time to Leave**

A new attribute called Time to Leave (TTL) was added to each candidate parent node. When an MN receives a DIO message from a candidate parent, it calculates the minimum time to remain in communication range of the candidate parent based on the distance and its speed. The approximate distance was calculated based on the RSSI value of the DIO message using Equation (3.11). The Remaining Distance (RD) was computed by subtracting the approximate distance from the Communication Range (CR) of the candidate parent. It is assumed that all nodes in the network are in the same communication range. Then, the TTL was computed by dividing the remaining distance with the speed of the MN as given in Equation (5.1).

$$RD = CR - Dist$$

$$TTL = \frac{RD}{S} \quad (5.1)$$

Where, RD is the remaining distance of the MN before moving out of communication range and S is the maximum speed of the MN.

#### **Freshness Timer**

A new attribute called freshness was added to the candidate parent to keep the candidate parent list updated. When the MN adds a new candidate parent to the candidate parent list, the freshness timer is initialized. The freshness timer was calculated by a fraction of the maximum communication range of the node to the maximum speed of the MN. The timer was reset whenever any activity was detected from the candidate parent. When the timer expired, all the routes established from the candidate parent were removed, along with its entry in the candidate parent list.

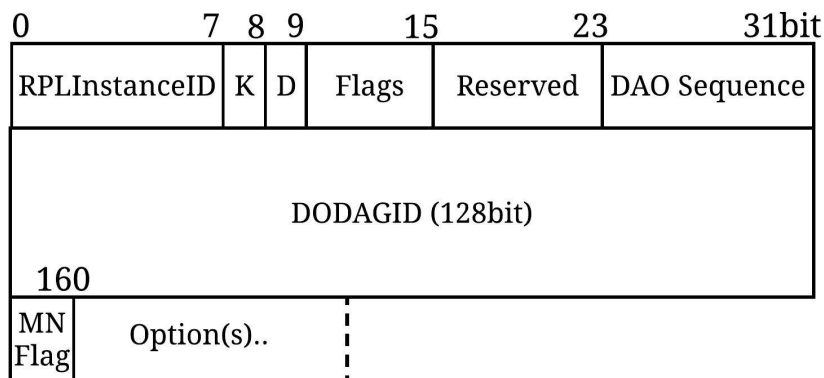


Figure 5.1: Modified DAO message

### DIO Timer

In the RPL, the DIO messages are transmitted based on the trickle algorithm. The main goal of the trickle algorithm is to reduce the number of control messages disseminated into the network. In a steady state, the trickle algorithm significantly reduces the number of DIO messages in the network. Thus, the MN fails to discover new candidate parents when they move from one location to another, and therefore, start a discovery process by sending DIS messages, which in turn increases the total number of control messages in the network. In order to overcome this problem, the Fixed Router Node (FRN) added a new attribute called the DIO timer. This timer was initialized whenever an MN selected a PPN based on the distance and speed. Whenever the timer expired, the FRN broadcasted a DIO message into the network.

### Unreachability Detection Timer

To avoid sending traffic to the unavailable node, the unreachability detection timer was used. This timer was initialized based on DAO latency between the sender and the receiver.

### Backward Compatibility

To allow the MNs in the RPL, the control messages were enhanced to incorporate mobility information, rather than create new control messages. The proposed EM-RPL works without interfering with the RPL. Figure 5.1 shows a modified DAO message to inform the FRN about the node type. If the Mobile Node Flag (MNF) bit is set to 1, then it is understood that the type of the node is MN, otherwise it is considered as an

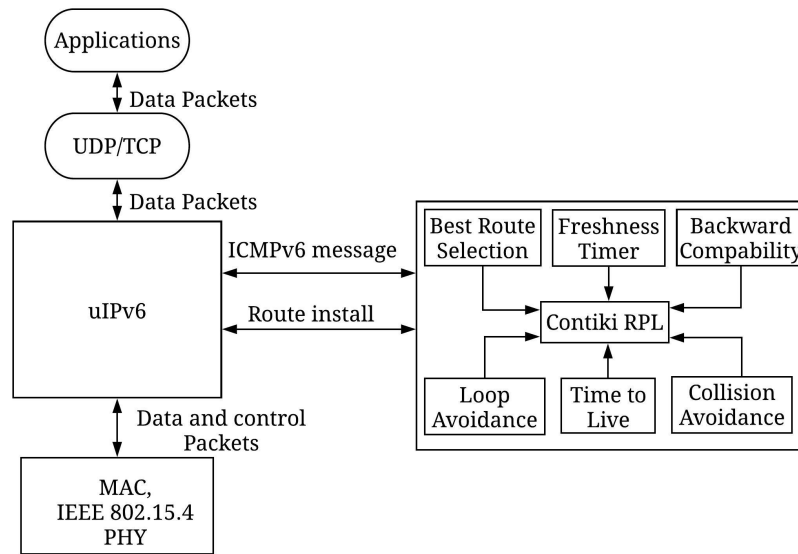


Figure 5.2: Enhanced Mobility RPL in Contiki Operating System

FRN.

#### Leaf Node

The trickle algorithm controls the number of DIO messages that enter the network. The algorithm increases the interval value if it receives a consistent message, otherwise, the interval becomes shorter, and the DIO messages are transmitted frequently in order to stabilize the network. Due to the mobility of the nodes, the nodes often reset the interval time and start sending DIO messages more frequently. To overcome this problem, the MNs were configured as leaf nodes so that inconsistent messages were not received by the FRNs. MNs can select same FRN as their PPN based on the OF.

#### Loop Avoidance

During local routing table update, where the node initializes its rank to infinite, there may be a chance that the node may select a PPN, which is its child creating a loop in the DODAG tree. In order to avoid this, the nodes were not allowed to select its children as PPN.

#### Best Route Selection

The MN selects a candidate parent as its PPN based on the duration it remains in the communication range of the node. The MN selects a candidate parent, which remains for a longer duration based on the TTL timer to avoid frequently changing a PPN.

Figure 5.2 shows the overall architecture of the modified RPL in the Contiki operating system. The mobility modules were added to the Contiki RPL, which helped to identify the best and consistent path towards the root node for the FRNs and MNs.

### 5.1.3 Procedure of the Enhanced Mobility RPL

The modules discussed in Section 5.1.2 were implemented into the RPL node based on node type, i.e., FRN or MN, which is assumed to be known during its deployment. Initially, there were no candidate parents in the candidate parent list and no PPN. Therefore, the MN broadcasted a DIS message into the network. All the neighbour nodes which heard the DIS message broadcasted their DIO message into the network. After receiving a DIO message from a neighbour node, the MN checks whether it is already present in its candidate parent list. If it is present, then the corresponding timers, i.e., TTL and freshness timers are reset. If the CPN is not present in its candidate parent list, then based on the RSSI of the DIO message, the MN approximately calculates its distance to compute the approximate duration the MN remains in communication range of the CPN, and also initializes the freshness timer.

From the candidate parent list, the MN selects a CPN, which is going to remain for a longer duration as a PPN. An MN Flag in the DAO message is set and sent to the selected PPN. The unreachability detection timer is initialized to detect the presence of the selected PPN. After receiving the DAO message, the CPN checks if a DAO message has been received from the MN or FRN based on the MNF bit. If received from the MN, then the DIO timer is initialized and a DAO acknowledgment is sent to the MN. On receipt of the DAO acknowledgment message, the node resets the unreachability detection timer and continues sending data traffic to the PPN. If the unreachability detection timer expires, then a new CPN from the candidate parents list is selected as the PPN. Algorithm 5 shows the step-by-step procedure of the MN in selecting a PPN and Procedure 2 shows the procedure for selecting the PPN among the candidate parents.

Figure 5.3 illustrates an example of the different scenarios that occur during the mobility of a node while selecting a PPN. These scenarios are discussed in detail in following sub-sections.

1. T1:T2 Discovery Phase
2. T2:T3 MN Selecting PPN

---

**Algorithm 5:** Selecting PPN for the Mobile Node

---

**Input** : Mobile Node MN  
**Output:** PreferredParentNode of MN

```
1 Candidate_Parent_List = NULL
2 do
3   send(Broadcast DIS message)
4   if DIO Message == TRUE then
5     Instance = DIO.Instance
6     RSSI = cc2420_last_rssi
7     TTL = Calculate_Remaining_Time(RSSI)
8     Candidate_Parent_List_Add(Instance)
9     Start_timer(CPN.freshness)
10 while Candidate_Parent_List != NULL;
11 Call Procedure 2
12 if DAO.MNF == 1 then
13   Calculate(DIO_Timer)
14   ctimer_set(&Instance->DIO_Timer, DIO_Timer, DIO_Output, Instance)
15 if DIO message == TRUE then
16   Instance = DIO.Instance
17   CPN = Candidate_Parent_List_Find(Instance.ID)
18   if CPN == NULL then
19     RSSI = cc2420_last_rssi
20     TTL = Calculate_Remaining_Time(RSSI)
21     Candidate_Parent_List_Add(Instance)
22     Start_timer(CPN.freshness)
23   else
24     Timer_reset(CPN.freshness) Update_timer(CPN.TTL)
25 if CPN.Freshness == 0 then
26   if CPN == dag->Preferred_Parent_Node then
27     dag->Preferred_Parent_Node = NULL
28     dag->Rank = INFINITE_RANK
29     dag->Instance->Def_route = NULL
30   Candidate_Parent_List_Remove(CNP)
31 if DAO.ACK == TRUE then
32   Start_timer(CPN.Unreachability)
33 if timer_expired(&CPN->Unreachability) then
34   Call Procedure 2
```

---



---

**Procedure 2 Preferred Parent Node**

---

```
1 PreferredParentNode = NULL
2 TTL = Minimum_TTL
3 if Candidate_Parent_List != NULL then
4   foreach CPN ∈ Candidate_Parent_List do
5     if CPN.TTL > TTL then
6       TTL = CPN.TTL
7       PreferredParentNode = CPN
8 if PreferredParentNode then
9   Set MNF=1
10  Send(DAO message to PreferredParentNode)
11 else
12  repeat Algorithm 5
```

---

### 3. T3:T4 MN Update PPN

#### Discovery Phase

At time T1 as shown in Figure 5.3, the MN does not have a PPN and its candidate parent list is empty. The MN solicits a DIS message from the network until it hears a DIO message from its neighbours. At time T2, the MN hears a DIO message from FRN6. Then it calculates the TTL from the RSSI of the DIO message and also initializes the freshness timer for the FRN6. Then, the FRN6 is added to its candidate parent list.

#### Mobile Node Selects PPN

At time T2 as shown in Figure 5.3, since the FRN6 is the only CPN available for the MN, it is selected as the PPN and a DAO message with MNF is sent to it. After receiving a DAO message from the MN, the FRN6 initializes a DIO timer based on the RSSI value and sends a DAO acknowledgment back to the MN. At time T3, the FRN6 continues as the PPN since the unreachability timer is reset each time the MN receives a DAO acknowledgment from FRN6, although the MN has candidate parents FRN5, FRN4, and FRN1.

#### Mobile Node Updates PPN

At time T4 as shown in Figure 5.3, the MN moves out of FRN6's communication range, and hence, the MN does not receive a DAO acknowledgment from it. When the un-

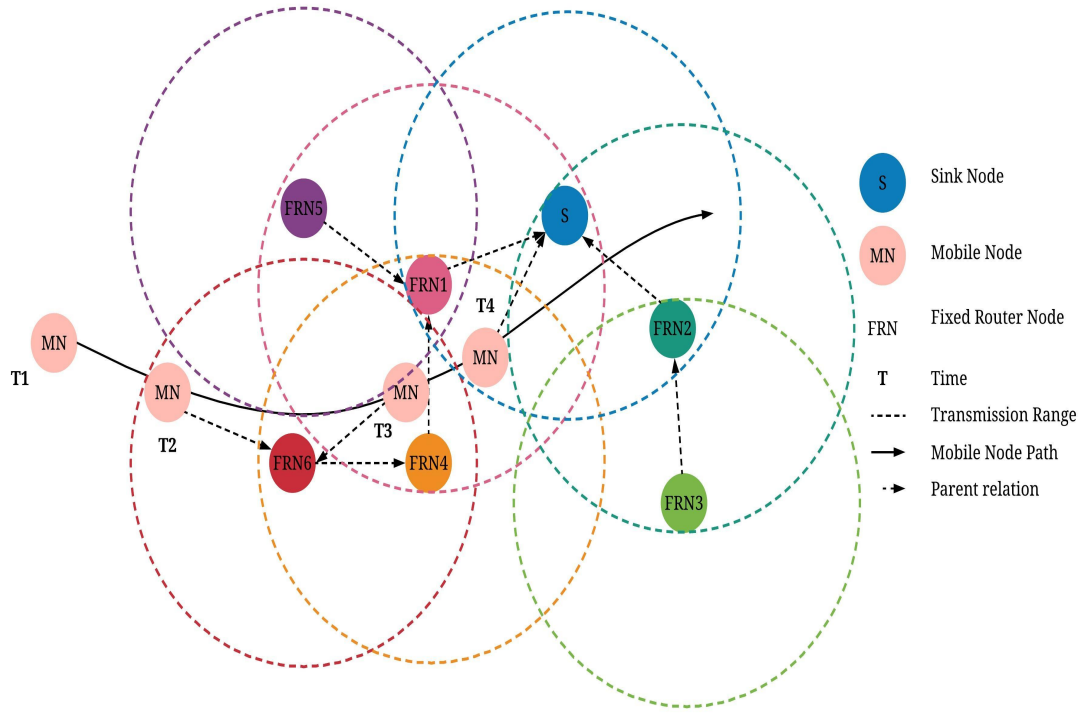


Figure 5.3: Example of different mobility scenario  
Table 5.1: Simulation parameters

Simulation parameter	Values
Simulation area	100m × 100m
Simulation time	600 seconds
Communication range	30 meters
Sensor Mote	Tmote Sky
Speed	(0.5, 1, 1.5, 2) m/s
Radio model	UDGM

reachability detection timer expires, the MN removes a route established through FRN6 and updates the PPN. In the candidate parent list, the MN has FRN4, FRN1, and the sink node. The MN selects the sink as its new PPN, since the sink's TTL value is more compared with the other candidate parents.

#### 5.1.4 Performance Evaluation of the proposed Enhanced Mobility RPL

##### Simulation Setup

The proposed EM-RPL was implemented in the Cooja simulator. The simulations were focused on two applications, namely, elderly monitoring application and hospital environment monitoring application. The simulation parameters were common for both the

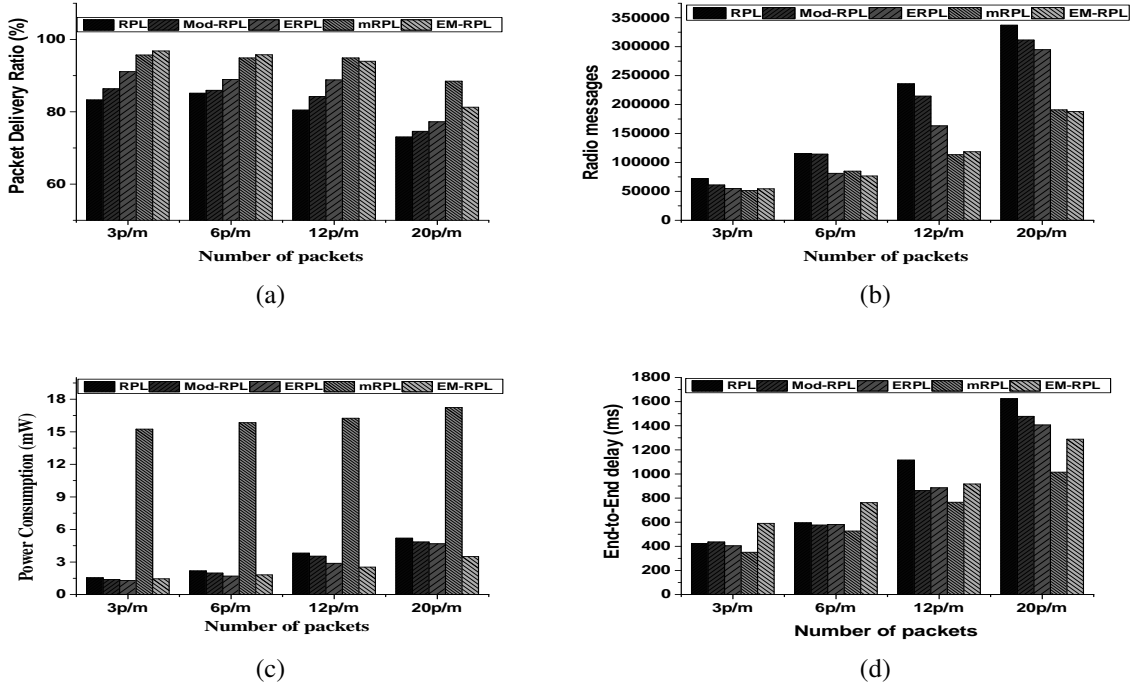


Figure 5.4: Impact of Data Traffic on (a) Packet Deliver Ratio, (b) Radio Messages, (c) Power Consumption, and (d) end-to-end delay

applications and are shown in Table 5.1. The simulation results were compared with the standard RPL (Winter et al. (2012)), the Mod-RPL (Gara et al. (2015)), the mRPL (Fotouhi et al. (2015)), and the ERPL (Sanshi & Jaidhar (2017)). Different evaluation metrics, namely, the PDR, power consumption, end-to-end delay, and number of radio messages were considered to evaluate the performance of the proposed EM-RPL.

#### Simulation of Elderly patient Monitoring Application

In elderly monitoring applications, sensor nodes were attached to the patients for continuous monitoring in the elderly care unit. The sensor nodes send measurements such as blood pressure, respiration rate, and pulse besides others to the doctor in-charge to take the appropriate decisions. Meanwhile, the patients are free to move around the unit. Fixed router nodes were deployed all around the unit to collect information from the patients and to forward the same to the sink node. In the simulation, a small elderly care unit of  $100m \times 100m$  area with 9 patients (mobile) was considered, where thirty fixed nodes were deployed to cover the whole area. The patients were assumed to move around the care unit based on the RWP model. The sensor nodes attached to the patient sent the data every 10 seconds (6p/m) to the sink node. The speed of the mobile node

was set to 1.5m/s, which is the average walking speed of humans. Further, the number of fixed nodes was varied to 15, 20, 25, and 30, the data rate to 3p/m, 6p/m, 12p/m, and 20p/m, and the speed to 0.5m/s, 1m/s, 1.5m/s, and 2m/s to analyze the behaviour of the proposed EM-RPL at different settings for purposes of comparison.

**Impact of Data Traffic:** Figure 5.4 shows the performance of the proposed EM-RPL compared with the RPL, Mod-RPL, mRPL, and the ERPL. It can be observed that the PDR decreases with the increase in data transmission rate as shown in Figure 5.4a. The EM-RPL has approximately 14%, 11%, and 6% higher PDR compared with the RPL, Mod-RPL, and the ERPL. The EM-RPL showed better performance by maintaining seamless connectivity by updating the PPN. However, the mRPL showed 2% better compared with the EM-RPL. From Figure 5.4b, it can be observed that the number of radio messages transmitted in the EM-RPL is less compared with the RPL, Mod-RPL, ERPL, and the mRPL with an improvement of around 38%, 32%, 17%, and 1%, respectively. The EM-RPL minimizes the number of radio messages by allowing the node to select a PPN that remains for a longer duration.

As illustrated in Figure 5.4c, the power consumption of the node increased with the increase in data traffic. The average power consumption of the node in RPL was found to be 3.1823mW; in the Mod-RPL, it was 2.93mW; the ERPL consumed an average of 2.6335mW, the mRPL consumed an average of 16.4mW, and in the EM-RPL, it was 2.3266mW. The mRPL consumed more power due to the fact that the node waited to listen for the burst messages for a longer time. From Figure 5.4d, it can be observed that the delay in the proposed EM-RPL was more compared with the other protocols. However, the EM-RPL showed an average improvement of 19% when the data traffic was set to 12p/m and 20p/m compared with the RPL and 8% compared with the ERPL when the data traffic was set to 20p/m.

**Impact of Speed:** Figure 5.5 shows the simulation results obtained for the RPL, Mod-RPL, ERPL, mRPL, and the EM-RPL by varying the speed of the MNs to 0.5m/s, 1m/s, 1.5m/s, and 2m/s. At low speed, the PDR of the RPL was 87%, which decreased with the increase in speed and reached 79% when the speed of the MNs was set to 2m/s as it was slow to react to topology changes. Similarly, the PDR for the Mod-RPL was 85% when the speed was 2m/s. The PDR of the ERPL was 90% when the speed was

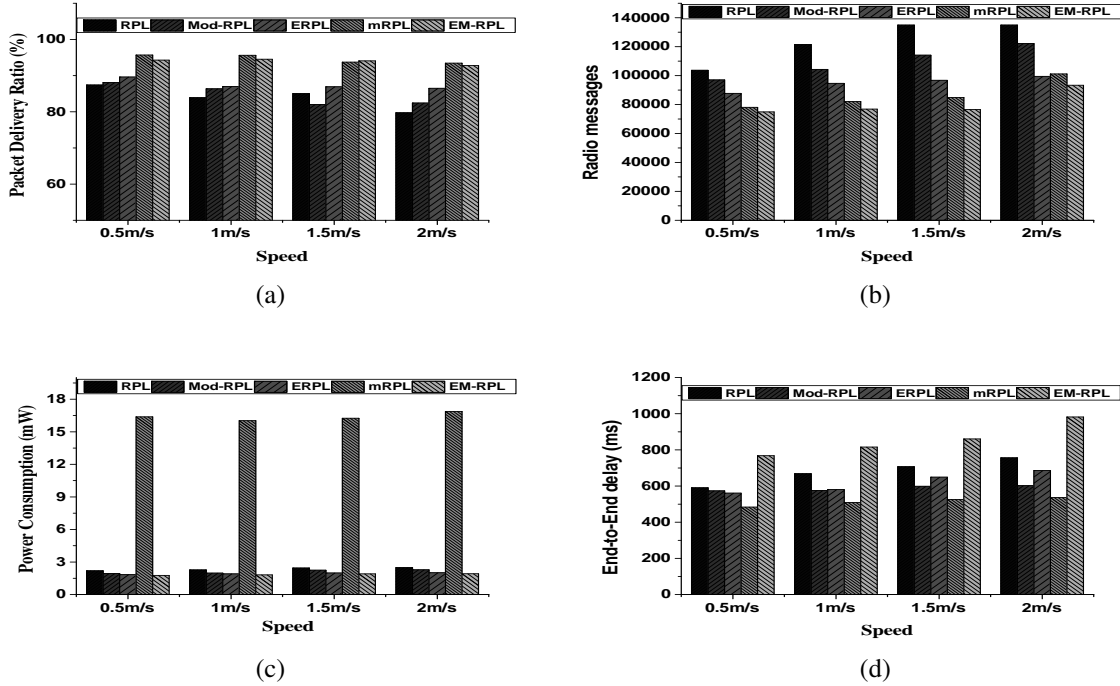


Figure 5.5: Impact of Speed on (a) Packet Deliver Ratio, (b) Radio Messages, (c) Power Consumption, (d) and end-to-end delay

0.5m/s, which decreased to 87% when the speed was 2m/s. Interestingly, the mRPL and the proposed EM-RPL achieved 95% and 94%, respectively, when the speed was 0.5m/s, and both achieved 92% when the speed was 2m/s as shown in Figure 5.5a. The improved performance in EM-RPL was because it responded quickly to topology changes compared with the other protocols. Figure 5.5b shows that the number of radio messages transmitted in the EM-RPL is less compared with the other protocols. It was found that the EM-RPL has 36% and 26% fewer radio messages compared with the RPL and Mod-RPL, and approximately 13% and 7% fewer radio messages compared with the ERPL and the mRPL.

The power consumption increased with the increase in speed of the MNs as illustrated in Figure 5.5c. The average power consumption of the node in the RPL was 2.3445mW; in the case of Mod-RPL, it was 2.112mW, and the ERPL consumed an average of 1.9369mW for the successful transmission of the packets. The mRPL consumed the highest power of 16.3856mW among the considered protocols by keeping the radio on for a longer time, whereas in the EM-RPL, it was 1.85mW for the successful transmission of the packets. However in Figure 5.5d, it was observed that the EM-RPL experienced higher delay compared with the other protocols as the packets

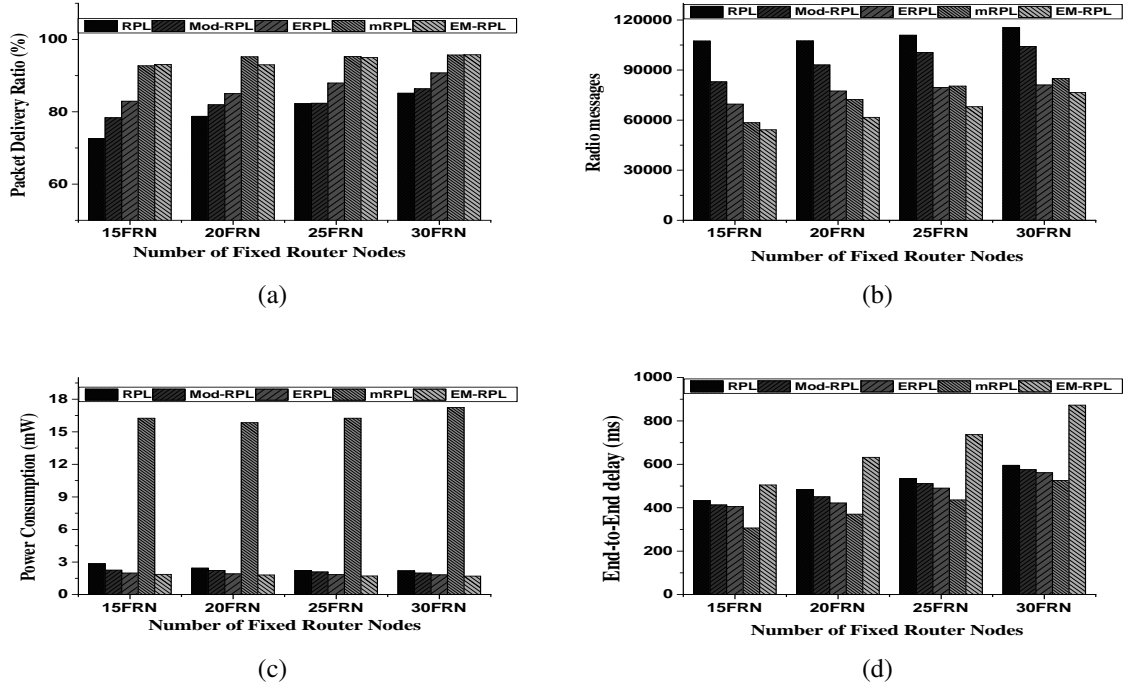


Figure 5.6: Impact of Fixed Router Node on (a) Packet Deliver Ratio, (b) Radio Messages, (c) Power Consumption, and (d) end-to-end delay

had to traverse a longer path to reach the sink node.

**Impact of Fixed Router Node:** Figure 5.6 shows the performance of the EM-RPL compared with the RPL, Mod-RPL, mRPL, and the ERPL by varying the number of FRNs to 15, 20, 25, and 30 and maintaining the data rate at 6p/m and the speed at 1.5m/s. Figure 5.6a shows the performance with respect to the PDR. As seen, the number of FRNs directly affects the PDR. The PDR increases with the increase in density of the FRNs as more options are available for the MN to choose the best PPN. The PDR in the RPL and the Mod-RPL achieved an average of 79% and 82%, and in the case of ERPL, it reached an average of 87%, whereas, the mRPL and EM-RPL reached an average of 94%. Figure 5.6b illustrates the number of radio messages communicated during the simulation. It was found that the EM-RPL used 41% and 31% fewer radio messages compared with the RPL and Mod-RPL. Whereas, in the case of the ERPL and the mRPL, the proposed EM-RPL required 16% and 12% fewer radio messages, respectively.

Figure 5.6c shows the performance with respect to power consumption. It can be observed that the power consumption decreases with the increase in FRNs. The av-

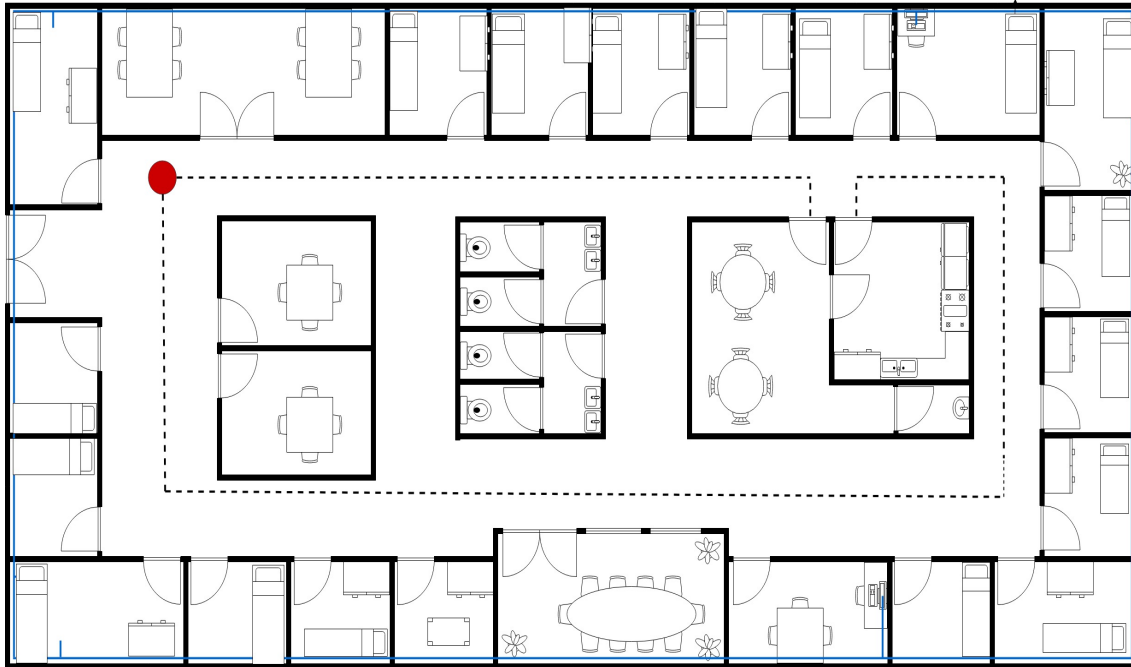


Figure 5.7: Hospital Environment Monitoring

average power consumption of the RPL and the Mod-RPL was found to be 2.4179mW and 2.129mW, respectively. Similarly, the power consumption of the ERPL decreased with the increase in FRNs at an average of 1.88mW. In the case of the mRPL, the average power consumption was 16.3995mW. The proposed EM-RPL consumed the lowest power at an average of 1.764mW. The reason that the EM-RPL was able to perform better was because it had found a consistent path to the root node. The candidate parents were removed from the candidate parent list when the timer expired so as to maintain consistent neighbours, and therefore, candidate parents out of communication range could not take part in the selection of a PPN in contrast to the other protocols. However in Figure 5.6d, it can be observed that the EM-RPL experienced higher delay compared with the other protocols.

#### Simulation of Hospital Environment Monitoring System

In this application, a hospital scenario was considered in which thirty FRNs were deployed to cover the entire area of the hospital to collect data from the MNs and forward the same to the administrator (sink node). The wearable sensors collected useful data such as blood pressure, respiration rate, pulse rate, etc. and the fall detection sensors that alerted the medical staff were attached to the patients to monitor their health. In the

scenario as shown in Figure 5.7, a patient (MN) is moving around the hospital. The MN speed has been varied to 0.5m/s, 1m/s, 1.5m/s, and 2m/s to match with the real-life scenario. The transmission rate has been set to 2p/s since healthcare applications require higher data rate.

Figure 5.8 shows the simulation results for this application for five protocols, viz., the RPL, Mod-RPL, ERPL, mRPL, and the EM-RPL. Figure 5.8a shows the PDR for each protocol using different speed settings. It can be seen that the EM-RPL outperformed the RPL, Mod-RPL, and the ERPL, thereby confirming its effectiveness in achieving rapid assessment of link quality and updating the PPN when the MN changed its position. In contrast, the RPL and the Mod-RPL experienced low PDR every time the MN changed its location due to lack of an active strategy. The ERPL performed better than the RPL and the Mod-RPL, but it was less efficient than both the mRPL and the EM-RPL. This can be explained by considering that the PPN was updated only after receiving consecutive DIO messages, and therefore, more time was needed to discover a better PPN when moving. However, the mRPL achieved 3% higher PDR than the EM-RPL.

Figure 5.8b quantifies the radio messages produced by each strategy. The number of radio messages in the RPL and the Mod-RPL was high due to topology changes that occurred during the mobility of the node. The ERPL showed a slight decrease in the number of radio messages as the PPN updated based on the DIO messages. The responsiveness of the mRPL to node mobility was obtained at the cost of sending burst control messages, whereas the EM-RPL reduced the radio messages by selecting a node, which remained for a longer time.

Figure 5.8c shows the average power consumption for each strategy. It can be observed that the power consumption of the RPL and the Mod-RPL by each strategy was almost equivalent. This can be explained by considering that both the strategies required more control messages. The ERPL consumed less power compared with the RPL and the Mod-RPL, but consumed more power compared with the EM-RPL. The mRPL consumed more power compared with all the other protocols because the MN remained awake for a longer period. On the other hand, the EM-RPL consumed less power by sending fewer control messages and maintained consistent neighbour nodes.



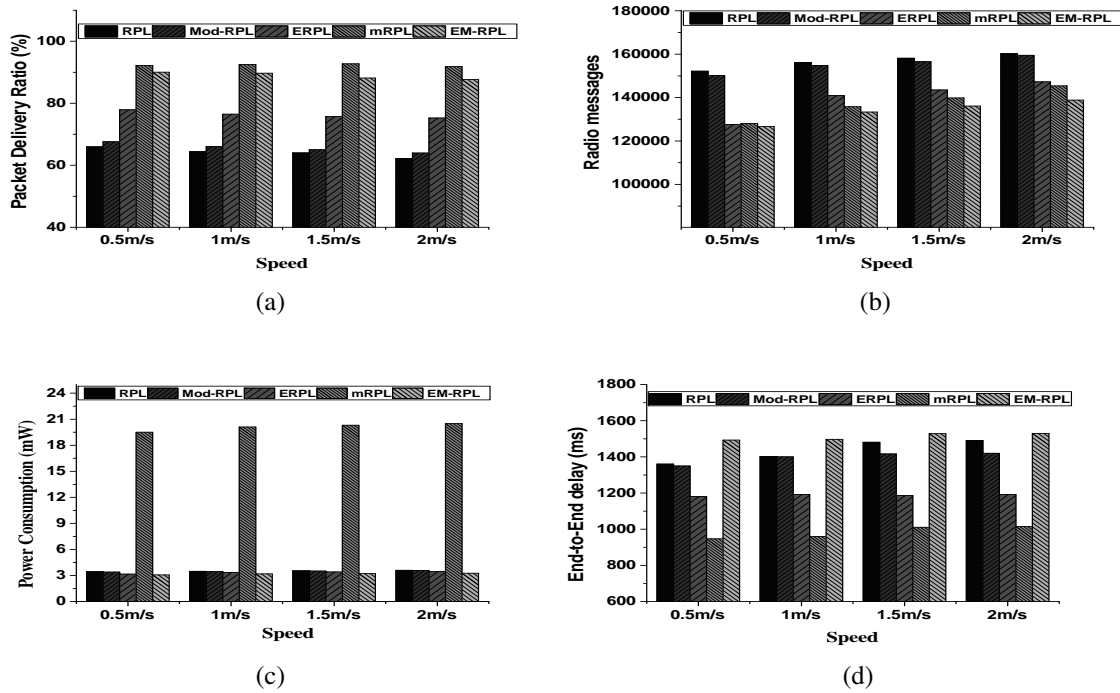


Figure 5.8: Hospital Monitoring Application (a) Packet Deliver Ratio, (b) Radio Messages, (c) Power Consumption, (d) and end-to-end delay

Therefore, it outperformed compared with the other chosen protocols.

Figure 5.8d shows the average end-to-end delay for packets to reach the sink node. It can be observed that the mRPL performed better compared with the other chosen protocols, whereas the EM-RPL showed higher delay compared with the other protocols. This can be explained by considering that in the EM-RPL the PPN was selected based on the node, which remained for a longer time.

### 5.1.5 Discussions

From the performance analysis of EM-RPL for different scenarios with different parameter settings, it was found that the proposed EM-RPL is more reliable and efficient in terms of PDR, packet overhead, and power consumption. Nevertheless, there were some concerns regarding its viability such as:

- The EM-RPL required the nodes to configure as MN or fixed node prior to deployment in order to perform different operations;
- To achieve better performance, the MNs had to be present within communication range of at least one fixed node as the MNs did not forward the data packets;

- The end-to-end delay in the EM-RPL was high, which affected the performance of the applications since they are delay sensitive; and
- The performance of the EM-RPL may be affected in a real-world scenario as the mobility timers were calculated based on the RSSI value, which is susceptible to interference.

## **5.2 FUZZY OPTIMIZED ROUTING METRIC WITH MOBILITY SUPPORT FOR RPL**

In the present work, the Fuzzy optimized routing metric was proposed along with timer modules for enhancing the performance of the RPL with mobility support in terms of packet delivery and energy consumption. The new PPN was selected based on the Fuzzy Inference System by considering node and link metrics. Further, timer functions were defined to maintain seamless connectivity of the MN. The proposed FL-RPL has the following advantages: 1) The selection of the PPN with Fuzzy Inference System can balance the energy consumption of the sensor nodes and increase the overall network lifetime; 2) The PPN is selected based on the node that remains for the longest period, thereby, reducing the number of control messages; 3) The PPN is updated when its timer expires, and a new PPN is selected from the candidate parent list to maintain seamless connectivity to the sink node; and 4) The CPNs that are out of communication range are removed from the candidate parent list, and thus, consistent neighbours are maintained.

The fuzzy logic is used due to its capability to reason precisely even in cases of imprecise or ambiguous input information. In addition, it allows combination of multiple routing metrics and evaluates the system effectively. It characterizes the generic behaviour of the neighbouring nodes to determine the PPN towards the sink node. Moreover, its use in LLN is an excellent option due to the execution of the requirements that can be easily supported by the sensor devices, while it enhances the network performance. In the present work, the Mamdani fuzzy logic ([Mamdani & Assilian \(1975\)](#)) was used due to its intuitive, widespread acceptance and convenience to human instinct.

### **5.2.1 Routing Metric Selection**

The choice of selecting a PPN was made based on the OF which depended on the routing metrics. Therefore, the selection of routing metrics is vital to enhance over-

all network performance. The Fuzzy Inference System uses the ETX, RE, RSSI, and Mobility Timer (MT) metrics.

The routing metrics ETX and RE are explained in the earlier chapters. The MT metric is discussed in the next sub-section.

### **Mobility Timer**

In a mobile environment, a radio link may suddenly be unavailable due to the mobility of the node. If that link is in use for forwarding packets to the sink node, then all the packets thus forwarded are dropped until the link failure is detected and a new link is identified. To overcome this problem, an MT is used. It is calculated based on the distance and maximum speed of the MN. When an MN receives a message from the CPN, it calculates the approximate distance based on the RSSI value using Equation (5.2).

$$RSSI = -10n \log(D) + C \quad (5.2)$$

Where,  $D$  is the distance between the nodes,  $n$  is the path loss exponent factor, and  $C$  is some fixed constant. The RD is computed by subtracting the approximate distance from the CR of the CPN. Then, the MT is calculated by dividing the remaining distance with the maximum speed of the MN as given in Equation (5.3). The maximum speed ensures the minimum time required by the node to move out of communication range.

$$RD = CR - D$$

$$MT = \frac{RD}{S} \quad (5.3)$$

Where,  $RD$  is the remaining distance of the MN before moving out of communication range and  $S$  is the maximum speed of the MN.

### **5.2.2 Fuzzy Inference System**

The Fuzzy Inference System consists of three parts, i.e., Fuzzification, Fuzzy Inference Engine, and Defuzzification as illustrated in Figure 5.9. The input metrics are assigned to one of the linguistic values to determine the membership degree. Three linguistic values are defined for each of the input metrics, for example, ETX has three linguistic

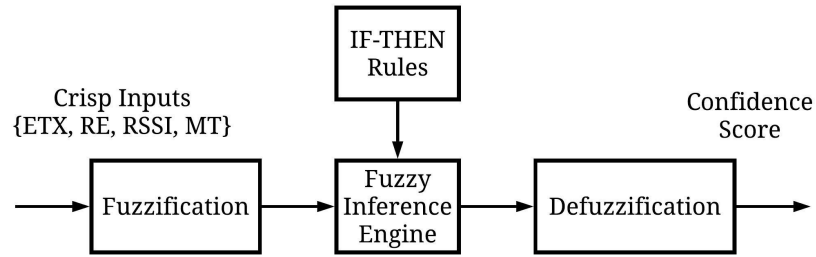


Figure 5.9: Block diagram of Fuzzy Inference System

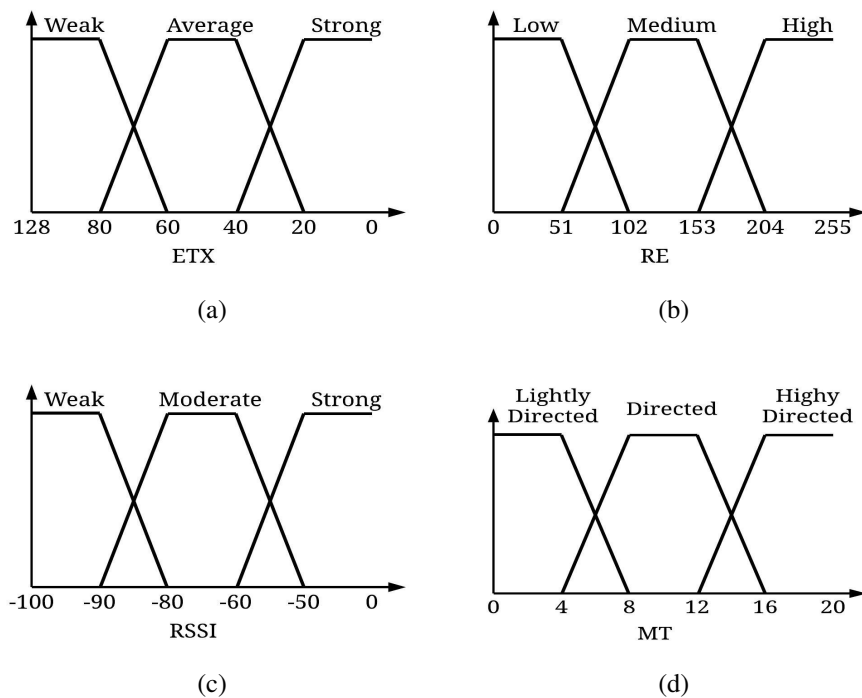


Figure 5.10: Membership function for input routing metrics: (a) ETX (b) RE (c) RSSI (d) MT

values: Weak, Average, and Strong. Figure 5.10 shows the membership function of each of the input variables. Here, the triangle and trapezoidal forms are used for membership functions since these forms are simple to evaluate and largely used in the Fuzzy Inference System. The outputs of the fuzzification are fuzzy values that are processed by the fuzzy inference engine.

The fuzzy inference engine applies IF-THEN rules that are kept in the fuzzy database to the fuzzy inputs using the Mamdani model (Mamdani & Assilian (1975)). Fuzzy rules have several antecedents containing a combination of different fuzzy inputs connected by fuzzy operators, such as OR, AND, and NOT. In the present work, four fuzzy inputs were used with each of them having three fuzzy sets, and therefore, the rule base consisted of  $3^4 = 81$  rules. Some of the 81 rules are defined as follows:

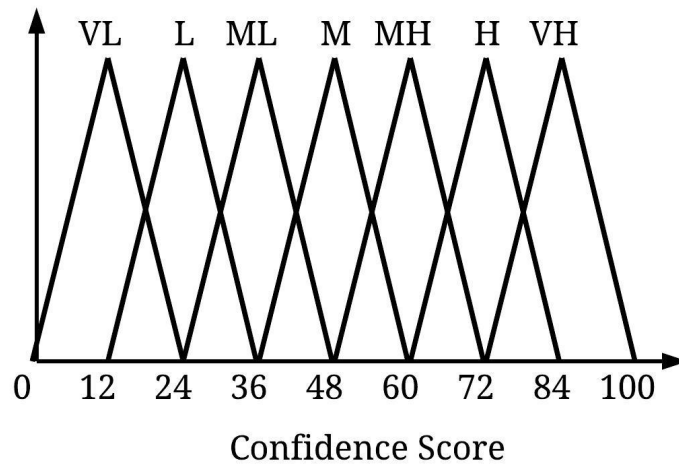


Figure 5.11: Membership Function of output variable: VL:Very Low, L:Low, ML:Moderate Low, M:Moderate, MH:Moderate High, H:High, VH:Very High

1. IF ETX is weak, and RE is low, and RSSI is weak, and MT is lightly directed THEN Confidence Score is very low
2. IF ETX is weak, and RE is low, and RSSI is weak, and MT is highly directed THEN Confidence Score is low
3. IF ETX is average, and RE is medium, and RSSI is moderate, and MT is directed THEN Confidence Score is moderate
4. IF ETX is medium, and RE is full, and RSSI is strong, and MT is directed THEN Confidence Score is high
5. IF ETX is high, and RE is full, and RSSI is strong, and MT is highly directed THEN Confidence Score is very high.

Similarly, the remaining rules are defined by a combination of different fuzzy sets. The consequent of the rules is the Confidence Score of the CPN. The output fuzzy set, which is the Confidence Score, consists of "Very Low" to "Very High". A Confidence Score from 0 to 100 is assigned to each CPN. Figure 5.11 shows the membership function for the Confidence Score.

In defuzzification, one output value is produced from several membership values

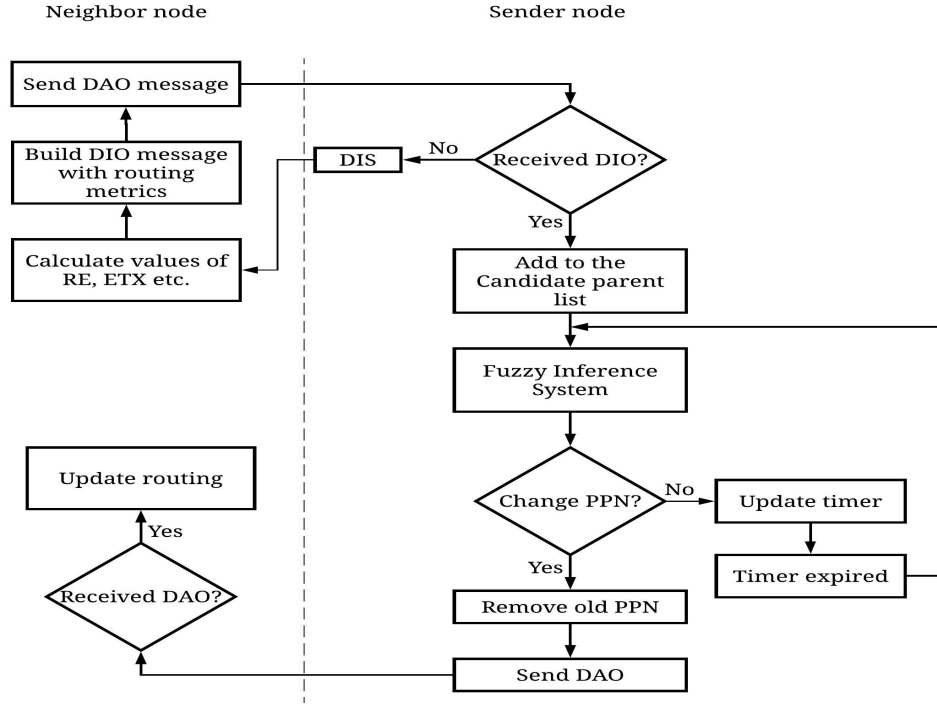


Figure 5.12: Route Construction in FL-RPL

using the centroid defuzzification method as given in Equation 5.4.

$$C = \frac{\sum_{i=1}^N W_i \times \mu_A(W_i)}{\sum_{i=1}^N \mu_A(W_i)} \quad (5.4)$$

Where,  $C$  is the weighted mean of the fuzzy region  $A$ ,  $W_i$  is the domain value of the corresponding rule  $i$ ,  $N$  is the number of activated rules, and  $\mu_A$  is the predicate truth of that domain value.

The Leaf node, Freshness timer and Loop avoidance modules are explained in the earlier sections.

#### Selection of Preferred Parent Node

The node selects its PPN based on the Confidence Score determined by the Fuzzy Inference System. The  $C$  value for the CPNs in the candidate parent list is compared and the CPN with the highest  $C$  value is selected as the PPN, and it is updated when the PPN's MT expires.

---

**Algorithm 6:** PPN selection for Mobile Node

---

**Input** : MN

**Output** : PPN of the MN

```
1 Candidate_Parent_List = NULL
2 do
3   send(DIS message)
4   if DIO Message == TRUE then
5     Instance.ID = DIO.InstanceID
6     RSSI = cc2420_last_rssi
7     MT = Calculate_MT(RSSI)
8     Candidate_Parent_List_Add(Instance)
9     Start_timer(CPN.Freshness)
10  while Candidate_Parent_List != NULL;
11  Call Algorithm 7
12  if Message == TRUE then
13    Instance.ID = DIO.InstanceID
14    CPN = Candidate_Parent_List.Find(Instance.ID)
15    if CPN == NULL then
16      RSSI = cc2420_last_rssi
17      MT = Calculate_MT(RSSI)
18      Candidate_Parent_List_Add(Instance)
19      Start_timer(CPN.freshness)
20    else
21      Timer_reset(CPN.freshness)
22      Update_MT(CPN)
23  if timer_expired(CPN.Freshness) then
24    if CPN == dag->Preferred_Parent_Node then
25      dag->Preferred_Parent_Node = NULL
26      Call Algorithm 7
27    Candidate_Parent_List_Remove(CNP)
28  if timer_expired(PPN.MT) then
29    Call Algorithm 7
```

---

### Procedure of the FL-RPL

Figure 5.12 shows the procedure for creating a DODAG in the FL-RPL, whereas Algorithm 6 shows the step-by-step procedure of the MN to select a PPN and Algorithm 7 shows procedure for selecting the PPN among candidate parents. Initially, there are no candidate parents in the candidate parent list and no PPN, and therefore, the MN broadcasts a DIS message into the network. All the neighbouring nodes on hearing this message in turn broadcast their DIO message into the network. After receiving a DIO message from a neighbour node, the MN checks to see if it is already present in its candidate parent list. If it is present, then the corresponding timers, i.e., the MT and the freshness timers are reset. If the CPN is not present in its list, then it extracts routing metrics and based on the RSSI of the DIO message, the MN approximately calculates its MT and also initializes the freshness timer. These routing metrics are given as input to the fuzzy inference system to obtain a Confidence Score for the CPN. If the Confidence Score is higher than the current PPN's Confidence Score, then the CPN is updated as the current PPN.

---

#### Algorithm 7: Preferred Parent Node

---

```
1 PPN = NULL
2 MAX_CS = NULL
3 if Candidate_Parent_List == TRUE then
4     foreach CPN ∈ Candidate_Parent_List do
5         C = Fuzzy_Inference_System(CPN)
6         if  $C > MAX\_C$  then
7             PPN = CPN
8             Start_timer(PPN.MT)
9 if PPN == TRUE then
10     Send(DAO message to PPN)
11 else
12     repeat Algorithm 6
```

---

If a node does not hear any activity from the CPN, then that CPN is removed from the candidate parent list when the freshness timer expires, otherwise the freshness timer and the MT are updated. When a PPN's MT expires, the node selects a PPN from the candidate parent list based on the Confidence Score.



Table 5.2: Simulation parameters

Simulation parameter	Values
Simulation area	$100m \times 100m$
Communication range	30 meters
Sensor Mote	Tmote Sky
Data Traffic	(3, 6, 12, 20) p/m
Number of Nodes	Fixed:(15, 20, 25, 30) MN:9
Speed	(0.5, 1, 1.5, 2) m/s
Mobility model	RWK
Radio model	UDGM

### 5.2.3 Results and Discussion

In the simulation,  $100m \times 100m$  area was considered with 9 MNs where 30 fixed nodes were deployed to cover the whole area. The sensor nodes sent their data for every 10 seconds (6p/m) to the sink node. The speed of the mobile node was set to 1.5m/s, which is the average walking speed of humans. Further, the number of fixed nodes was varied to 15, 20, 25, and 30; the data rate to 3p/m, 12p/m, and 20p/m, and the speed to 0.5m/s, 1m/s, 1.5m/s, and 2m/s to analyze the behaviour of the proposed scheme at different settings for purposes of comparison. The detailed simulation parameters are shown in Table 5.2. To simulate the environment, a Contiki-based Cooja simulator (Jevtić et al. (2009)) was used and RWK mobility traces were generated using the BonnMotion tool (Aschenbruck et al. (2010)).

#### Impact of Data Traffic

Figure 5.13 shows the performance of the RPL, ERPL, and the FL-RPL under different traffic conditions. The PDR is high for all the protocols (above 80%) when the traffic is low, which decreases with the increase in data traffic as shown in Figure 5.13a. The RPL goes down to 80% at 12p/m and to 67% at 20p/m. The ERPL reaches around 87% at 12p/m and around 77% at 20p/m. The FL-RPL achieves around 91% at 12p/m and around 84% at 20p/m. The FL-RPL outperforms the RPL by an average 16% and the ERPL by an average of 7%. With the high data rate, the RPL and the ERPL performance is reduced due to the delay in switching off of the routes when the PPN changes.

Figure 5.13b shows the number of radio messages with varying data traffic. The FL-

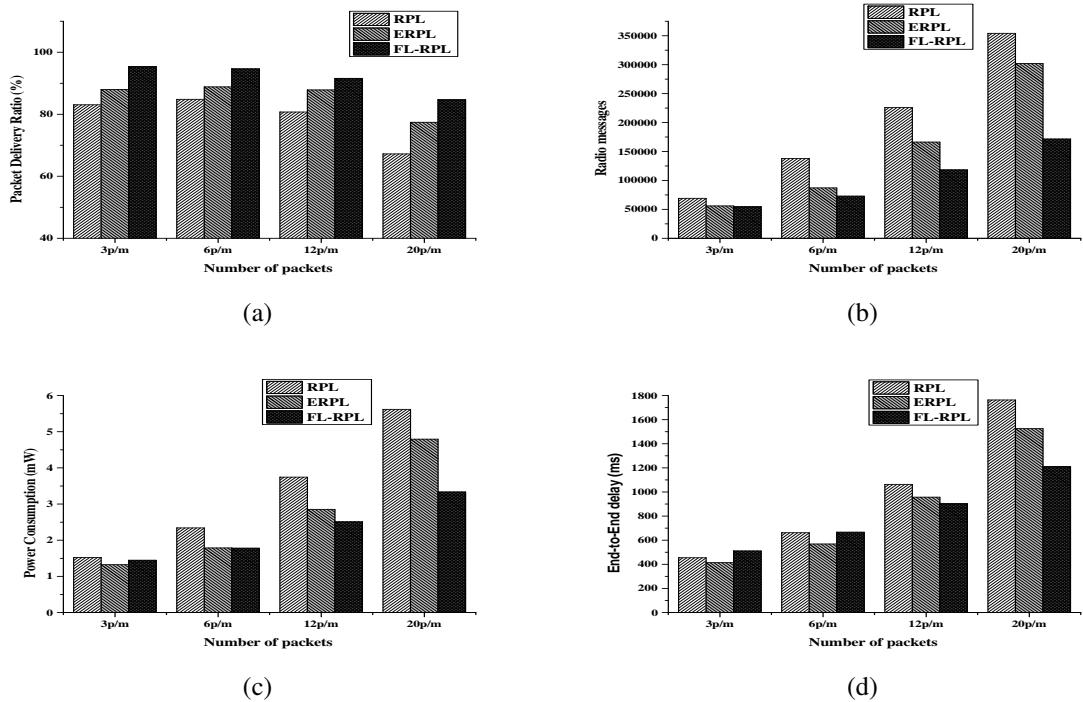


Figure 5.13: Impact of Data Traffic on (a) Packet Deliver Ratio, (b) Radio Messages, (c) Power Consumption, and (d) end-to-end delay

RPL requires an average 41% and 22% fewer radio messages compared with the RPL and the ERPL, respectively. In the RPL, the main reason for the high number of radio messages is because the node continues to send messages even when the PPN is out of communication range and until a new PPN is selected. In the ERPL, the candidate parent list contains inconsistent neighbours, and therefore, requires more messages when an inconsistent neighbour is selected as the PPN. Whereas in the FL-RPL, the candidate parent is removed from the candidate parent list whenever the freshness timer expires and thus maintains consistent neighbours.

Figure 5.13c shows power consumption with varying data traffic. At a low data rate, the ERPL performs better compared with the FL-RPL. However, the ERPL is not optimized for higher data rate. The FL-RPL takes into consideration the RSSI value and the MT while selecting a PPN, and therefore, shows average improvement of 25% and 8% compared with the RPL and ERPL, respectively.

Figure 5.13d shows end-to-end delay with varying data traffic. The end-to-end delay in the FL-RPL is high during low data rate compared with both the RPL and the ERPL. At a transmission rate of 12p/m and 20p/m however, the FL-RPL has an average of

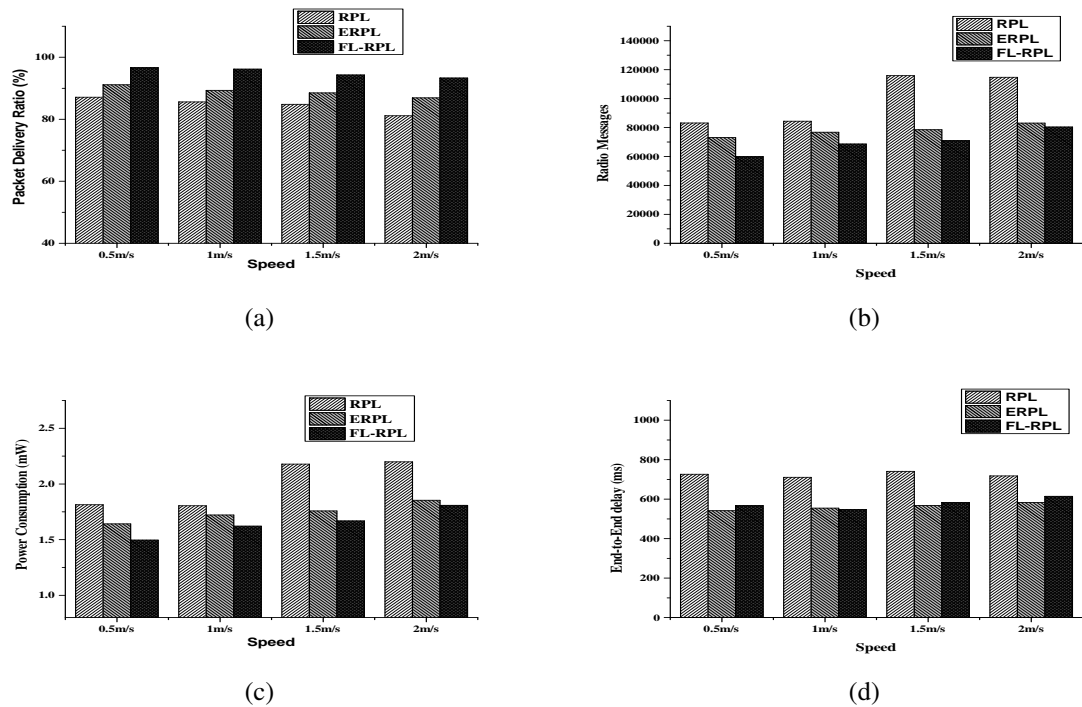


Figure 5.14: Impact of Speed on (a) Packet Deliver Ratio, (b) Radio Messages, (c) Power Consumption, (d) and end-to-end delay

23% and 13% improvement compared with the RPL and ERPL, respectively. The main reason for the delay in the RPL and the ERPL is the frequency of retransmission of the packets to reach the sink node successfully, whereas the FL-RPL is optimized to deliver the data packets even in high data traffic.

### Impact of Speed

Figure 5.14 shows the performance of the RPL, ERPL, and the FL-RPL with different speeds of the MN. The PDR of the FL-RPL reaches around 97% when the speed is at its lowest, and around 93% at its maximum. In the case of ERPL, the PDR is around 91% at minimum speed, and around 86% at its maximum, whereas in the standard RPL, the PDR is 87% at minimum speed and around 81% at maximum speed as shown in Figure 5.14a. Therefore, the FL-RPL has 12% and 7% better PDR compared with the RPL and ERPL, respectively. From Figure 5.14b, it can be observed that the radio messages increase as the speed of the MN increases due to the overhead in finding the right path for the MN to reach its destination, and thus the FL-RPL requires an average of 28% and 10% fewer radio messages compared with the RPL and ERPL, respectively. Similarly from Fig 5.14c, the power consumption for FL-RPL outperforms the RPL and ERPL by

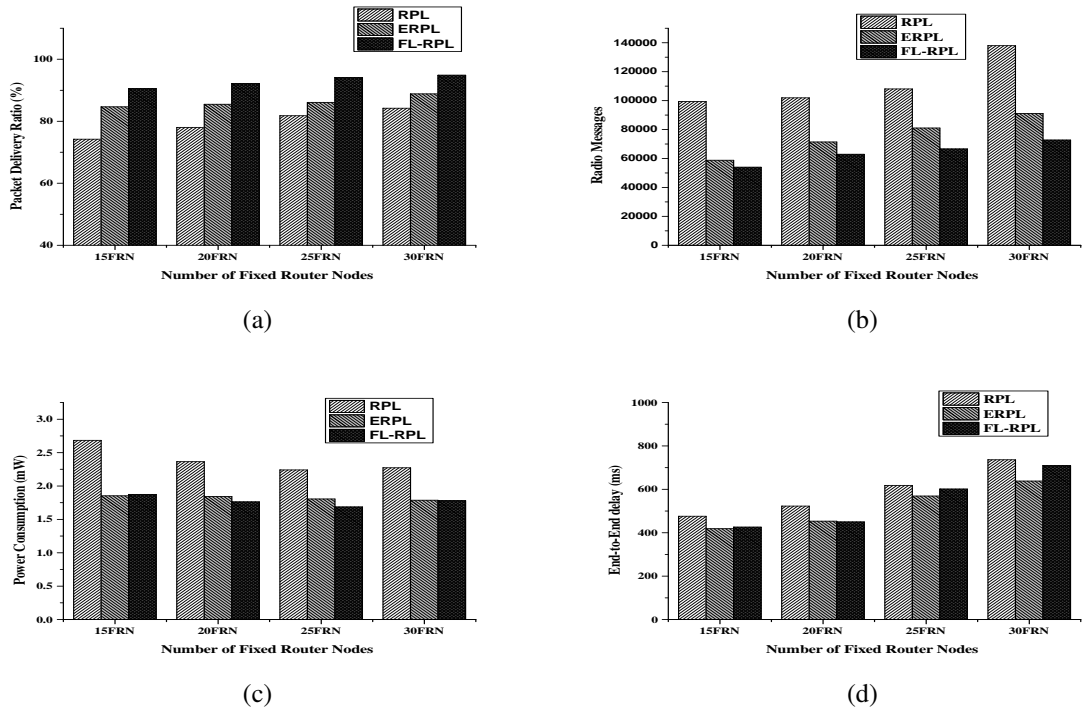


Figure 5.15: Impact of Fixed Nodes on (a) Packet Deliver Ratio, (b) Radio Messages, (c) Power Consumption, and (d) end-to-end delay

17% and 6%, respectively. The main reason that the FL-RPL performs better compared with the other protocols is that it updates the PPN whenever the MT of the current PPN expires, and thus always find the right path to its destination. However, the end-to-end delay in the FL-RPL is higher compared with the ERPL due to the path length as shown in Figure 5.14d.

### Impact of Fixed Node

Figure 5.15 illustrates the impact of fixed nodes on the performance of the RPL, ERPL, and the FL-RPL. The node selects a PPN from the candidate parent list based on the OF. The number of CPNs affects the performance of all the protocols since the probability of selecting an optimal PPN increases. Figure 5.15a shows the performance of all the protocols with respect to PDR. The RPL achieved 74% PDR when the fixed nodes were 15 and 84% when the fixed nodes were increased to 30. In case of ERPL, the PDR reaches 84% when the fixed nodes were 15 and 88% when the fixed nodes were increased to 30, whereas the FL-RPL achieved 90% and 94% when the fixed nodes were 15 and 30, respectively.

Figure 5.15b shows the number of radio messages with varying fixed nodes. The

FL-RPL takes an average 40% and 14% fewer radio messages to find an optimal PPN in the presence of MN compared with the RPL and ERPL, respectively. Similarly from Figure 5.15c, it can be observed that the FL-RPL consumes an average 25% and 3% less power compared with the RPL and ERPL, respectively. The main reason that the FL-RPL performs better is that it updates the candidate parent list in a timely manner and selects the PPN based on the fuzzy optimized metric. However, the end-to-end delay is high compared with the ERPL protocol as shown in Figure 5.15d.

### 5.3 SUMMARY

Section 5.1 proposed an EM-RPL to support mobility in WSN. The EM-RPL increased the network reliability and efficiency by selecting a route that was more stable. The TTL and Freshness Timers were used in the proposed EM-RPL to prevent the MNs from selecting a PPN that was not in communication range and to select a candidate parent, which would be present for a longer duration to avoid frequent changing of the PPN. Further, to reduce the frequency of the discovery process, the FRN broadcasted a DIO message based on the DIO timer in the presence of an MN within communication range. This is crucial for minimizing the number of control messages in the network. The proposed EM-RPL was implemented and evaluated using the Cooja simulator over the Contiki operating system and compared with the RPL, Mod-RPL, mRPL and the ERPL. From the simulation results, it was found that the EM-RPL showed a maximum of 18% PDR improvement along with 26% improved power consumption compared with the other protocols.

Section 5.2 proposed an FL-RPL to improve the performance of the RPL. The Fuzzy Inference System considered multiple routing metrics to select a suitable candidate parent as the preferred parent node to forward the data packets to the sink node. Further, timer functions were added to maintain consistent neighbours to support mobility and seamless connectivity. The FL-RPL was implemented and tested with different parameter settings for real-life scenarios. The simulation results showed that the proposed solution increased packet delivery ratio by approximately 12% while reducing power consumption by 20% compared with other related works.

## Chapter 6

### Conclusions and Future Work

The RPL was mainly designed to work in a network, where the sensor nodes are static. However, many emerging applications demand mobility as a fundamental requirement and require transmission of data in real-time. For instance, in healthcare based applications, patients are equipped with body sensors to measure glucose rate, pulse rate, respiration rate, and other physiological signs. The gathered data is then forwarded to the sink node, where the doctors can examine it and make appropriate and rapid decisions to treat the patient. In such real-world applications, the doctors or patients freely move around. Due to this mobility of the nodes, the RPL experiences packet loss and requires packet retransmission, which significantly consumes node energy.

The OF, which plays a central role in the RPL, affects overall performance under mobility. Therefore, a detailed study of the RPL under mobility was carried out by considering different OFs. The results obtained from the simulations demonstrated that under mobility, the OFs have a direct effect on PDR, power consumption, and latency. Furthermore, the MRHOF performed better in terms of PDR and power consumption, whereas the OFDE achieved better results in terms of latency compared with the other OFs. The default OF used in the RPL did not consider mobility and used a single routing metric. A new MMOF, by considering node and link metrics, was proposed. Its performance was analyzed by varying the system and traffic parameters. The simulation results showed that the MMOF minimized the energy consumption of the nodes by selecting a PPN based on a combination of minimum distance, maximum energy, high quality link, and the direction of the MN.

The RPL protocol suffered due to the movement of the MNs, as their neighboring nodes and the link quality changed frequently. If the MN is effectively distant from its PPN then the route towards the PPN becomes inconsistent and continues to exist until the route expires. All the packets transmitted to the PPN, which is out of communication range, are lost and require retransmission to reach the destination successfully. In the MARPL, the MN is aware of its mobility and updates the PPN without waiting for route expiration time. The simulation results showed that the MARPL performed better with respect to healthcare applications compared with the standard RPL. An enhanced

routing protocol, ERPL was proposed to provide mobility support to the standard RPL, in which a different OF was used during the selection of the PPN based on the node type. Further, a new mechanism to update PPN information whenever the MN moved away from the already selected PPN was proposed. The obtained simulation results showed that the proposed ERPL selected the PPN based on high quality link, high availability, and low power consumption. The ERPL updated the PPN quickly whenever the MN moved away from the already selected PPN. The ERPL outperformed in terms of PDR, control messages, power consumption, and latency compared with the existing protocols.

The EM-RPL was proposed to increase network reliability and efficiency by selecting a route that was more stable and to reduce the frequency of the route discovery process. In order to do that, the EM-RPL used multiple routing metrics to ensure an optimal path to the destination and timer modules to maintain seamless connectivity to the destination by updating the PPN whenever the MN moved out of communication range. Further, the candidate parent list was updated to maintain consistent neighbours based on the neighbour nodes' activity. The EM-RPL increased network reliability and efficiency by selecting a route that was more stable, and reduced the frequency of the route discovery process. From the simulation results, it was found that the EM-RPL showed a maximum of 18% PDR improvement with 26% improved power consumption compared with the other protocols.

The proposed FL-RPL took into consideration of link failures due to wireless propagation issues, node mobility, and battery depletion while selecting the PPN. Further, the timer modules maintained consistent neighbours and updated the PPN in a timely fashion to support seamless connectivity. The simulation results showed that the FL-RPL outperformed the RPL and the ERPL in terms of PDR and power consumption with the exchange of fewer control messages.

The proposed mobility aware routing protocols for the LLN achieved better performance in terms of network reliability and power consumption. Among the proposed protocols, the EM-RPL protocol performs better compare to the other proposed approaches as the MN updates its PPN when the unreachability timer expires and update the PPN based on time to leave value. It is evident from the simulation results that

EM-RPL achieves high PDR and consumes less energy. However, the performance was evaluated using the simulator.

As a future work, the proposed mobility management routing protocols can be evaluated in real test bed environment for real-time applications. The proposed routing protocols considered the root (sink) node as static, which may not be true for all scenarios. Hence, the performance of these protocols can be evaluated in scenarios where the sink node is mobile. Additionally, the performance can also be evaluated in the presence of multiple root nodes in the network.



## References

- Adams, J. T. (2006). "An introduction to IEEE STD 802.15. 4". In *2006 IEEE Aerospace Conference*, 1–8.
- Amiri, M. (2010). "Measurements of energy consumption and execution time of different operations on Tmote Sky sensor nodes". PhD thesis, Masarykova univerzita, Fakulta informatiky.
- Ancillotti, E., Vallati, C., Bruno, R., & Mingozzi, E. (2017). "A reinforcement learning-based link quality estimation strategy for RPL and its impact on topology management". *Computer Communications*, *112*, 1–13.
- Aschenbruck, N., Ernst, R., Gerhards-Padilla, E., & Schwamborn, M. (2010). "Bonn-Motion - A mobility scenario generation and analysis tool". In *Proc. of the 3rd Int. ICST Conference on Simulation Tools and Techniques*, 51.
- Atzori, L., Iera, A., & Morabito, G. (2010). "The internet of things: A survey". *Computer networks*, *54*(15), 2787–2805.
- Bag, G., Mukhtar, H., Shams, S. S., Kim, K. H., & Yoo, S.-w. (2008). "Inter-PAN mobility support for 6LoWPAN". In *Convergence and Hybrid Information Technology, 2008. ICCIT'08.*, volume 1, 787–792.
- Bag, G., Raza, M. T., Kim, K.-H., & Yoo, S.-W. (2009). "LoWMob: Intra-PAN mobility support schemes for 6LoWPAN". *Sensors*, *9*(7), 5844–5877.
- Bag, G., Shams, S. S., Akbar, A. H., Raza, H. M. T., Kim, K.-H., & Yoo, S.-w. (2009). "Network assisted mobility support for 6LoWPAN". In *2009 6th IEEE Consumer Communications and Networking Conference*, 1–5. IEEE.
- Barcelo, M., Correa, A., Vicario, J. L., Morell, A., & Vilajosana, X. (2016). "Addressing Mobility in RPL With Position Assisted Metrics". *IEEE Sensors Journal*, *16*(7), 2151–2161.
- Bouaziz, M., Rachedi, A., & Belghith, A. (2017a). "EC-MRPL: An energy-efficient and mobility support routing protocol for Internet of Mobile Things". In *2017 14th IEEE Annual Consumer Communications Networking Conference (CCNC)*, 19–24.
- Bouaziz, M., Rachedi, A., & Belghith, A. (2017b). "EKF-MRPL: Advanced mobility support routing protocol for internet of mobile things: Movement prediction approach". *Future Generation Computer Systems*, *93*, 822 – 832.
- Cao, Z. & Lu, G. (2010). "S-AODV: Sink Routing Table over AODV Routing Protocol for 6LoWPAN". In *2010 Second Int. Conference on Networks Security, Wireless Communications and Trusted Computing*, volume 2, 340–343.
- Chakeres, I. (2008). "Dynamic MANET on-demand (DYMO) routing". <http://tools.ietf.org/html/draft-ietf-manet-dymo-14>.

- Chang, J.-M., Chi, T.-Y., Yang, H.-Y., & Chao, H.-C. (2010). "The 6LoWPAN Ad-Hoc On Demand Distance Vector Routing with multi-path scheme". In *IET Int. Conference on Frontier Computing, Theory, Technologies and Applications*, 204–209.
- Chen, Y.-S., Hsu, C.-S., & Lee, H.-K. (2014). "An enhanced group mobility protocol for 6lowpan-based wireless body area networks". *IEEE Sensors Journal*, 14(3), 797–807.
- Cobârzan, C., Montavont, J., & Noel, T. (2015). "Integrating Mobility in RPL". In Abdelzaher, T., Pereira, N., & Tovar, E. (Eds.), *Wireless Sensor Networks*, 135–150.
- Cobârzan, C., Montavont, J., & Noël, T. (2014). "Analysis and performance evaluation of RPL under mobility". In *2014 IEEE Symp. on Computers and Communications (ISCC)*, 1–6.
- Dunkels, A. (2012), "Contiki Operating System". <http://www.contiki-os.org/> [Accessed: 24 January 2017 ].
- Dunkels, A., Alonso, J., & Voigt, T. (2003). "Making TCP/IP viable for wireless sensor networks". *SICS Research Report*, 1–9.
- Dunkels, A., Eriksson, J., Finne, N., & Tsiftes, N. (2011). "Powertrace: Network-level power profiling for low-power wireless networks". Technical report.
- Dunkels, A., Osterlind, F., Tsiftes, N., & He, Z. (2007). "Software-based On-line Energy Estimation for Sensor Nodes". In *Proc., of the 4th Workshop on Embedded Networked Sensors, EmNets '07*, 28–32.
- Durvy, M., Abeille, J., Wetterwald, P., OFlynn, C., Leverett, B., Gnoske, E., Vidales, M., Mulligan, G., Tsiftes, N., Finne, N., et al. (2008). "Making sensor networks IPv6 ready". In *Proc., of the 6th ACM conference on Embedded network sensor systems*, 421–422.
- Fotouhi, H., Moreira, D., & Alves, M. (2015). mRPL: Boosting mobility in the Internet of Things. *Ad Hoc Networks*, 26, 17 – 35.
- Fotouhi, H., Moreira, D., Alves, M., & Yomsi, P. M. (2017). mRPL+: A mobility management framework in RPL/6LoWPAN. *Computer Communications*, 104, 34 – 54.
- Gaddour, O., Koubää, A., Rangarajan, R., Cheikhrouhou, O., Tovar, E., & Abid, M. (2014). "Co-RPL: RPL routing for mobile low power wireless sensor networks using Corona mechanism". In *Proc., of the 9th IEEE Int. Symposium on Industrial Embedded Systems (SIES 2014)*, 200–209.
- Gara, F., Saad, L. B., Ayed, R. B., & Tourancheau, B. (2015). "Rpl protocol adapted for healthcare and medical applications". In *Wireless Communications and Mobile Computing Conference (IWCMC), 2015*, 690–695.
- Gara, F., Saad, L. B., Hamida, E. B., Tourancheau, B., & Ayed, R. B. (2016). "An adaptive timer for RPL to handle mobility in wireless sensor networks". In *2016 Int. Wireless Communications and Mobile Computing Conference (IWCMC)*, 678–683.

- Ghosh, A. & Das, S. K. (2008). “Coverage and connectivity issues in wireless sensor networks: A survey”. *Pervasive and Mobile Computing*, 4(3), 303–334.
- Gnawali, O. (2012). “The minimum rank with hysteresis objective function in RFC 6719”. Technical report.
- Gonizzi, P., Monica, R., & Ferrari, G. (2013). “Design and evaluation of a delay-efficient RPL routing metric”. In *2013 9th Int. Wireless Communications and Mobile Computing Conference (IWCMC)*, 1573–1577.
- Ha, M., Kim, D., Kim, S. H., & Hong, S. (2010). “Inter-MARIO: a fast and seamless mobility protocol to support Inter-PAN handover in 6LoWPAN”. In *Global Telecommunications Conference, 2010 IEEE*, 1–6.
- Ha, M., Kim, S. H., & Kim, D. (2017). “Intra-MARIO: A Fast Mobility Management Protocol for 6LoWPAN”. *IEEE Transactions on Mobile Computing*, 16(1), 172–184.
- Hong, K. S. & Choi, L. (2011). “DAG-based multipath routing for mobile sensor networks”. In *ICTC 2011*, 261–266.
- Hui, J. W. & Culler, D. E. (2008). “IP is dead, long live IP for wireless sensor networks”. In *Proc., of the 6th ACM conference on Embedded network sensor systems*, 15–28.
- Islam, M. M., Hassan, M. M., & Huh, E.-N. (2010). “Sensor proxy mobile IPv6 (SPMIPv6)-a framework of mobility supported IP-WSN”. In *Computer and Information Technology (ICCIT), 2010 13th Int. Conference on Computer and Information Technology*, 295–299.
- Jabir, A. J., Subramaniam, S. K., Ahmad, Z. Z., & Hamid, N. A. W. A. (2012). “A cluster-based proxy mobile IPv6 for IP-WSNs”. *EURASIP J. Wireless Communications and networking*, 2012(1), 1–17.
- Jara, A. J., Silva, R. M., Silva, J. S., Zamora, M. A., & Skarmeta, A. F. (2011). “Mobile ip-based protocol for wireless personal area networks in critical environments”. *Wireless Personal Communications*, 61(4), 711–737.
- Jara, A. J., Zamora, M. A., & Skarmeta, A. F. (2009). “HWSN6: hospital wireless sensor networks based on 6LoWPAN technology: mobility and fault tolerance management”. In *Computational Science and Engineering, 2009. CSE’09, Int. Conference on Computational Science and Engineering.*, volume 2, 879–884.
- Jevtić, M., Zogović, N., & Dimić, G. (2009). “Evaluation of wireless sensor network simulators”. In *Proc., of the 17th Telecommunications Forum (TELFOR 2009), Belgrade, Serbia*, 1303–1306.
- Kamgueu, P. O., Nataf, E., Djotio, T. N., & Festor, O. (2013). “Energy-based Metric for the Routing Protocol in Low-power and Lossy Network.”. In *SENSORNETS*, 145–148.
- Kharrufa, H., Al-Kashoash, H., & Kemp, A. H. (2018). “A Game Theoretic Optimization of RPL for Mobile Internet of Things Applications”. *IEEE Sensors Journal*, 18(6), 2520–2530.

- Kim, J., Haw, R., Cho, E. J., Hong, C. S., & Lee, S. (2012). “A 6LoWPAN sensor node mobility scheme based on proxy mobile IPv6”. *IEEE Transactions on Mobile Computing*, 11(12), 2060–2072.
- Kim, K. (2005). “Hierarchical routing over 6LoWPAN (HiLow)”. *draft-daniel-6lowpan-hilow-hierarchical-routing-00.txt, Internet draft*.
- Kim, K., Montenegro, G., Park, S., Chakeres, I., & Perkins, C. (2007). “Dynamic MANET On-demand for 6LoWPAN (DYMO-low) Routing”. *Internet Engineering Task Force, Internet-Draft*.
- Ko, J. & Chang, M. (2015). “MoMoRo: Providing Mobility Support for Low-Power Wireless Applications”. *IEEE Systems Journal*, 9(2), 585–594.
- Korbi, I. E., Brahim, M. B., Adjih, C., & Saidane, L. A. (2012). “Mobility Enhanced RPL for Wireless Sensor Networks”. In *2012 Third Int. Conference on The Network of the Future (NOF)*, 1–8.
- Kuhn, F., Wattenhofer, R., & Zollinger, A. (2003). “Ad-hoc networks beyond unit disk graphs”. In *Proc., of the 2003 joint workshop on Foundations of mobile computing*, 69–78.
- Kumar, P., Reddy, L., & Varma, S. (2009). “Distance measurement and error estimation scheme for RSSI based localization in Wireless Sensor Networks”. In *2009 Fifth Int. Conference on Wireless Communication and Sensor Networks (WCSN)*, 1–4.
- Kuntz, R., Montavont, J., & Noël, T. (2013). Improving the medium access in highly mobile Wireless Sensor Networks. *Telecommunication Systems*, 52(4), 2437–2458.
- Kushalnagar, N., Montenegro, G., & Schumacher, C. (2007). “IPv6 over low-power wireless personal area networks (6LoWPANs): overview, assumptions, problem statement, and goals in RFC 4919”. Technical report.
- Lee, K. C., Sudhaakar, R., Dai, L., Addepalli, S., & Gerla, M. (2012). “RPL under mobility”. In *2012 IEEE Consumer Communications and Networking Conference (CCNC)*, 300–304.
- Levis, P., Patel, N., Culler, D., & Shenker, S. (2004). “Trickle: A Self-regulating Algorithm for Code Propagation and Maintenance in Wireless Sensor Networks”. In *Proc., of the 1st Conference on Symposium on Networked Systems Design and Implementation - Volume 1, NSDI’04*, 2–2.
- Mamdani, E. & Assilian, S. (1975). An experiment in linguistic synthesis with a fuzzy logic controller. *Int. J. Man-Machine Studies*, 7(1), 1 – 13.
- Mulligan, G. (2007). “The 6LoWPAN architecture”. In *Proc., of the 4th workshop on Embedded networked sensors*, 78–82. ACM.
- Oliveira, L. M., De Sousa, A. F., & Rodrigues, J. J. (2011). “Routing and mobility approaches in IPv6 over LoWPAN mesh networks”. *Int. J. Communication Systems*, 24(11), 1445–1466.

- Park, J., Kim, K.-H., & Kim, K. (2017). “An Algorithm for Timely Transmission of Solicitation Messages in RPL for Energy-Efficient Node Mobility”. *Sensors*, 17(4), 1–13.
- Perkins, C., Belding-Royer, E., & Das, S. (2003). “Ad hoc on-demand distance vector (AODV) routing RFC 3561”. Technical report.
- Petajajarvi, J. & Karvonen, H. (2011). “Soft handover method for mobile wireless sensor networks based on 6lowpan”. In *2011 Int. Conference on Distributed Computing in Sensor Systems and Workshops*, 1–6.
- Pister, K., Thubert, P., Dwars, S., & Phinney, T. (2009). Industrial routing requirements in low-power and lossy networks, rfc 5673. Technical report.
- Rodrigues, J. J. & Neves, P. A. (2010). “A survey on IP-based wireless sensor network solutions”. *Int. J. Communication Systems*, 23(8), 963–981.
- Sanshi, S. & Jaidhar, C. D. (2017). “Enhanced mobility aware routing protocol for Low Power and Lossy Networks”. *Wireless Networks*, 10.1007/s11276–017–1619–6.
- Shelby, Z. & Bormann, C. (2011). “6LoWPAN: The wireless embedded Internet”, volume 43. John Wiley & Sons.
- Silva, R., Silva, J. S., & Boavida, F. (2014). “Mobility in wireless sensor networks—Survey and proposal”. *Computer Communications*, 52, 1–20.
- Singh, C. K., Kumar, A., & Ameer, P. (2008). “Performance evaluation of an IEEE 802.15. 4 sensor network with a star topology”. *Wireless Networks*, 14(4), 543–568.
- Sky, T. (2006). “Ultra low power IEEE 802.15. 4 compliant wireless sensor module”. *Moteiv Corporation*.
- Somaa, F., Korbi, I. E., Adjih, C., & Saidane, L. A. (2016). “A modified RPL for Wireless Sensor Networks with Bayesian inference mobility prediction”. In *2016 Int. Wireless Communications and Mobile Computing Conference (IWCMC)*, 690–695.
- Sundmaeker, H., Guillemin, P., Friess, P., & Woelffle, S. (2010). “Vision and challenges for realising the Internet of Things”. *Cluster of European Research Projects on the Internet of Things, European Commission*, 3(3), 34–36.
- Tahir, Y., Yang, S., & McCann, J. (2018). “BRPL: Backpressure RPL for High-Throughput and Mobile IoTs”. *IEEE Transactions on Mobile Computing*, 17(1), 29–43.
- Teo, K. H., Subramaniam, S., & Sinniah, G. R. (2015). “Node Mobility Support Between Multi-hop 6LoWPAN Networks Based on Proxy Mobile IPv6”. *Wireless Personal Communications*, 85(3), 959–986.
- Texas-Instruments, “CC2420 datasheet”. <http://www.ti.com/lit/ds/symlink/cc2420.pdf/>.

- Thubert, P. (2012). “Objective function zero for the routing protocol for low-power and lossy networks (RPL) in RFC 6552”. Technical report.
- Tian, B., Hou, K. M., Shi, H., Liu, X., Diao, X., Li, J., Chen, Y., & Chanet, J. P. (2013). “Application of Modified RPL Under VANET-WSN Communication Architecture”. In *2013 Int. Conference on Computational and Information Sciences*, 1467–1470.
- Vasseur, J.-P., Kim, M., Pister, K., Dejean, N., & Barthel, D. (2012). “Routing metrics used for path calculation in low-power and lossy networks, RFC 6551”. Technical report.
- Wang, X., Zhong, S., & Zhou, R. (2012). “A mobility support scheme for 6LoWPAN”. *Computer Communications*, 35(3), 392–404.
- Winter, T., Thubert, P., Brandt, A., Hui, J., Kelsey, R., Levis, P., Pister, K., Struik, R., Vasseur, J. P., & Alexander, R. (2012). “RPL: IPv6 routing protocol for low-power and lossy networks, RFC 6550”. Technical report.
- Xiaonan, W. & Hongbin, C. (2016). “Research on seamless mobility handover for 6LoWPAN wireless sensor networks”. *Telecommunication Systems*, 61(1), 141–157.
- Zinonos, Z. & Vassiliou, V. (2010). “Inter-mobility support in controlled 6LoWPAN networks”. In *2010 IEEE Globecom Workshops*, 1718–1723.

# Publications

## Journal Papers

1. **Shridhar Sanshi**, and Jaidhar CD (2017), "Enhanced Mobility Aware Routing Protocol for Low Power and Lossy Networks", *Journal of Wireless Networks*, DOI 10.1007/s11276-017-1619-6.
2. **Shridhar Sanshi**, and Jaidhar CD (2018), "Enhanced mobility routing protocol for wireless sensor network", *Journal of Wireless Networks*, DOI 10.1007/s11276-018-1816-y.
3. **Shridhar Sanshi**, and Jaidhar CD (2018), "Fuzzy optimized routing metric with mobility support for RPL", *Journal of IET Commun*, DOI: 10.1049/iet-com.2018.5562.

## Conference Papers

1. **Shridhar Sanshi**, and Jaidhar C.D. (2018), "Assessment of Objective Functions under mobility in RPL", In *Proc. of the 5<sup>th</sup> International Conference on Advanced Computing, Networking, and Informatics (ICACNI 2017), Recent Findings in Intelligent Computing Techniques*, Singapore, 565-576.
2. **Shridhar Sanshi**, and Jaidhar C.D. (2018), "Multimetrics-based objective function for low power and lossy networks under mobility", In *Proc. of the 7<sup>th</sup> International Conference on Soft Computing for Problem Solving (SocProc 2017), Advances in Intelligent Systems and Computing, SocPros*, Singapore, 391-403.
3. **Shridhar Sanshi**, and Jaidhar C.D. (2018), "Mobility Aware Routing Protocol based on DIO message for Low power and Lossy Networks", In *18<sup>th</sup> International Conference on Intelligent Systems Design and Applications (ISDA 2018)*. Vellore, India, [**Accepted and Presented**].

# Curriculum Vitae

## **Shridhar Sanshi**

Full-Time Research Scholar  
Department of Information Technology  
National Institute of Technology Karnataka  
P.O. Srinivasanagar, Surathkal  
Mangalore-575 025

## **Permanent Address**

Shridhar Sanshi  
Plot No. S-142, Sector No. 63  
Navanagar  
Bagalkot-587 103  
Email: shridhar.sanshi@gmail.com  
Mobile: +918095202962.

## **Academic Records**

1. M.Tech. in Information Technology from National Institute of Technology Karnataka (NITK) Surathkal, 2013.
2. B.E. in Information Science and Engineering from Basaveshwar Engineering College (BEC) Bagalkot, 2011.

## **Research Interests**

Wireless Sensor Networks  
Low power Lossy Networks  
Internet of Things

## **Programming Languages**

C, CPP, Python, Matlab, Scripts.